Materials Today Bio 30 (2025) 101415

Contents lists available at ScienceDirect

Materials Today Bio

journal homepage: www.journals.elsevier.com/materials-today-bio

From innovation to clinic: Emerging strategies harnessing electrically conductive polymers to enhance electrically stimulated peripheral nerve repair

Rajiv Borah [a,b,c], Daniel Diez Clarke [a,c], Jnanendra Upadhyay [d], Michael G. Monaghan [a,b,c,e,*]

[a] Discipline of Mechanical, Manufacturing and Biomedical Engineering, School of Engineering, Trinity College Dublin, Dublin 2, Ireland
[b] Advanced Materials and BioEngineering Research (AMBER), Centre at Trinity College Dublin and the Royal College of Surgeons in Ireland, Dublin 2, Ireland
[c] Trinity Centre for Biomedical Engineering, Trinity College Dublin, Dublin 2, Ireland
[d] Department of Physics, Dakshin Kamrup College, Kamrup, Assam, 781125, India
[e] CÚRAM, Research Ireland Centre for Research in Medical Devices, University of Galway, H91 W2TY Galway, Ireland

ARTICLE INFO

Keywords:
Nerve repair
Conductive polymer
Nerve guidance conduit (NGC)

ABSTRACT

Peripheral nerve repair (PNR) is a major healthcare challenge due to the limited regenerative capacity of the nervous system, often leading to severe functional impairments. While nerve autografts are the gold standard, their implications are constrained by issues such as donor site morbidity and limited availability, necessitating innovative alternatives like nerve guidance conduits (NGCs). However, the inherently slow nerve growth rate

Abbreviations: (SN)x, poly(sulfurnitride); 2D, 2 dimensional; 3D, 3 dimensional; 3HT, 3-hexylthiophene; 3 MT, 3-methylthiophene; AC, alternating current; ADMSCs, adipose-derived mesenchymal stem cells; Akt, protein kinase B; ATP, adenosine triphosphate; BDNF, brain-derived neurotrophic factor; BMSC, bone marrow mesenchymal stem cells; BNCs, brain neuroglioma cells; cAMP, cyclic adenosine monophosphate; CGO, carboxylic graphene oxide; CIC, charge injection capacity; CNS, central nervous system; CNTs, carbon nanotubes; CREB, cAMP response element-binding protein; CS, chondroitin sulfate; CSC, charge storage capacity; DAG, diacylglycerol; DC, direct current; DNA, deoxyribonucleic acid; DRGs, dorsal root ganglions; DS, dextran sulfate; EC, electrospun cellulose; ECM, extracellular matrix; ECP, electrically conductive polymer; EDOT, 3,4-ethylenedioxythiophene; ERK, extracellular signal-regulated kinases; ES, electrical stimulation; FAK, focal adhesion kinase; FDA, Food and Drug Administration; $FeCl_3$, ferric chloride; fMWCNTs, functionalized multiwall carbon nanotubes; GAP-43, growth associated protein-43; GDNF, glial cell line-derived neurotrophic factor; GelMA, gelatin methacrylate; GO, graphene oxide; GPCR, G-protein-coupled receptors; HA, hyaluronic acid; HEC, hydroxyethyl cellulose; IL-4/6/10, Interleukin-4/6/10; IL-4Rα, Interleukin-4Rα; IP3, inositol 1,4,5-trisphosphate; ITO, indium tin oxide; JNK1/2/3, Jun amino-terminal kinases; KATP, ATP-sensitive potassium; M1, pro-inflammatory macrophage; M2, pro-regenerative/reparative macrophage; MAH, methacrylate anhydride modified hyaluronan; MAPK, mitogen-activated protein kinase; MEH-PPV, poly[2-methoxy-5-(2-ethylhexyloxy)-1,4-phenylenevinylene]; Mg, magnesium; Mo, molybdenum; MSCs, mesenchymal stem cells; NGCs, nerve guidance conduits; NGF, nerve growth factor; NIR, near-infrared; NPs, nanoparticles; Nrf2, nuclear factor erythroid 2-related factor 2; NSCs, neural stem cells; NT-4/5, neurotrophin-4/5; OptoES, optoelectronic stimulation; P(VDT-VI), poly(2-vinyl-4,6-diamino-1,3,5-triazine)/poly(1-vinylimidazole); p38 MAPK, P38 Mitogen-activated protein kinase; P3HT, poly(3-hexylthiophene); P3HT-b-PPI, poly(3-hexylthiophene)-block-poly(phenylisocyanide); P3MT, poly(3-methylthiophene); p75-NgR, p75 Neurotrophin Receptor-Nogo Receptor; PA, polyacetylene; PAni, polyaniline; PbS, lead sulfide; PBS, phosphate buffer saline; PC12, Rat pheochromocytoma cell line; PC60BM, [6,6]-Phenyl C61-butyric acid methyl ester; PCL, polycaprolactone; PCLF, polycaprolactone fumarate; PDA, polydopamine; PEDOT, poly(3,4-ethylenedioxythiophene); PEDOT:PSS, poly(3,4-ethylenedioxythiophene):polystyrene sulfonate; PEG, polyethylene glycol; PEGDA, polyethylene glycol diacrylate; PELA, poly(d,l-lactide)-co-poly(ethylene glycol); PENGs, piezoelectric nanogenerators; PEO, polyethylene oxide; PGA, poly(glycolic acid); PHBV, poly(3-hydroxybutyrateco-3-hydroxyvalerate); PI3K, phosphoinositide 3-kinase; PKA, protein kinase A; PKC, protein kinase C; PLC, phospholipase C; PLCL, poly(L-lactide-co-ε-caprolactone); PLGA, poly lactic-co-glycolic acid; PLL, polylysine; PLLA, poly-l-lactic acid; PMAS, poly(2-methoxyaniline-5-sulfonic acid); PNI, peripheral nerve injury; PNR, peripheral nerve repair; PNS, peripheral nervous system; PPV, poly(p-phenylenevinylene); PPy, polypyrrole; PSS, poly(styrenesulfonate); PT, polythiophene; Pt, platinum; PTCDI-C8, N,N′-dioctyl-3,4,9,10-perylenedicarboximide; PVA, polyvinyl alcohol; PVDF, polyvinylidene fluoride; RCS rats, Royal College of Surgeons rats; R_{ct}, charge storage resistance; RGD, arginine-glycine-aspartic acid; rGO, reduced graphene oxide; ROS, reactive oxygen species; RuO_2, ruthenium oxide; SCs, Schwann cells; SD rat, Sprague-Dawley rat; SF, silk fibroin; SO_3^-, tosylate ions; SPI, soy protein isolate; STAT6, signal transducer and activator of transcription 6; Tab2, TGF-beta activated Kinase 1 (MAP3K7) binding protein 2; TCA, tricarboxylic acid; TENGs, triboelectric nanogenerators; Ti_3C_2Tx, titanium carbide; TiN, titanium nitride; TLR4, Toll-like receptor 4; TRAF6, tumor necrosis factor receptor-associated factor 6; TRKb, tyrosine kinase B; TRPM7, transient receptor potential cation channel subfamily member 7; VEGF, vascular endothelial growth factor; VGCCs, voltage gated calcium channels; ZnO, zinc oxide.

* Corresponding author. Discipline of Mechanical, Manufacturing and Biomedical Engineering, School of Engineering, Trinity College Dublin, Dublin 2, Ireland.
E-mail addresses: borahr@tcd.ie (R. Borah), diezclad@tcd.ie (D. Diez Clarke), jnanendra2015@gmail.com (J. Upadhyay), monaghmi@tcd.ie (M.G. Monaghan).

https://doi.org/10.1016/j.mtbio.2024.101415
Received 11 September 2024; Received in revised form 7 December 2024; Accepted 17 December 2024
Available online 19 December 2024

Electrical stimulation (ES)
Optoelectronic stimulation (OptoES)
Photovoltaic biomaterials
Wireless electrical stimulation

(~1 mm/day) and prolonged neuroinflammation, delay recovery even with the use of passive (no-conductive) NGCs, resulting in muscle atrophy and loss of locomotor function. Electrical stimulation (ES) has the ability to enhance nerve regeneration rate by modulating the innate bioelectrical microenvironment of nerve tissue while simultaneously fostering a reparative environment through immunoregulation. In this context, electrically conductive polymer (ECP)-based biomaterials offer unique advantages for nerve repair combining their flexibility, akin to traditional plastics, and mixed ionic-electronic conductivity, similar to ionically conductive nerve tissue, as well as their biocompatibility and ease of fabrication. This review focuses on the progress, challenges, and emerging techniques for integrating ECP based NGCs with ES for functional nerve regeneration. It critically evaluates the various approaches using ECP based scaffolds, identifying gaps that have hindered clinical translation. Key challenges discussed include designing effective 3D NGCs with high electroactivity, optimizing ES modules, and better understanding of immunoregulation during nerve repair. The review also explores innovative strategies in material development and wireless, self-powered ES methods. Furthermore, it emphasizes the need for non-invasive ES delivery methods combined with hybrid ECP based neural scaffolds, highlighting future directions for advancing preclinical and clinical translation. Together, ECP based NGCs combined with ES represent a promising avenue for advancing PNR and improving patient outcomes.

1. Introduction

Neurological disorders due to injury of the peripheral nervous system (PNS) and central nervous system (CNS) comprise 6.3 % of global disease burden, affecting circa one billion people. A recent pilot study estimates nearly 10 million deaths due to neurological disorders in 2019 alone [1]. Nerve injury can occur in the CNS or PNS, and is a serious healthcare burden with few treatment options available. Various ischemic, chemical, mechanical, or thermal factors can induce damage in CNS or PNS, but the responses of CNS and PNS to such damages are fundamentally different. Specifically, and also the focus of this review: the PNS, which can regenerate on its own if the damage is minor, but surgical intervention is necessary for a larger nerve defect. Peripheral nerve injury (PNI) remains a significant unresolved healthcare challenge due to its high incidence, debilitating effects that can lead to irreversible disability, and substantial financial burden. PNIs are commonly caused by motor vehicular accidents, penetrating trauma after stabbing incidents, gunshot injuries, and stretching or crushing injuries after falls [2]. It has been estimated that 13–23/100,000 persons and 2–5% trauma patients are being exposed to PNI annually [3,4]. There are 360,000 PNI per year in the USA alone leading to an economic burden of $150 billion [5,6], with a similar figure of 300,000 PNI per year in Europe [7]. More significantly, the majority of PNIs result from vehicular accidents involving the most economically productive age group (16–35 years) in society [8]. Moreover, as CNS trauma can accompany PNI, an early diagnosis of PNI remains problematic. This is exemplified by the fact that 10–34 % of the patients with traumatic brain injury admitted to rehabilitation units are found to have associated PNIs [2].

PNS can recover naturally, but larger defects require surgery to join the proximal and distal nerve stumps directly to each other or using a biological or synthetic bridging graft. Despite advances in microsurgical techniques and a deeper understanding PNI pathophysiology and regeneration, only 50 % of traumatic PNI patients achieve good to normal function after surgery, regardless of the repair strategy or injury location [9]. It has been also reported that 80–90 % of patients show permanent sensory or motor deficit following nerve repair [10]. While the regenerative capacity of PNS is higher than CNS, complete recovery is rare, misdirected, or linked with persistent neuropathic pain. Moreover, age-related structural and biochemical changes cause a gradual loss of neurons, with mature neurons unable to divide [11]. This significantly reduces the regenerative and reinnervation capabilities of nerve fibers, posing a serious threat to mobility and sensory function.

Current clinical treatments for PNI include surgical end-to-end coaptation, autologous nerve grafts, allografts, and nerve conduits [12,13]. The gold standard is autologous nerve grafting, but it has significant drawbacks, such as sensory loss, scarring, donor site dysfunction, nerve size mismatch, and limited donor tissue availability. Neural tissue engineering: combining tissue engineering with cellular seeding, offers a potential alternative. This approach has sparked interest in engineered nerve guidance conduits (NGCs) made from various natural and synthetic polymers, which feature porosity, biocompatibility, biodegradability, and infection resistance [14–16]. However, bioactive but electrically passive NGCs fail to replicate the native bioelectrical environment of nerve tissue and are ineffective in repairing long defect gaps, especially those ranging from over 30 mm to as much as 15 cm [15]. Additionally, patients undergoing immediate peripheral nerve repair (PNR) face a prolonged denervation period of the distal target, as the regeneration rate in humans is approximately 1 mm/day. This delay can lead to significant atrophy of the denervated tissue by the time regenerating axons reach it. Therefore, accelerating nerve regeneration can lead to improved functional outcomes for the affected tissue.

Just like endogenous electric fields generated after injury have a vital role in natural wound healing, electric fields following a nerve injury have been demonstrated to affect regeneration [17]. Such endogenous electric fields are generated by disruption of transcellular potential differences due to breaches in ionic gradients at the injury site. Endogenous electric fields play a pivotal role in nerve regeneration by directing neurite growth, promoting branching, and accelerating growth rates through mechanisms such as the regulation of asymmetric Ca^{2+} influx, polarization of epidermal growth factor (EGF) receptors, cytoskeletal reorganization, activation of Rho GTPases (small signalling G protein like Cdc42 and Rac, involved in regulation in cell morphology, cytoskeleton reorganization), and modulation of specific signaling pathways, including neuronal nicotinic acetylcholine receptors and phospholipase C (PLC) [17–19].

Acknowledging the role of endogenous electric field, one potential method for improving nerve regeneration and the effective restoration of function is exogenous electrical stimulation (ES), which is a versatile and powerful technique used across a broad spectrum of medical and therapeutic applications [20–22]. Electrical impulses and ion fluxes drive the firing of neurons, the beating of hearts, and the contraction of muscles in every living organism through a complex network of bioelectrical signals. Therefore, ES provides a potent way to control tissue and cellular responses with the goal of enhancing or restoring physiological processes that have been disrupted by disease or injury. Exogenous ES accelerates nerve repair by promoting axonal growth through galvanotaxis, enhancing Schwann cell (SC) migration, proliferation, and neurotrophic factor secretion, and modulating cellular function via calcium influx and activation of regeneration-associated gene expression [21,22]. Additionally, externally applied ES can also minimize inflammation through macrophage polarization to the M2 phenotype, creating a favorable microenvironment for nerve regeneration and functional recovery.

ES is commonly used in rehabilitation medicine to help with muscle re-education and injury recovery, as well as to treat neurological diseases like Parkinson's disease, epilepsy, and neurotrophic pain, using various types of microelectrodes (e.g., deep brain stimulating electrodes, nerve cuff, percutaneous leads, microneedles, etc.). These

microelectrodes are generally smaller in size and are designed to deliver highly localized ES to specific nerve fibers or regions. Additionally, most of these microelectrodes are rigid, not suitable for long-term implantation and most importantly, lack ability to support any regenerative function. However, administrating exogenous ES to a nerve injury site to stimulate reparative processes should be evenly distributed across the regenerating neural tissue and potentially enable the injured nerve ends to communicate electrically. In this context, a conductive neural scaffold or bioelectronic interface not only provides localized stimulation but also serves as a conductive bridge between injured nerve ends, facilitating neural signal transmission and axonal growth.

A wide range of conductive materials have been explored for fabricating electroconductive neural scaffolds including electrically conductive polymers (ECPs) [23–26], carbon nanotubes (CNTs) [27,28], graphene [29,30], graphene oxide (GO), reduced graphene oxide (rGO) [31,32], MXenes [33,34], metals [35,36], and others [37,38]. Out of those, this review will specifically focus on ECPs; a unique class of organic conducting polymers having traditional plastic-like flexibility and metal-like electrical conductivity [39]. Though both ECPs and carbon based nanomaterials (e.g., graphene, GO, rGO, CNTs) are organic conducting materials, they are significantly distinct in terms of their molecular arrangement. ECPs are composed of long chain of organic monomers with alternating single and double bonds, resulting in a partial delocalization of π-electrons which enables them to conduct electricity upon doping [40–43]. In contrast, carbon based nanomaterials are composed of carbon atoms arranged in 2D hexagonal lattices with fully delocalized π-electrons, resulting in excellent conductivity without any need of doping. Also, ECPs show excellent redox activity, leading to its enhanced charge transfer and charge storage behaviour through Faradaic mechanisms, while carbon based nanomaterials show electric double layer capacitance (EDLC) behaviour for charge transfer (only electron) and storage. Charge carriers in ECPs (e.g., solution, polaron, bipolarons, discussed in details in Section 4) are also different from carbon based nanomaterials (electron & hole). Thus, ECPs are unique type of conducting organic polymers and exhibit exceptional electrochemical properties, including superior charge transfer, charge storage, and charge injection capacity, as well as mixed ionic and electronic conductivity that aligns with the ionic conductivity in biological tissues [20,44,45]. In this context, ECPs have been extensively explored for building electroconductive neural scaffolds, while providing ES, for faster nerve regeneration [20,23,25].

Effective solutions are required due to the catastrophic consequences of PNIs, as previously mentioned. Researchers have investigated a variety of innovative tissue engineering techniques that concentrate on the development of materials and strategies for the repair of damaged nerves following an injury, in recognition of this imperative need. Several reports have reviewed such innovative nerve repair techniques, emphasizing the use of natural and synthetic material-based hydrogels as bioengineered scaffolds [46], piezoelectric polymers in neural tissue regeneration that emphasise the generation of bioelectric cues [47], and cell-derived extracellular matrices as biomimetic materials [48]. The promising aspects of conductive and growth-factor-loaded hydrogels are also highlighted. Liu et al. have discussed both natural and synthetic hydrogels, including their hybrid thereof, with a particular emphasis on how they can be tailored for PNR by modifying their mechanical, biochemical, and electrical properties [46].

Shlapakova et al. have comprehensively highlighted how piezoelectric polymers like polyvinylidene fluoride (PVDF), and poly-l-lactic acid (PLLA) can convert mechanical energy due to body movements, ultrasound, and magnetic fields into electrical signals for nerve repair. They highlight that magnetoelectric scaffolds, composed of piezoelectric matrices doped with magnetic materials, exhibit a greater potential than ultrasound-driven piezoelectric scaffolds due to their non-invasive nature with safe penetration into tissue without attenuation or adverse effects. These magnetoelectric materials can activate the piezoelectric response through magnetostriction, i.e., mechanical deformation caused by magnetic fields [49], offering an alternative for nerve repair. Another recent review on a wide range electroactive biomaterials, has discussed the potential of combining electrical and mechanical cues for advanced scaffold design for neural tissue engineering purposes [50]. However, here the focus spanned a broad range of neural tissues, including CNS repair, and primarily discussed general challenges in biomaterial engineering. Additionally, other reviews have investigated graphene-based scaffolds combined with ES for PNR, highlighting their unique ability to promote SC proliferation and neuronal growth, as well as their mechanical strength and conductivity [51]. However, challenges such as standardization of ES protocols and biocompatibility remain unresolved.

Although valuable insights into a diverse array of materials and strategies, including a wide variety of conductive biomaterials have been reported, this current review is distinctive in that it concentrates on the integration of ECPs, a distinct class of organic polymer-based NGCs, together with ES approaches to improve PNR. With ES and ECP as the primary emphasis of this review, it not only investigates the engineering of ECP based NGCs to imitate endogenous electrical fields, but also evaluates emerging non-invasive ES delivery methods. These technologies seek to overcome the limits of typical wired ES systems, which provide significant impediments to the therapeutic application of this technology. Here, we emphasise the progress, challenges, and emergent techniques for the integration of ECP based NGCs with ES modules for functional nerve repair. Due to the slow progress in the clinical translation of ECP-based neural scaffolds, it is crucial to identify the gaps in knowledge and technology that are hindering advancement. The fundamentals of peripheral nerve physiology post-PNI, especially the roles of SCs and macrophages in nerve regeneration are discussed, alongside the effects of ES on regeneration and immunoregulation. The basic underlying mechanisms of electronic and electrochemical properties of ECPs are also discussed in light of their ability to electrically stimulate neurons effectively. Recent strategies using ECP based scaffolds combined with ES for nerve regeneration, both in vitro and in vivo, are reviewed with particular discussion to electrical and electrochemical properties, biomaterial architecture, ES protocols, and delivery methods. Finally, the challenges are highlighted, emphasizing the need to improve material characteristics (e.g., electrical and electrochemical properties, biodegradability, and bioresorbability) and develop non-invasive ES delivery methods. These advancements could provide valuable insights for necessary interventions to support the potential clinical translation of the technology for functional nerve repair.

2. Peripheral nerve injuries and regeneration

The nervous system controls organs and processes throughout the body. The PNS consists of a vast network of nerves, including the spinal nerves that come from the spinal cord, cranial nerves that originate from the brain, and the sensory nerve cell bodies along with their processes [Fig. 1(a)]. The peripheral nerves are responsible for transmitting sensory inputs to the CNS and relaying signals from the CNS to muscles and glands in the body. The PNS is composed of various cell types, each with distinct roles in the maintenance of the nervous system. These include neurons, SCs, satellite glia, fibroblasts, endothelial cells, macrophages, and pericytes. A peripheral nerve has motor and sensory axons in a nerve trunk enclosed by connective tissue [Fig. 1(b)] [13], whereby SCs form myelin sheaths around axons to speed up signal transmission. Axons and myelin sheaths are surrounded by endoneurium, orientated collagen fibers and the perineurium, made of flattened fibroblasts and collagen, bundles axons into fascicles. A fibrocollagenous epineurium holds the fascicles and vasculature (artery and vein) together to form a nerve trunk. Nerve damage or injury affects the complete or partial microstructure of the nerve trunk. Hence, when injury occurs to the PNS, it can either be non-degenerative, without axonal loss, or degenerative, involving axonal damage [52]. Seddon classified nerve injuries into three broad categories: neuropraxia, axonotmesis, and neurotmesis, depending on the severity of the damage [52,53]. Segmental

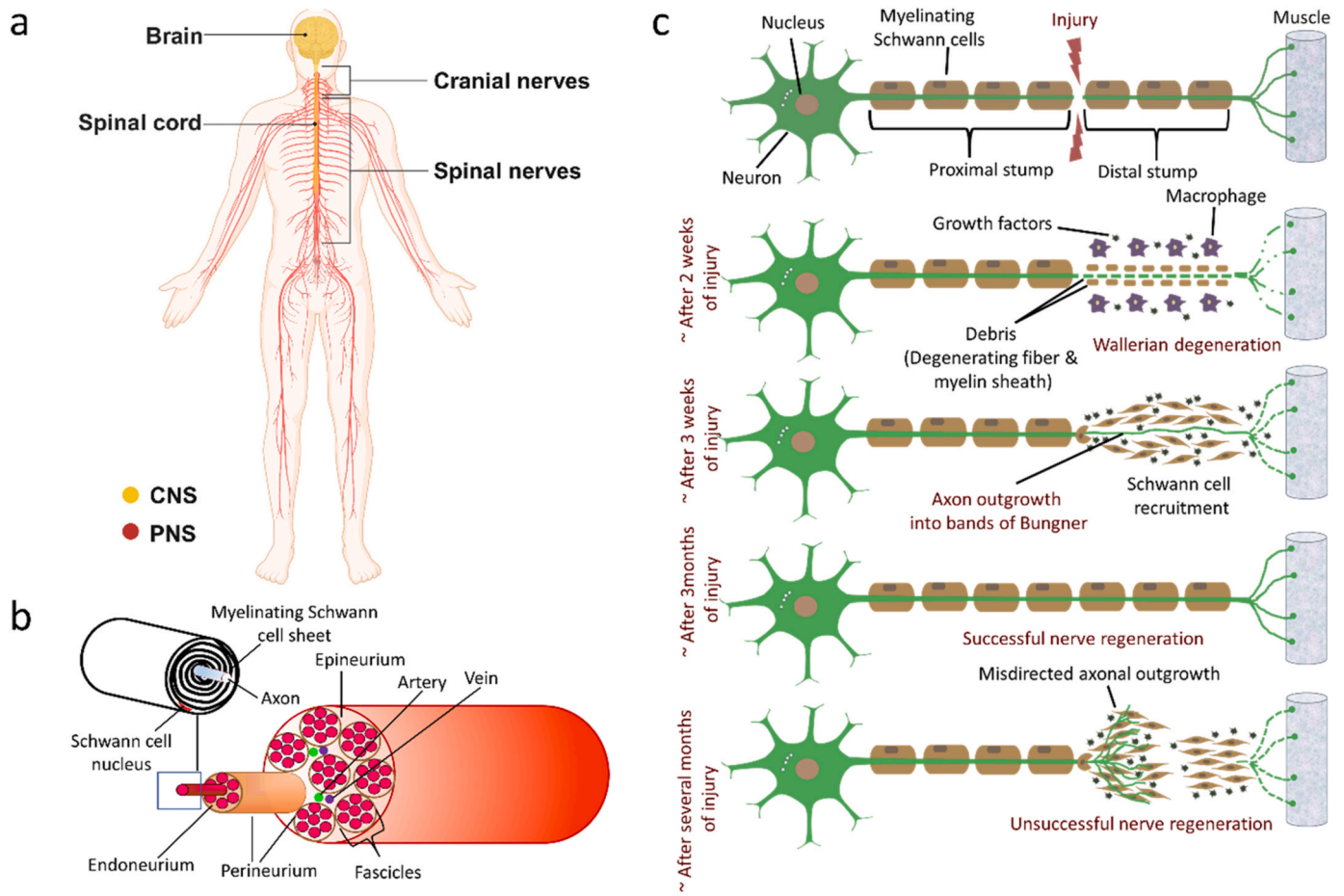

Fig. 1. (a) Human nervous system showing distribution of CNS and PNS. (b) Anatomical structure of peripheral nerve trunk showing the nerve bundles grouped together by connective tissue and vasculature. (c) Schematic illustration of cellular responses at different stages after PNI showing degenerative processes followed by regeneration. *Created with* BioRender.com.

demyelination of axons causes partial or total signal transmission failure in the least severe neuropraxia. When myelin is regenerated, this condition goes away in healthy people. Axonotmesis occurs when the axon is injured but the supporting connective tissue is intact. Axonal regeneration along the myelinating SC sheet from the proximal end restores neuronal activity after distal degeneration or demyelination. The worst injury is neurotmesis, which destroys the nerve trunk and connective tissue and requires surgery. In 1951, Sunderland divided axonotmesis damage into three grades, extending this categorization to five. Mackinnon and Dellon introduced a mixed injury grade with numerous layers [52]. The latest grade of injury type is a mixed one associated with multiple layers of injury, introduced by Mackinnon and Dellon [54].

PNS damage can produce nerve transection, disruption of neuronal transmission and the blood nerve barrier, and inflammatory response with fibrin deposition, fibrosis, scarring, and neurotoxic cytokine release. Axonal constancy breaches cause phenotypic alterations at the lesion site, damaging sensory and motor neurons [55–57]. Wallerian degeneration under protease activity occurs after PNI because the distal end is separated from the neuronal body and has no metabolic resources [Fig. 1(c)]. PNS specific Wallerian degeneration is a well-coordinated morphological and biochemical event at the distal end that clears debris to create a milieu for axon regeneration [58]. Disassemblement of cytoskeleton components, cell membrane breakdown, and distal axonal fragmentation initiate this degeneration process. Meanwhile, SCs lose myelin and along with macrophages, they remove degenerated axons, myelin, and other waste. An array of cellular and molecular activities, including retrograde reactions and chromatolysis, occur in the cell body. Nucleic induction upregulates regeneration-associated genes, which are necessary for axonal regrowth and growth cone formation from the proximal stump [59]. SCs recruited migrate towards injury site and start to proliferate. They provide scaffolding by forming well-orchestrated "Bands of Bunger" to proximal stump-derived regenerating axonal sprouts. Additionally, SCs release neurotrophic growth factors and cytokines that aid axonal regeneration. Recent advances in neuroimmunology have shown that macrophage polarization is essential to PNR [60,61]. Macrophages, which make up 2–9% of peripheral nerve cells, are phagocytic. After an injury, SCs dedifferentiate and express pro-inflammatory cytokines including tumor necrosis factor-α (TNF- α) and Interleukin-6 (IL-6), which activate local macrophages and draw circulating monocytes to the region [60–62]. Pro-inflammatory (crudely denoted as M1) macrophages clear myelin debris, breaking it down into cholesterol and lipid molecules essential for new myelin sheath formation [Fig. 2]. After Wallerian degeneration, macrophages/monocytes gradually polarize to a pro-regenerative macrophage phenotype, aiding nerve regeneration. M2 (pro-regenerative) macrophages secrete vascular endothelial growth factor-A (VEGF-A), promoting blood vessel formation, which allows SCs to cross nerve defects and guide axon regeneration. Of course, macrophages do not exist on a binary scale and a wide spectrum and degree of heterogeneity exist among their populations. A recent study showed that 'M2' polarization enhances SC migration, proliferation, and remyelination, improving sciatic nerve function restoration. The diverse role of pro-inflammatory (M1) and pro-regenerative (M2) is shown in Fig. 2. New axonal sprouts extend until they reach the distal target ideally at 1 mm/day. If they cannot reach the distal target (e.g. muscle), axonal regeneration becomes misdirected leading to neuroma and the denervated muscle fiber becomes

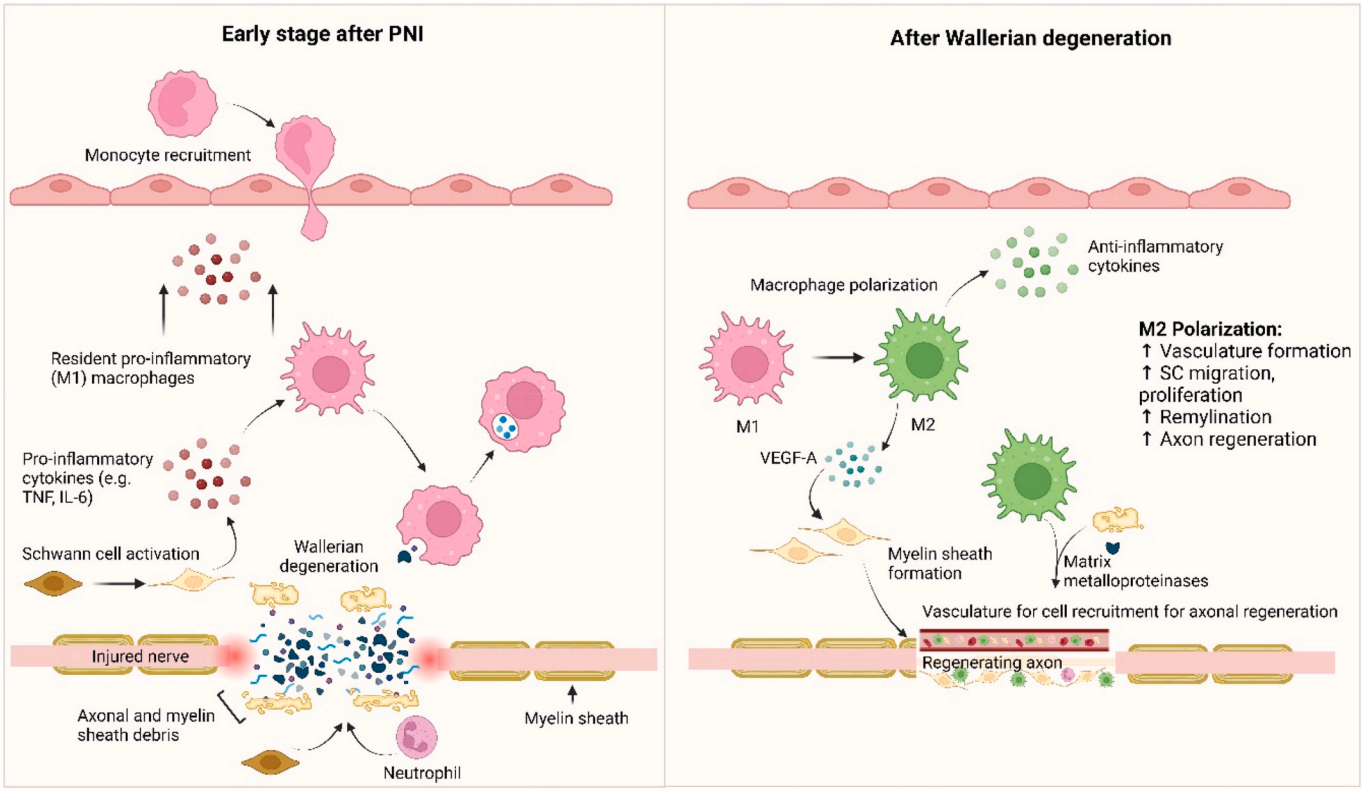

Fig. 2. Schematic illustration of cascade of biochemical events induced by pro-inflammatory (M1) macrophages after PNI in clearing axonal and myelin sheath debris. Subsequent polarization to pro-regenerative (M2) phenotypes after Wallerian degeneration contributes to regeneration of injured nerve by promoting SC migration, proliferation, remyelination and vasculature formation. *Created with* BioRender.com.

atrophic. In case of a severe nerve injury, axonal regeneration becomes more disorganized with additional scarring and end-to-end suturing is not possible. In that case, nerve grafts or nerve guidance channels are needed to bridge the gap between the proximal stump and the distal stump.

3. Impact of electrical stimulation (ES) on nerve regeneration

Bioelectricity plays a pivotal role in normal functioning of our body including movement, cognition, sensation, sight, sensation, blood transportation through our circulatory system and healing of an injury [63]. All biological processes in the body are governed by charge transport phenomena such as transport of ions across the plasma membranes and of electrons along biomolecules. Electrical potentials (−60 mV to −100 mV) exist inside and outside cells. Changes in the transmembrane potential influence cellular functions and continuous electrical signals through neurons are responsible for the internal body function. In case of neurons, a transient change in steady state transmembrane potential, known as resting potential, represents a specific electrical event, termed as action potential and it effects the ion influx through the membrane to condition the intracellular signal transduction pathways through second messengers such as cAMP and Ca^{2+}, which in turn regulate enzyme phosphorylation and gene expression [64]. During an action potential, information is transmitted from one place to another accompanied by a change in the transmembrane potential from negative to positive [65]. This action potential event is involved with several processes, such as depolarization, repolarization and hyperpolarization of cell membrane. For a typical nerve cell, the resting potential of the interior of a cell is −70 mV and the membrane starts to depolarize when the interior potential is drawn to −55 mV, leading to opening of Na^+ channels. When the ion influx through the Na^+ channels propel the interior potential to +30 mV, the membrane becomes completely depolarized [Fig. 3] [66]. Subsequently, the membrane begins to repolarize towards its resting potential by the opening of K^+ channels. However, during the process of a signal transmission, the repolarization process goes past the resting potential and peaks to approximately −90 mV. At this point, the membrane becomes hyperpolarized and prevents the neuron receiving additional stimulus. It also prevents any stimulus sent to an axon from inducing another action potential in the reverse direction, ensuring unidirectional signal transduction. After hyperpolarization, the membrane attains the resting potential. It has been documented that for inducing a brief action potential of ~1 ms, the membrane must be depolarized by ~10–20 mV [67].

Several theories and hypotheses regarding the effect of intervening electrical signals and its impact on the development and organization of nervous system have been put forward by scientists since 1891 [68], with the first reported by Ingvar in 1920 to experimentally demonstrate the effect of external ES on the orientation of chick nerve growth along the electrical field lines of action [69]. Later, several studies not only confirmed this but also reported that neurites facing the cathode grew several times faster than those facing the anode under a steady direct current (DC) electric field [68,70,71]. Since then, the clinical success of ES in cochlear and visual prosthetics, and deep brain stimulation for managing neurological disorders e.g. Parkinson's disease, epilepsy, and dementia; has been established [72]. Given the prominent electrical activity of neurons, there is an obvious growing interest among research communities in utilizing external electrical signals to manipulate the electrical environment of the nervous system in order to achieve efficient regeneration of a damaged nerve.

ES modulates cellular responses via a sophisticated and intricately interconnected network of cellular mechanisms that are precisely designed to convert external electrical signals into cellular actions via receptor-based cell signaling. Tailored ES parameters can induce functional tissue repair with a higher degree of efficiency than conventional

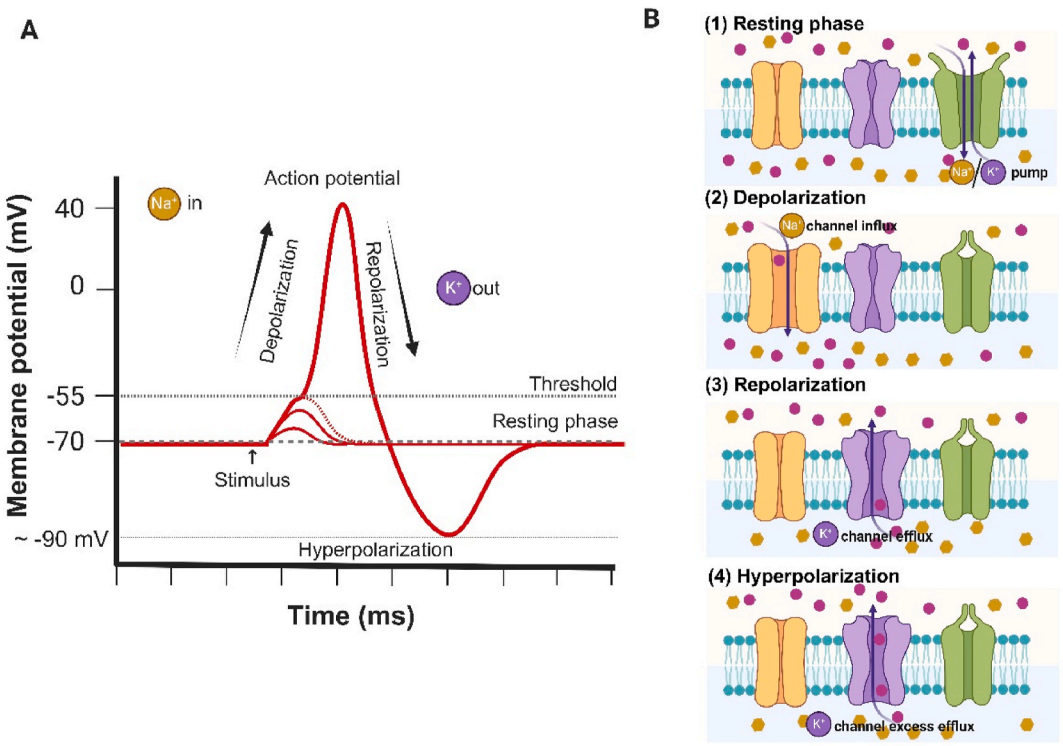

Fig. 3. Scheme of membrane polarization processes of a neuronal cell leading to the generation of an action potential. (A) The action potential graph shows changes in membrane potential over time, including the resting phase (~−70 mV), depolarization due to Na^+ influx, repolarization from K^+ efflux, and hyperpolarization (~−90 mV) caused by prolonged K^+ channel activity. (B) Schematic representation of ion channel states during the four phases: (1) Resting phase with Na^+/K^+ pump maintaining resting potential, (2) Depolarization with Na^+ channels open, (3) Repolarization with K^+ channels open, and (4) Hyperpolarization due to excess K^+ efflux. *Created with* BioRender.com.

existing tissue engineering options, contingent upon the specific cell types. More details regarding general cellular responses under electrical signals can be found elsewhere [20,73–76]. A variety of cellular responses, such as proliferation, differentiation, apoptosis, cytoskeleton reorganization, and axonal growth, can be induced by ES-mediated cascades of intricate molecular events. ES induces an asymmetric redistribution of charged receptors on the cell membrane, activating signaling cascades such as mitogen-activated protein kinases (MAPK), which regulate transcription of specific mRNAs and molecular pathways including extracellular signal-regulated kinases (ERK), p38 MAPK, and phosphatidylinositol-3 kinase (PI3K), driving various cellular processes like neurite outgrowth in nerve cells [Fig. 4]. Patel and Poo, 1982 were one of the first to document an increase in neurite length of single dissociated *Xenopus* neurons under a steady electric field [77]. They hypothesized that ES acted directly in the cell body by altering the potential of cytoplasm, which in turn may induce electrophoretic distribution of cytoplasmic materials important for axonal growth. Further, ES acting along plasma membrane can aid electrophoretic accumulation of surface molecules that promote neurite adhesion and outgrowth. ES can also change the membrane potential through depolarization, thereby activating growth controlling transport processes across the plasma membrane. ES directly influences ion dynamics by promoting Na^+ influx and K^+ efflux, while increasing intracellular Ca^{2+} levels via plasma membrane ion channels and calcium release from endoplasmic reticulum stores. This release of intracellular Ca^{2+} has been shown to activate cyclic adenosine monophosphate (cAMP) cAMP, boosting adenosine triphosphate (ATP) production and driving cAMP response element-binding protein (CREB)-mediated transcription, which is critical for facilitating enhanced nerve regeneration [51] [Fig. 4]. This is also supported by the evidence of direct current stimulation enhancing ATP production by directing proton migration towards mitochondrial H1-ATPases [78], which is essential for cytoskeletal reorganization and related cellular processes [79]. Additionally, ES can induce G-protein-coupled receptors (GPCR) activation for phospholipase C (PLC) mediated synthesis of inositol 1,4,5-trisphosphate (IP3) and diacylglycerol (DAG), which in turn induce endoplasmic reticulum to release its stored Ca^{2+} [76,80]. ES can significantly enhance the intracellular electrical and metabolic signaling between cells via mediating cell gap junctions and promoting transfer of signalling molecules like Ca^{2+}, K^+, cyclic nucleotides, and inositol phosphates, like IP3 [81]. Another possible mechanism is the emergence of endogenous currents at the filopodial tips of growth cones carried by Ca^{2+} ions, which play a significant role in neuronal growth including vesicle fusion into growing membranes and aligning actin and myosin fibers [82]. Other important effects of the induced Ca^{2+} current include the release of neuromodulators and hormones, tubulin polymerization for microtubule formation and protein phosphorylation, thereby contributing towards assembly and molecular organization of the growing nerve. Thereafter, a series of studies followed to elucidate the effect of ES on nerve regeneration at a molecular level, which found upregulation of various growth factors and regeneration associated genes both in neurons and supporting cells. ES has been shown to activate voltage gated calcium channels (VGCCs) to induce increased intracellular calcium production in SCs, which leads exocytosis of nerve growth factor (NGF) [83,84]. ES mediated Ca^{2+} influx plays a crucial role in F-actin polymerization at the growth cone of a regenerating axon [85]. Ca^{2+} signalling activates protein kinase C (PKC), a calcium-dependent kinase, which subsequently triggers the MAPK signalling pathway and promotes neuronal growth [Fig. 4] [86]. This pathway, comprising key cascades such as ERK1/2, Jun amino-terminal kinases (JNK1/2/3), p38-MAPK, and ERK5, are responsible for regulating various cellular behaviours by modulating specific mRNA transcription in response to ES [76]. The Ras-Raf-MEK-ERK pathway, part of the MAPK family, facilitates proliferation and differentiation, whereas the JNK route, triggered by

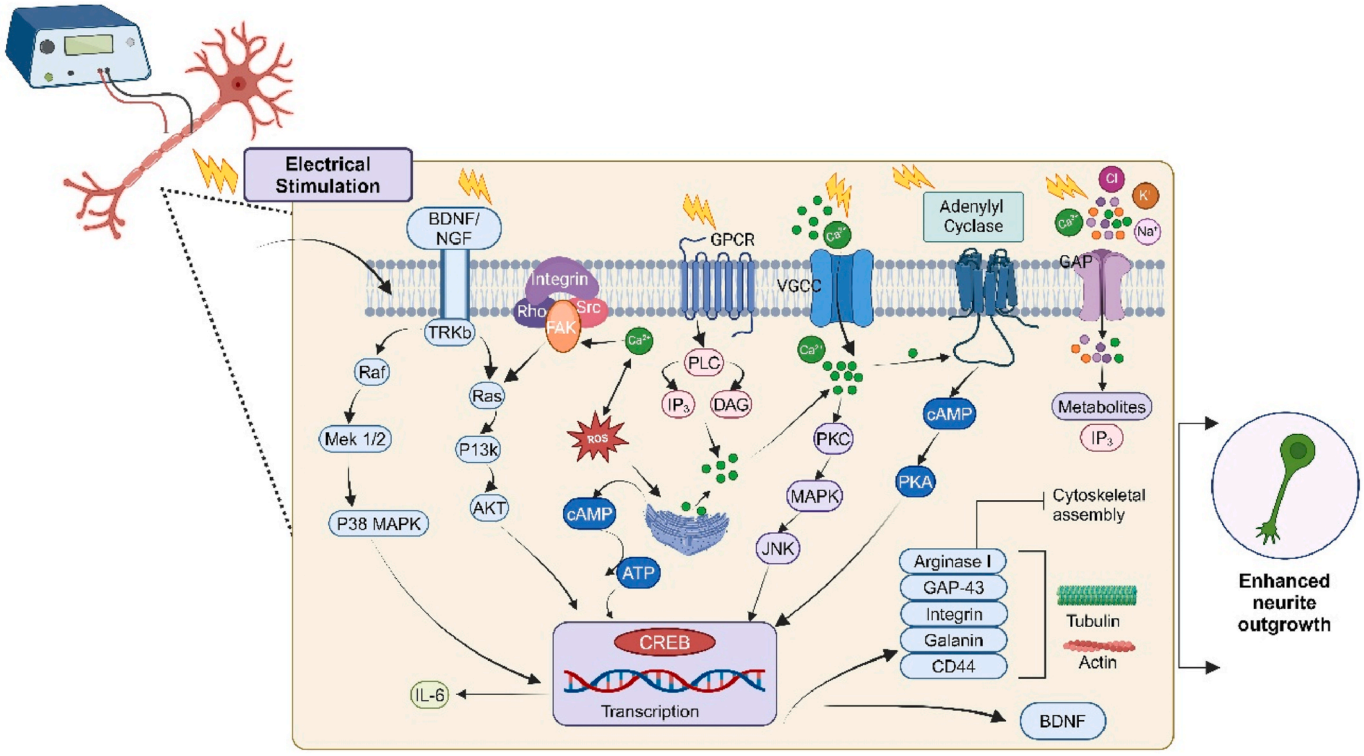

Fig. 4. Molecular pathways associated with ES mediated enhanced nerve regeneration, as reported in previous studies. ES upregulates BDNF and its receptor TRKb by elevating intracellular cAMP levels through the activation of VGCCs. Activation of TRKb initiates the Ras-MAPK (Raf-MEK1/2-ERK) and PI3K/AKT signaling cascades, promoting transcription factor CREB activity, which regulates the expression of genes like Arginase I, GAP-43, integrins, and CD44, essential for axonal growth and cytoskeletal reorganization. ES also enhances intracellular Ca^{2+} signaling via VGCCs, activating PLC to synthesize IP_3 and DAG, and also activates PKC and MAPK signaling cascades. This triggers JNK and p38 MAPK pathways, further supporting cellular responses such as cytokine modulation (e.g., IL-6) and cytoskeletal assembly. Additionally, adenylate cyclase is activated, producing cAMP and further stimulating PKA, contributing to CREB-mediated transcription. ES activated FAKs promote cytoskeletal dynamics and promoting cellular migration and axonal guidance. ES also effects cell gap junctions (GAP) promoting intracellular metabolic signaling, which influence cytoskeletal assembly and metabolic activity. Collectively, these pathways orchestrate cellular responses that enhance neurite outgrowth, axonal guidance, and nerve regeneration. *Created with* BioRender.com.

intermediates such as Rac1 or PKC, regulates stress responses, apoptosis, and inflammation. ES has also been demonstrated to upregulate expression of glial cell line-derived neurotrophic factor (GDNF), brain-derived neurotrophic factor (BDNF) and their receptor tyrosine kinase B (TRKb) for accelerated axonal growth [87–90]. These neurotrophic factors elevates the gene expression of various regeneration associated proteins such as actin, tubulin, galectin-1, growth associated protein-43 (GAP-43), and neurotrophin-4/5 (NT-4/5). Elevated intracellular neuronal cAMP further promotes of transcription of regeneration associated proteins by activating PKA and CREB for increased cytoskeletal protein production as discussed [91,92]. Elevated BDNF expression also inhibit phosphodiesterase by preventing cAMP degradation. ES mediated p38 MAPK pathway is critical for neurite outgrowth via CREB activation, as p38 MAPK inhibition downregulates both CREB activity and neurite outgrowth [93]. In addition, ES also stimulates focal adhesion kinase (FAK) through increased intracellular Ca^{2+} level, leading to stimulation of MAPK signalling and P13/Akt pathway for CREB activation [Fig. 4] [76,80]. All these ES mediated processes ultimately induce accelerated axonal regeneration in PNS, which is summarized in Fig. 4.

Beyond the direct impact on neurons, ES influences interleukin-6 (IL-6) production, which plays dual roles at different phases of PNI. In the early phase, increased IL-6 expression fosters an inflammatory environment that aids in clearing axonal debris, while in the chronic phase, controlled ES induces transient IL-6 expression, which supports SC proliferation and enhances the secretion of neurotrophic factors such as NGF and GDNF [92,94,95]. ES also upregulates angiogenic factors such as VEGF and IL-8 for enhanced blood vessel formation [96], which then helps in the axonal growth as mentioned in the previous discussion. Additionally, moderate levels of reactive oxygen species (ROS), elevated via Ca [2]⁺ signalling during ES, activate MAPK cascades (ERK1/2, JNK, and p38), likely through miR-210 activation, facilitating proliferation and differentiation [76,80,97,98]. ROS also help control the immune system by working with myeloid-derived suppressor cells to stop the immune system from overreacting [99].

Given the essential role of macrophages in clearing tissue debris and promoting repair after PNI, it is clear that modulating the immune microenvironment can enhance functional nerve regeneration [100]. While the pro-inflammatory response is crucial for phagocytosing axonal and myelin debris to create a path for axonal regrowth, excessive inflammation can hinder repair. Elevated levels of inflammatory proteins and ROS can lead to muscle atrophy and impair locomotor function after PNI [76,93]. Therefore, timely activation of pro-regenerative functions of macrophages, by promoting their polarization to a regenerative M2 phenotype, is critical for supporting nerve repair and reducing inflammation. The endogenous electric field generated after injury has been shown to play a key role in recruiting various cell types, including circulating immune cells, to regulate the local microenvironment and trigger an anti-inflammatory response to initiate healing [101–104]. The role of ES in macrophage polarization or regulation of inflammation for bone tissue engineering has been reviewed by others [76,105,106]. However, the precise role of ES in the context of PNR through immunoregulation is limited. There is also a limited understanding of the impact of ES on macrophage behaviour currently. However, some past studies have shown that the use of ES can lead to the polarization of macrophages towards the M2 phenotype, thereby

enhancing their ability to promote wound healing and osteogenesis [105–110]. Most of such studies are limited to murine or J774A.1 macrophages and THP-1 cell lines. Recently, Gu et al. showed that ES promoted M2 polarization of mouse bone marrow derived macrophages by upregulating IL-4Rα and toll-like receptor 4 (TLR4) receptors, which activates ion channels like transient receptor potential cation channel subfamily member 7 (TRPM7), which in turn activates signal transducer and activator of transcription 6 (STAT6) pathway [Fig. 5] [106]. Hu et al. showed that ES through a MXene/SF hydrogel enhances M2 polarization by upregulating M2 markers such as CD206 and F4/80 and improving macrophage infiltration potential compared to other conditions such as IL-4 treatment or only material-based interventions for bone regeneration [111]. Similarly, Li et al. showed that ES through graphene oxide based scaffolds mediates M2 polarization through key signalling pathways, including the RhoA/ROCK pathway, which upregulates Cdc42, Rac1, and ROCK while suppressing hypoxia-inducible factor-α (HIF-α) protein synthesis and TNF signalling [112]. ES also inhibits pro-inflammatory MAPK/JNK cascades, promotes ATP synthesis, and maintains an intact tricarboxylic acid (TCA) cycle, essential for oxidative phosphorylation and M2 polarization [113].

A few studies also report increased M1 polarization due to elevated Ca $[2]^{+}$ signalling, which activates the NF-κB phosphorylation [Fig. 5] and its translocation into the nucleus, where it facilitates the transcription of pro-inflammatory cytokines such as TNF-α and IL-1β [114]. Such approaches might be useful in early phase of injury for debris removal from the injury site and creating space new tissue growth or axonal sprouting, while ES can further be optimized to downregulate pro-inflammatory behaviour to create reparative microenvironment. This is supported by the study reported by Yan et al., who showed ES mediated downstream PI3K and NF-κB signaling pathways, reducing M1-type polarization while promoting the M2 phenotype [Fig. 5] [115]. Dai et al. also demonstrated localized ES through a $BaTiO_3$/P(VDF-TrFE) piezoelectrical scaffold downregulated the P13K-Akt2-IRF5 signalling pathway, reducing pro-inflammatory responses and promoting glycolysis and HIF-1α-mediated processes associated with M2 macrophage polarization [Fig. 5] [116]. Another study showed that elevated intracellular Ca^{2+} due to ES activates transforming growth factor β (TGF-β) receptor, which subsequently phosphorylates SMAD2. The phosphorylated SMAD2 forms a complex with SMAD4, which activates regulates the transcription of M2-associated genes such as Arg1 and IL-10 in the nucleus [117]. ES downregulates the proteins like Tab2 and TRAF6 to prevent TLR signalling components, thereby reduces inflammation and further supporting M2 polarization [Fig. 5]. Li et al. showed that by effectively manipulating the ATP-sensitive potassium (KATP) channels through membrane polarization, macrophage phenotype can be fine-tuned, for instance inducing M2 polarization and creating an immunosuppressive and reparative microenvironment [118]. However, further detailed investigations are needed to fully understand the underlying mechanisms of ES-driven immunomodulation, which is crucial for enhancing the therapeutic efficacy of this approach in PNR. Although numerous electroactive biomaterials have been explored to influence macrophage behaviour, ECP-based biomaterials have rarely been dedicated for immunomodulation. A recent study, however, demonstrated the use of a PEDOT-based conductive piezoelectric nerve conduit to regulate the immune microenvironment by activating the PI3K/AKT-Nrf2 signalling pathway [Fig. 5] [100]. This approach promoted macrophage polarization toward the anti-inflammatory M2 phenotype and supported the repair of the rat sciatic nerve. Owing to the piezoelectric nature, self-generated electricity was proposed to activate the M2 polarization in vivo, facilitating repair process. This highlights

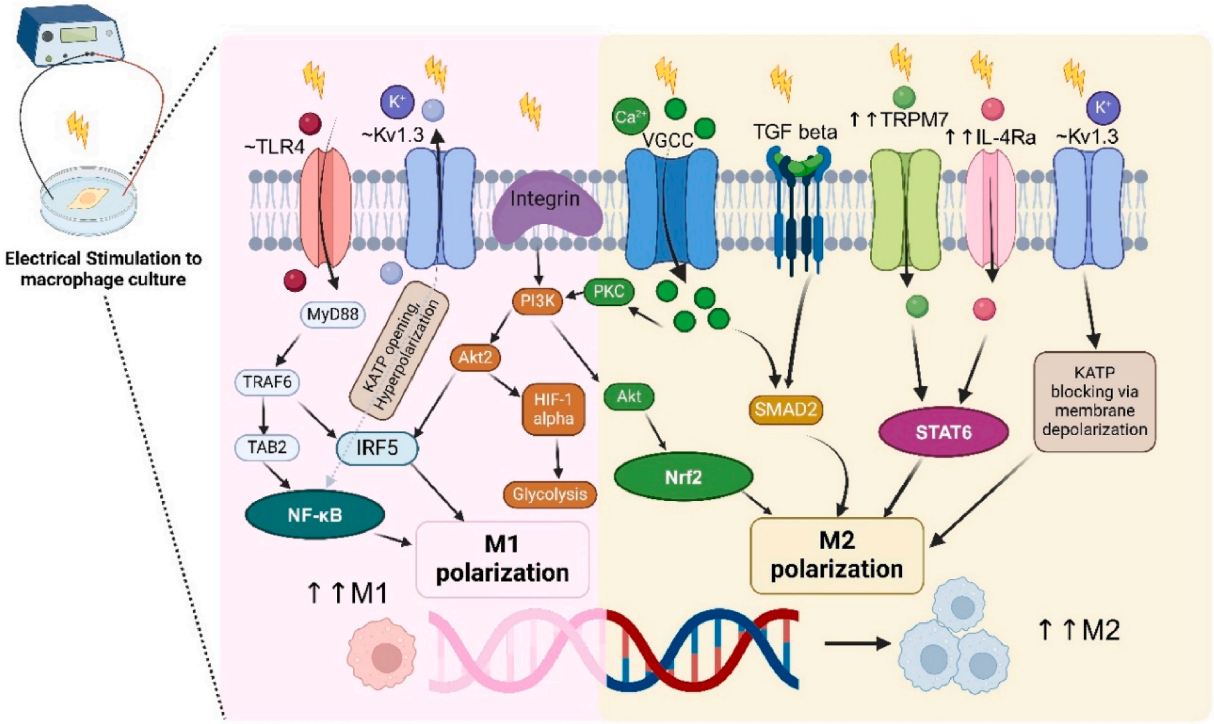

Fig. 5. Molecular pathways of macrophage polarization under the effect of ES, as proposed by previous studies. ES influences macrophage polarization by modulating ion channels, signaling pathways, and receptor activity. For M1 polarization, ES upregulates TLR4 activity, activating Kv1.3 potassium channels and increasing MyD88-dependent signaling through TRAF6 and Table 2, ultimately leading to NF-κB activation and downstream pro-inflammatory gene expression. Concurrently, Akt2 and HIF-1α pathways promote glycolysis, supporting M1 metabolic activity. In contrast, ES facilitates M2 polarization by activating TRPM7 ion channels and IL-4Rα, triggering the STAT6 pathway to enhance anti-inflammatory gene expression. ES mediated Ca^{2+} levels stimulate PKC and PI3K signaling. This promotes Akt and Nrf2 pathways for antioxidant and anti-inflammatory responses. Additionally, ES enhances TGF-β signaling to activate SMAD2, further driving M2 polarization. Blocking KATP channels via membrane depolarization also promotes M2 polarization by preventing hyperpolarization-associated M1 pathways. These mechanisms together regulate macrophage behavior and shift polarization based on the microenvironment and injury stage. *Created with* BioRender.com.

the potential of ECP based scaffolds to modulate the local immune microenvironment while simultaneously providing neuronal stimulation through ES.

4. Electrically conductive polymers (ECPs)

ECPs are a relatively recent class of organic polymers that merge the electrical, magnetic, and optical properties of metals and semiconductors with the mechanical properties of traditional polymers. Unlike conventional polymers or those blended with conductive materials, ECPs have a unique structure featuring alternating single and double bonds along a highly conjugated backbone, enabling efficient electron mobility and high electrical conductivity [119]. ECPs possess conductivities of 1–10^3 S/cm, while typical insulating polymers have 10^{-20} to 10^{-6} S/cm [120]. The first reference to the synthesis of ECPs was noted by Letherby in 1862, who observed the anodic oxidation of aniline in sulfuric acid forming a deep-blue powder [121,122]. Despite this early discovery of this material known as "aniline black" at that time, it was initially overlooked due to a lack of understanding regarding ECPs [123]. The breakthrough came between 1973 and 1975 with the discovery of the electrical properties of poly(sulfur nitride) (SN)x [121,123]. In 1976, Alan MacDiarmid, Hideki Shirakawa, and A. J. Heeger enhanced polyacetylene's conductivity by 10 fold by doping it with bromine and iodine, earning them the Nobel Prize in Chemistry in 2000 [124,125]. The electrochemical synthesis of conductive polypyrrole (PPy) films began in 1979 by Diaz et al. [126] Concurrently, Heeger reported ECPs synthesized through chemical and electrochemical redox processes having relatively higher electrical conductivities [127]. The flexibility of tuning conductivity of ECPs during oxidation has since drawn great scientific interest. Various ECPs like polyacetylene (PA), polypyrrole (PPy), polyaniline (PAni), polythiophene (PT), poly(3,4-ethylenedioxythiophene) (PEDOT), poly(p-phenylenevinylene) (PPV) and its derivatives, have been successfully synthesized. These materials have been extensively studied and applied in several critical areas such as optoelectronics such as organic light-emitting diodes and field-effect transistors [128,129], energy storage devices such as supercapacitors [130,131] and solar cells [132,133], electromechanical actuators [134,135], electronic textile [136,137], and anticorrosive coatings [138,139] to name but a few.

The electrical conductivity of ECPs is aided by intrinsic conjugated alternating of double bonds and doping [140]. In ECPs, the polymer backbone's conjugated alternate single-double carbon-carbon or carbon-nitrogen bonds distinguish ECPs from other insulating polymers [Fig. 6(a)] [141]. The backbone of ECPs has a strong 'sigma' (σ) bond

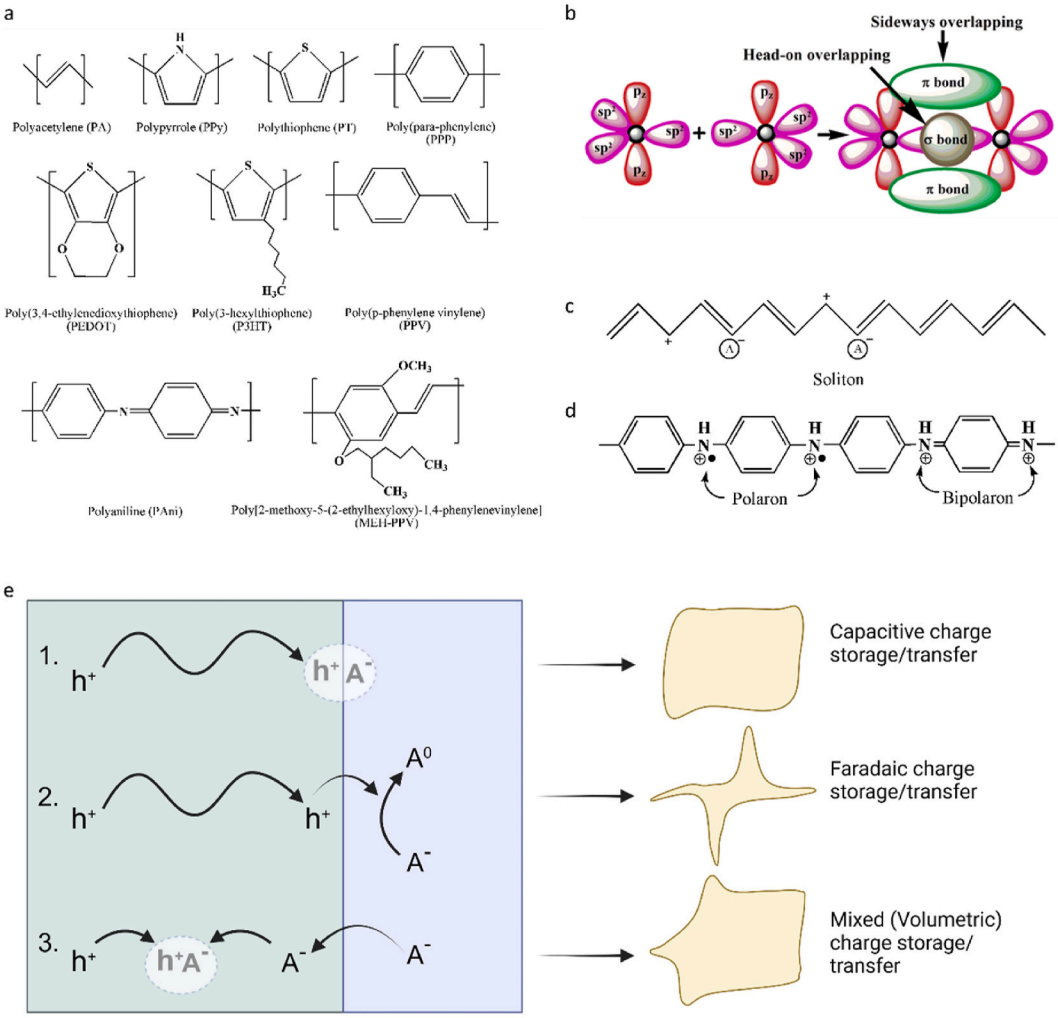

Fig. 6. (a) Molecular structures of some of the widely used ECPs for biomedical applications. (b) Schematic illustration of the formation of σ and π molecular orbitals from two sp^2 hybridized carbon atoms in ECP; sideways overlapping of p_z orbitals results in π electron cloud for electron delocalization. Charge carrier formation in the polymer backbone of ECPs showing (c) soliton in PA and (d) polaron & bipolaron in PAni. (e) Schematic of mixed ionic-electronic electroactivity in ECPs in presence of electrolyte (or biological fluid) showing capacitive/electric double layer capacitance (EDLC) charge, Faradaic charge and volumetric (mixed) charge transfer.

and a weaker 'pi' (π) bond with sp^2 hybridized atoms. Fig. 6(b) depicts sp^2 hybridized carbon atoms with 1 s and two p-orbitals, resulting in one unpaired electron (π electron) per atom. Overlapping out-of-plane p_z orbitals form a π-band, causing electron delocalization on the polymer backbone. One unhybridized p_z orbital remains unaffected when the 2s orbital hybridizes with two 2p orbitals, creating three sp^2 hybridized orbitals. The unhybridized p_z orbital is perpendicular to the hybridized orbitals, while the sp^2 hybridized orbitals are coplanar with 120° angles. The hybridized orbitals along the nuclear axis form strong σ (sigma) bonds, forming polymer chains, while the p_z orbital perpendicular to the chain plane overlaps laterally with another carbon atom to form π (pi) bonds [Fig. 6(b)]. Delocalization of electron clouds in the π (pi) bond enables charge mobility in polymer chains and between adjacent chains. The characteristics of the π band significantly impact the semi-conducting or metallic behaviour of ECPs.

ECPs are intrinsically insulators even with conjugated alternating double bonds, so they must be doped with simple anionic or cationic chemical species to conduct electricity. Interstitial doping in ECPs differs from substitutional doping in inorganic semiconductors [142]. Doping in ECPs is a charge transfer reaction that partially oxidizes (or reduces) the polymer, a reaction which is reversible. Doping can change the conductivity of an insulating or semiconducting polymer from 10^{-10}-10^{-5} S/cm to ~1–10^4 S/cm in the metallic regime. Doping causes loosely bound conjugated system electrons to jump around the polymer chain. The unique bond conjugation in CP's backbone delocalizes electrons, allowing many atoms to share them. Thus, delocalized electrons carry charges, making the polymer conductive. Indeed, charge delocalization alters ECP band structure, creating localized defects like polarons, bipolarons, solitons, and defect bands [Fig. 6(c&d)] [143]. Electrons can then be removed or added to create cations or anions, which can hop between polymer chain sites under an electrical field, thereby increasing the polymer's conductivity. Thus, these spatial defects (polarons, bipolarons, and solitons) act as regular charged particles in ECPs giving rise to its electrical conductivith property. However, it is entirely different from delocalized electrons in highly ordered lattices in metallic conductors. When a charge (electron or hole) is inserted into the polymer backbone of ECPs through a doping process, it changes their energy state. As ECPs are soft organic materials, the polymer chain can adjust its spatial configuration to a more energetically preferred alignment, causing a local distortion in the soft polymer chain at microscopic level coupled with the inserted charge [144]. A large collection of such spatial distortions or charge carriers (i.e., polarons, bipolarons, and solitons) collectively contribute to structural or volumetric change (due to charge insertion) in ECP based materials under the effect of an external electrical field at macroscopic level. Additionally, the volumetric swelling or shrinkage of ECPs are well documented when under a potential sweep due to electrochemical doping or dedoping process (reversible insertion/extraction of electrolyte ion), a characteristic which also makes it highly ion permeable [145]. This type of unique behaviour of ECPs are distinct whereby ECPs can interact chemically with the electrolyte ions through their intrinsic redox behaviors, in contrast to EDLC materials that undergo ion accumulation through physical adsorption [146–148]. In fact, due to their ion permeability and reversible oxidation/reduction behaviour, ECPs have been demonstrated to exhibit both electronic and ionic conuductive behaviour [discussed in subsequent Section 5] [44,45,149]. The "Intelligent material" term given to ECPs has been thus become more justified as they can engage more effectively with physiological events or any changes in local microenvironment by virtue of their mixed ionic & electronic conductive properties. This has also led to excellent electrical conductivity of ECPs in physiological environment, for instance, PEDOT:PSS hydrogels have shown conductivity of ~40 S/cm and ~20 S/cm in deionized water and phosphate buffer solution (PBS), respectively [149]. The same study showed a negligible decrease in conductivity (<10 %) after 3 months of incubation in PBS and water. Shi et al. also showed ~15 % conductivity retention of PPy/PDLLA composite after 1000 h of incubation in cell culture media [150]. Other studies have investigated electrolyte ion exchange properties using electrochemical techniques with ECPs such as PPy [151] and PAni [152] through oxidation (current increases) and reduction (current decreases), which evidence ion movement in and out within the polymer matrix with no indication of ion accumulation. Key properties of ECPs along with their limitations and applications are summarized in Table 1.

5. ECPs in peripheral nerve repair (PNR)

Over the last two decades, ECPs have transformed the development of electroconductive biomaterials and soft bioelectronics, owing to their flexibility and processability akin to traditional polymers, as well as their excellent electrical conductivity comparable to metals and semiconductors. Advancing research in tissue engineering and regenerative medicine consistently seeks to develop biomaterial scaffolds that can replicate the dynamic microenvironment of native tissue by mimicking the composition and topography of the natural ECM. The presence of electromotive forces in living tissues, which drives potential differences, controls current flow, and stores charge, has sparked a significant interest in electroconductive biomaterials [63]. In this context, ECP-based biomaterials provide added functionality by enabling ES of cells, which is advantageous for promoting regenerative processes in various stimuli-responsive cells, such as neurons and cardiomyocytes [153]. ECPs possess good optical properties, a high conductivity-to-weight ratio, the ability to entrap and controllably release biological molecules through reversible doping, and can transfer charge from biochemical reactions [154]. Their electrical, chemical, and physical properties can be easily modified for specific applications. ECPs can also be made biocompatible, biodegradable, and porous, with their properties further adjustable even after synthesis through external stimuli such as electricity, light, or pH [153]. Thus, several ECPs such as PPy, PT, PAni and PEDOT have been shown to effect positively various cellular activities including cell adhesion, proliferation and migration, DNA synthesis and protein secretion both in vitro and in vivo. Given the potential advantages, ECPs have been explored for various tissue engineering applications including nerve [155,156], bone [157,158], cardiac [159,160], muscle [159,161] and skin tissue engineering [162,163].

As discussed in the preceding sections, the beneficial effects of ES on nerve growth and importance of guiding neural scaffold, has inspired the utilisation of electrically conductive materials in the fabrication of NGCs. Due to their versatility in processing into various scaffold formats while maintaining electrical conductivity for efficient signal transmission to and between cells, ECPs have been utilized in the fabrication of neural scaffolds, such as NGCs, to stimulate cells or tissues for accelerated nerve regeneration. ES has facilitated the release and uptake of negative and positive ions by the polymer, the electrophoretic redistribution of cell surface receptor proteins, and the adsorption of cell adhesion molecules like fibronectin onto ECP based biomaterials, thereby accelerating neurite outgrowth [164]. When delivering ES to cells or tissues, ECP based biomaterials or bioelectronic interfaces stand out from other electroconductive biomaterials like piezoelectric materials, carbon nanostructures, and metals due to their ability to offer mixed ionic-electronic charge transport and reversible redox behaviour [26,44,45,151,152]. ECP based biomaterials are superior to the carbon based nanomaterials in terms of their flexibility, while choice of piezoelectric materials are limited. ECP based biomaterials allow for localized stimulation around the polymer, offering precise control over the level and duration of ES, in contrast to directly applied electrical signals. Uncontrolled ES can cause cells to depolarize recklessly, which can malfunction neuronal voltage-gated channels and elicit neuronal excitotoxicity and death. Numerous studies have also emphasised the significance of an efficient and secure ES that can be accomplished by employing ECPs with high charge density and charge-transfer efficiency to stimulate cells and tissues at low stimulation potentials [165]. ECPs

Table 1
Key properties of some commonly used ECPs and their limitations including their major biomedical applications (Refs. 140–143).

ECPs	Key properties	Synthesis Methods	Demerits	Biomedical applications
PPy	High conductivity with tunability, High stability in air, Stable redox state, Biocompatibility, Ease of synthesis and Surface modification, Can be doped with biomolecules	Electrochemical polymerization, Chemical oxidative polymerization	Poor solubility, Brittle, No biodegradability	Biosensors, Drug delivery, Tissue engineering, Neural interface, Bioactuators
PAni	High conductivity with tunability, Diverse structural forms and oxidation states, Environmental stability, Redox stability, Biocompatibility, Can be doped with biomolecules	Electrochemical polymerization, Chemical oxidative polymerization	Poor solubility, Poor processability, Poor biodegradability	Biosensors, Drug delivery, Tissue engineering, Neural interface, Bioactuators
PT	High conductivity, Biocompatibility, High doping levels, Good optical property	Electrochemical polymerization, Chemical oxidative polymerization	Instability in air, Poor solubility, Poor processability, No biodegradability	Biosensors, Tissue engineering, Neural interface
PEDOT	High conductivity (mixed electronic & ionic) and transparency, Excellent redox stability in biological environment, High charge-transfer efficiency, Biocompatibility, Easy post-synthesis modification, Can be made water dispersible	Electrochemical polymerization, Chemical oxidative polymerization	Poor biodegradability	Biosensors, Drug delivery, Tissue engineering, Neural interface
P3HT	Good solubility, Optoelectronic property, Biocompatibility	Electrochemical polymerization, Chemical oxidative polymerization	Poor biodegradability	Biosensors, Drug delivery, Tissue engineering, Neural interface
MEH-PPV	Good solubility, Easy processing, Electroluminescent properties, High density of holes-traps, Biocompatibility,	Chemical polymerization of vinylene monomers, precursor route, soluble derivatives for processing	Low conductivity Complex synthesis, Low mechanical strength,	Biosensors, Bioimaging, Tissue engineering

are capable to transport both holes and ions when sufficiently hydrated or when in contact with biological tissue [45]. Ions from an electrolytic medium can be injected into the ECP matrix during an electrochemical process, which can induce electrostatic interactions in the bulk of the polymer and thereby, modulate its conductivity, through a process called volumetric electrochemical doping [Fig. 6(e)] [25,44]. Biological tissues, such as nerves and muscles, communicate and function using a combination of ion and electronic signals. Therefore, as a mixed ionic and electronic conductor, ECP based biomaterials enables a more seamless integration with biological tissues. Due to their high trans-conductance, ECP based biomaterials can translate the electron flow into the ion flow in the tissue, which is crucial for evoking action potential in neurons. ECP-based biomaterials exhibit increased charge transfer efficiency, enabling membrane depolarization at low, tissue-safe stimulation voltages, along with superior charge transfer resistance (R_{ct}). The charge storage capacity (CSC), or available charge density within a voltage range, should be high to ensure that there are enough charges available for membrane depolarization during ES. ECP-based biomaterials allow charge/current injection via capacitive and faradaic mechanisms. Conventional capacitive neural electrode materials (such as titanium nitride (TiN), tantalum/tantalum oxide, and so on) store and transfer charge by charging and discharging the electrode-electrolyte double layer. While these reactions are stable and do not produce chemical species during ES, they reduce charge density, limiting the ability to achieve high charge-injection capacity. Mixed ionic and electronic conductors, like ECPs offer charge storage capacity through intrinsic redox reactions at the electrode-electrolyte interface, as well as electrostatic interactions via volumetric doping. They enable efficient electron and ion transport during ES, reducing the stimulation threshold, lowering power consumption, and supporting the possibility of minimally invasive stimulation, which is critical for long-term nerve implants. The following sections summarize the most recent research and developments using the various ECP based biomaterials for peripheral neural tissue engineering applications, with a focus on identifying specific polymer compositions, scaffold design, appropriate ES methods/parameters used, and the nature of the study, whether in vitro or in vivo.

5.1. Polypyrrole (PPy)

Because of its ease of synthesis and exceptional electrical conductivity, PPy is extensively researched in tissue engineering. It has excellent electrochemical and conductive properties, as well as biocompatibility, both in vitro and in vivo [156], and can be synthesized usually chemical polymerization and electrochemical methods [166]. Furthermore, PPy can easily incorporate anionic biomolecules into its structure, which improves its biocompatibility and potential for use in tissue engineering [5]. Thus, PPy allows for easy conjugation with negatively charged biologically active molecules, which increases its utility in this field [166].

Schmidt et al. were among the pioneers in evaluating the use of PPy in conjunction with ES to promote the growth of neurites in PC12 cells [26]. They tested an electrochemically synthesized poly(styrene sulfonate) (PSS) doped PPy thin film to culture PC12 cells with 100 mV ES for 2 h, resulting in a twofold increase in neurite length compared to the unstimulated group. Additionally, a 2-h constant current stimulation of 10 mA led to greater neurite growth compared to the unstimulated group. The study also demonstrated a minimal immune response in adult male Lewis rats after two-weeks implantation. In a subsequent study, Kotwal et al. found that ES of PC12 cells grown on PPy film at 10 mA for 2 h increased fibronectin adsorption, which favored longer neurite outgrowth [164]. These studies established that the application of ES in the form of a constant electrical field and current has a positive impact on nerve growth. Following this, Lee et al. investigated the impact of topographical cues and varied electric potential on neuronal growth using PC12 cells and primary hippocampal neurons [156]. They chemically polymerized PPy over aligned and randomly oriented PLGA nanofibers. The neuronal growth study conducted under ES of 10 and 100 mV/cm, showed that lower electrical potential favored more neurite outgrowth than the higher potential. The study also concluded that scaffolds with both topographical and electrical cues may be more beneficial for neural applications, as aligned PPy/PLGA nanofibrous meshes showed more neurite outgrowth and a higher percentage of neurite-bearing cells than random nanofibrous meshes. The application of ES was also found to accelerate SC migration on electrochemically synthesized PPy [167]. This study was the first to show that current flowing through the conductive biomaterials during ES, as well as the

Table 2
PPy based neural scaffolds or NGCs assessed for electrically stimulated neural regeneration in-vitro and in-vivo, highlighting their electrical or electrochemical properties and ES paradigms (parameters and delivery method).

Biomaterials	Electrical/ Electrochemical properties	ES Parameters	In-vitro/In-vivo	Outcome	Key points	References
PPy/PSS	Resistance: 1 kΩ	100 mV or 10 mA, 2 h	PC12 cells	Increased neurite outgrowth under ES both in voltage and current mode	• First demonstration of ECP based scaffold for ES mediated neurite growth • PPy film was synthesized electrochemically. • ES was delivered via wired connection	26
PPy film	Resistance: 10 kΩ	10 mA, 2 h	PC12 cells	ES induced increased fibronectin adsorption and neurite outgrowth	• PPy film was synthesized electrochemically • ES delivered through Ag wires connected to the PPy film	164
PPy/PLGA	Resistance: 10^3–10^4 Ω	100 mV/cm or 10 mV/cm	PC12 cells, Rat embryonic hippocampal neurons	ES induced increased neurite outgrowth on aligned nanofibers than random nanofibers	• PPy coating over electrospun PLGA nanofibers • ES delivered via wired connection	156
PPy/PSS	NA	0.1, 0.5 & 1.0 V, 2 h	SCs	ES induced elevated protein adsorption and increased SC migration	• Electrochemical synthesis of PPy • ES delivered via wired connection	167
PELA/PPy	Conductivity: 6.9 ± 1.6 mS/cm	N/A	PC12 cells, Spraguee-Dawley (SD) rats	Comparable nerve regeneration efficacy with the commercial autograft	• Electrospun nanofibers of blended PELA/PPy • Tubular scaffold tested in a 10 mm sciatic nerve injury model	170
PPy/Chitosan	Conductivity: 1.5 ± 0.2 × 10^{-2} S/cm	20 Hz, 0.1 ms, 3 V, 1 h	SD rats	Enhanced axon regeneration, remyelination, motor, and sensory functional recovery after ES	• Freeze drying process to longitudinally oriented microchannel •Cu wires connected to the scaffold were used for ES • Tested for a 15 mm sciatic injury model	171
PPy/PLCL	Conductivity: ~10^{-5} S/cm	In-vitro ES: 100 mV/cm, 4 h/day; In-vivo ES: 100 mV/cm, 1 h	PC12 cells, DRG neurons, SD rats	ES induced increased neurite extension and expression of GDNF, BDNF and NT-3; Comparable nerve regeneration similar to commercial autograft	• Electrospun PLCL nanofibrous tubular constructs coated with PPy via oxidative polymerization • Tested for a 15 mm sciatic injury model • Wired ES in direct contact with scaffold	172
Peptide-PEG-Thiazole/ PPy	Conductivity: 2.9 × 10^{-4} S/cm	10 mV, 30 min	Rat olfactory cell derived neurons	Increased axonal outgrowth under ES	• PPy was incorporated into self-assembled laminin derived peptide by layer by layer assembly • Pt electrodes were placed in culture media without in contact with the scaffold	173
PPy/SF	Conductivity: ~0.11 mS/mm	In-vitro ES: 100 mV/mm; In-vivo ES: 0.1 ms, 20 Hz, 3 V, 1 h	SCs, SD rats	ES induced increased SC migration along with BDNF, NT-4/5 and NGF expression; ES promoted nerve regeneration through activation of MAPKs pathway	• Tubular PPy/SF fabricated using 3D printing and electrospinning • Wired ES protocol in direct contact with the scaffold • Tested in a 10 mm sciatic nerve injury model	169
PDA/CGO/ PPy-PLLA	Conductivity: ~17.3 S/cm	50 mV/cm, 1 h	Primary rat SCs	ES induced improved SC alignment in applied current direction	• Electrodeposition of blended CGO/ PPy over electrospun PLLA fibers, followed by dip coating of PDA • Wired ES protocol in direct contact with the scaffold	174
PPy/PLGA	Conductivity: ~9–39 S/cm	Square wave, 0.1 ms, 2 Hz, 1 V, 20 s/day	Mouse neural stem cells	ES promoted enhanced neural differentiation	• Microgrooved PLGA scaffolds coated with PPy via oxidative polymerization • Wired ES protocol in direct contact with the scaffold	175
PPy	Conductivity: 7.65 ± 0.95 S/cm	In-vitro & In-vivo: 40 V/m,100 Hz,1 h	Human neural progenitor cells (hNPCs), immunodeficient RNU rats	ES promoted expression of VEGF-A, BDNF, and NTF-3 in vitro; ES through stem cell embedded NGC showed enhanced function peripheral nerve regeneration and recovery	• Electroplating of PPy on a 14 G metal wire to produce PPy tubes • Wired ES protocol in direct contact with the tube • First demonstration of ES of transplanted stem cells on conductive NGC for PNR in vivo.	168
PPy/Collagen	Conductivity: 2.06 ± 0.17 mS/cm	Biphasic charge balanced waveform, 20 Hz, 60 mV/cm, 1 h	Primary DRG rat neurons	Increased neurite outgrowth under ES	• Gel-aspirationejection (GAE), was used for manufacturing of aligned collagen constructs • Electrodes placed in the medium, not connected with the materials	176

(*continued on next page*)

Table 2 (*continued*)

Biomaterials	Electrical/ Electrochemical properties	ES Parameters	In-vitro/In-vivo	Outcome	Key points	References
PCLF/PPy	Resistance: 2 kΩ	20 Hz, 10 μA, 1 h	PC12 cells	Increased neural differentiation and neurite length under ES	• PPy was chemically polymerized over PCLF tube fabricated by injection moulding technique • Wired ES protocol in direct contact with the tube	177
CGO/PPy/ PLLA	Conductivity: 11.6 S/cm	In-vitro: 50 mV/ cm, 2 h/day; In-vivo: 0.1 ms, 20 Hz, 1 V	PC12 cells, SD rat	ES promoted nerve regeneration and muscle reinnervation in vivo	• Electrochemical deposition of CGO and PPy followed by dip coating of PLLA fiber film and the resultant films were wrapped into cylindrical format to obtain conductive NGC • Wired ES protocol in direct contact with the tube • Tested in 10 mm sciatic nerve injury model	178
Alginate-PPy/ PLL	Conductivity: 0.158 mS/m	Rectangular pulse, 1 Hz, 150 ms, 40 mV, 30 min	P19 embryonic stem cells	ES induced enhanced neural differentiation	• Chemical oxidative polymerization, freeze drying and ionic cross-linking/gelation method was to prepare the conductive hydrogels	179

ES-mediated oxidation PPy, which enables elevated protein adsorption, has a crucial role on SC migration and proliferation. The promising potential of a combined regenerative-rehabilitation approach was demonstrated using a PPy-based conductive nerve guide, fabricated by electroplating PPy onto nickel-chromium wires and, for the first time, integrating it with stem cell therapy and ES for improved functional recovery in a sciatic nerve injury model [Table 2 & Fig. 7] [168]. The PPy based conduit, embedded with hNPCs encapsulated in an alginate hydrogel and combined with ES, represents a milestone achievement, as this strategy not only promoted the regrowth of damaged nerves but also achieved motor and sensory recovery comparable to that of healthy nerve [Fig. 7 (ii)]. While this study had promising results, a conduit with only PPy has some inherent challenges like flexibility (brittle) and poor bioresorbable. A PPy/SF NGC with longitudinal guidance can be more mechanically robust and versatile with improved biodegradability, which was already tested in a 10 mm sciatic nerve defect in rats under ES with functional recovery than the control [Fig. 8 (i) & (ii)] [169]. Theses fabricated NGCs with its outcomes exhibited its significant potential for clinical use in nerve repair.

The poor solubility of most ECPs including PPy, limits its use alone to create aligned scaffolding matrices mimicking the neural anatomy to guide axonal regeneration. However, due its high reactivity or redox behavior, PPy has been successfully integrated with a range of natural (e.g., chitosan, collagen, silk fibroin, etc.) and synthetic polymers (e.g., PELA, PCL, PLGA, etc.) to fabricate smart electroconductive NGCs. Several conventional fabrication strategies (e.g., freeze-drying, dip coating, etc.) as well as additive manufacturing-based technologies (e.g., electrospinning, 3D printing, etc.) have been employed to fabricate these conductive NGCs mimicking the neural anatomy [Discussed in Section 6]. The published reports of PPy based conductive scaffolds in PNR in conjunction with ES are summarized in Table 2.

5.2. Polyaniline (PAni)

PAni and its composites have also emerged as strong contenders for nerve conduit fabrication, owing to their redox stability, which can enhance charge transfer between the polymer and cell membranes and promote membrane depolarization. Similar to PPy, the chemical and electrochemical polymerization methods are similar to obtain PAni [180]. Though PAni had been demonstrated to possess good biocompatibility in vitro and in vivo [181,182], it had to wait longer to see any demonstration in neural applications. Guo et al. were the first to report RGD functionalized oligomeric aniline to aid spontaneous neurogenesis in PC12 cells in absence of NGF [183].

The first ES application using PAni based scaffold was reported by Ghasemi-Mobarakeh et al., wherein of a high electrical potential of 1.5 V was administrated to stimulate NSC [184]. The study fabricated PAni/PCL/gelatin electrospun scaffold, which had a low conductivity (2×10^{-7} S) due to low volume ratio of PAni as compared to PCL and gelatin (highest was 15:85). The study demonstrated that 1 h of ES led to increased cell proliferation and longer neurite outgrowth compared to cells stimulated for 15 or 30 min, as well as those that were not stimulated. The limitation of a low conductivity of the PAni based scaffold was addressed by choosing and optimizing a suitable scaffold fabrication technique. For example, Zhang et al. employed a co-axial electrospinning technique to obtain aligned PAni/PLCL/SF nanofibrous scaffolds by increasing both mass content (upto 17 %) and w/v% of PAni against PLCL/SF composite (upto 20 %), which resulted enhanced conductivity of 30.5×10^{-3} S/cm [185]. This study demonstrated increased SC spreading in the direction of fibre alignment and enhanced neurite outgrowth under ES using a relatively low electrical potential of 100 mV/cm for 1 h/day for 5 days. Aside from applying a constant electric field, constant current stimulation together with a PAni based scaffold yielded improved neurite outgrowth. For instance, a highly conducting PAni nanoparticles coated ITO glass was shown to two-fold increase in neurite outgrowth using a very low current of 100 μA [185]. PAni based NGCs with various architectures mimicking nerve microstructure have been shown to promote nerve regeneration in vivo without ES [186–188], while studies conducted in conjunction with ES remains very limited. Even with a highly conductive NGC, nerve regeneration rate is slow in absence of ES. For instance, a tubular NGC of PAni/SF electrospun nanofibers (Resistance: 1×10^{12} Ω), embedded with SCs was shown successful regeneration and functional recovery in a 10 mm nerve gap in SD rat after 12 months [187]. The advantage of conductive PAni was also shown when it was used as a coating over a zein protein based intraluminal microtubes for a 10 mm sciatic nerve injury repair [186]. The PAni coated zein conduit showed recovery of proximal compound muscle action potential significantly in the regenerated nerve compared to the uncoated zein conduit. The study demonstrated enhanced functional nerve regeneration after 12 months when compared to pure silk scaffolds with improved nerve conduction velocity, motor unit potential, and muscle action potential. Zaman et al. also fabricated a highly conductive (0.3 S/cm) and bioactive multichannel NGC using decellularized plant tissue modified with PAni/GO [188]. Similar to PPy, PAni has poor solubility and limited mechanical flexibility. To mitigate these challenges and enhance bioactivity, PAni has been blended various natural materials (e.g., collagen, chitosan, silk fibroin, etc.) and synthetic polymers (e.g., PCL, PLGA, etc.), to fabricate conductive NGCs in various deign formats. Table 3 summarizes the evidence regarding PAni based conductive scaffolds in PNR.

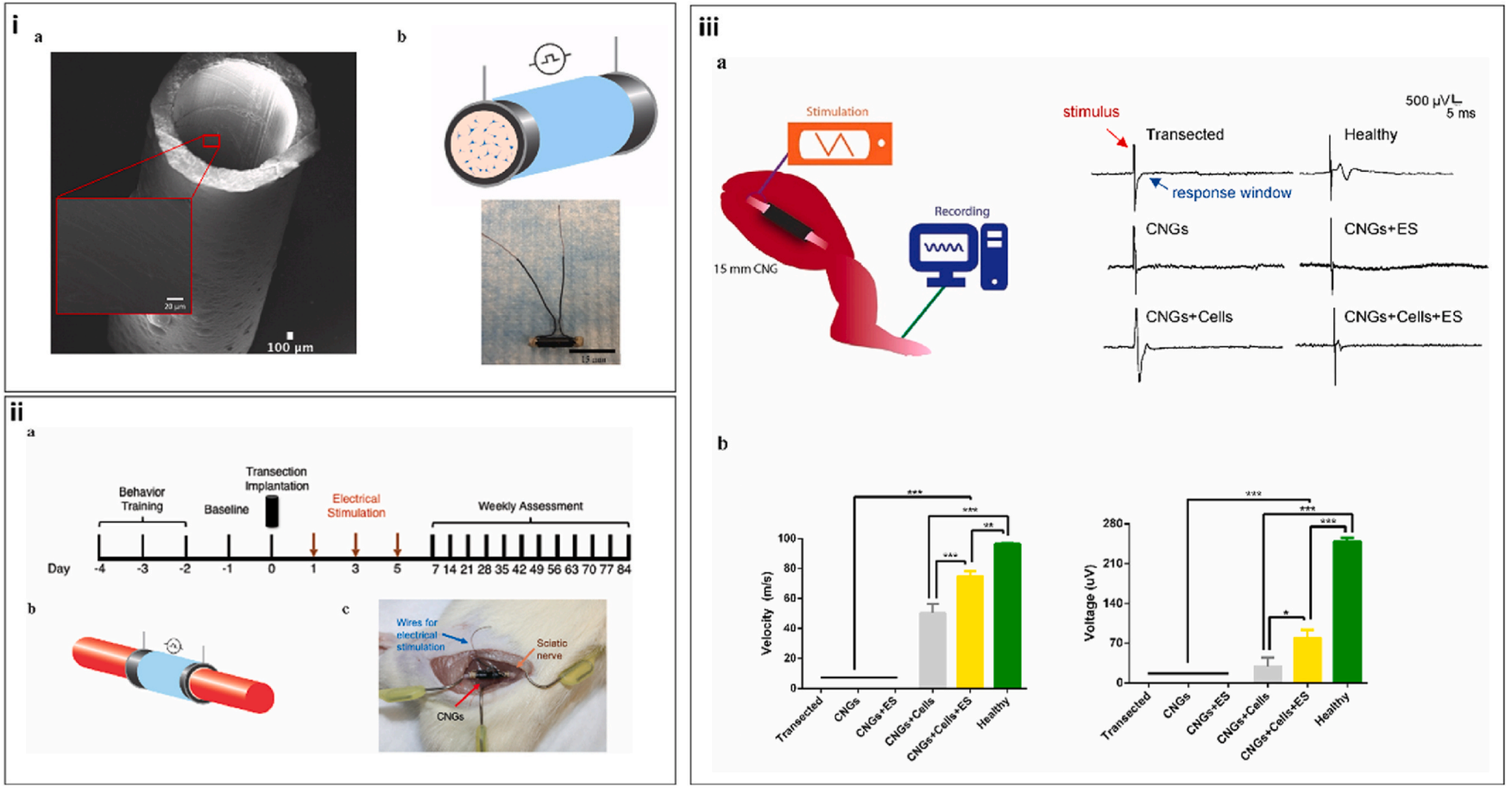

Fig. 7. PPy based conductive nerve guides (CNGs) for electrically stimulated PNR. i. (a) SEM images of PPy CNGs (scale bar: 100 µm) (b) Schematic showing a cross-section of insulated CNGs containing hNPCs (blue) encapsulated in alginate (orange) (top panel) and a longitudinal view with external wires for ES (bottom; scale bar: 15 mm); ii. In vivo implantation showing the (a) experimental timeline, (b) schematic of implanted CNG and (c) digital photo with insulated wires hidden under the skin for retrieval and ES. iii. The electrophysiological analysis showing (a) a schematic of the proximal stimulation and signal recording from the paw after 12 weeks of after CNG implantation (left panel) and (b) functional recovery results, with stimulated hNPC-containing CNGs (CNGs + Cells + ES) showing the highest conduction velocity and compound action potential amplitude compared to controls (*$p < 0.05$, **$p < 0.01$, ***$p < 0.001$; $n = 3$). Data were analyzed using one-way ANOVA and Tukey's test. *Reprinted and adapted from Song et al. 2021, Copyright Elsevier (2021) [Ref. 171].* (For interpretation of the references to colour in this figure legend, the reader is referred to the Web version of this article.)

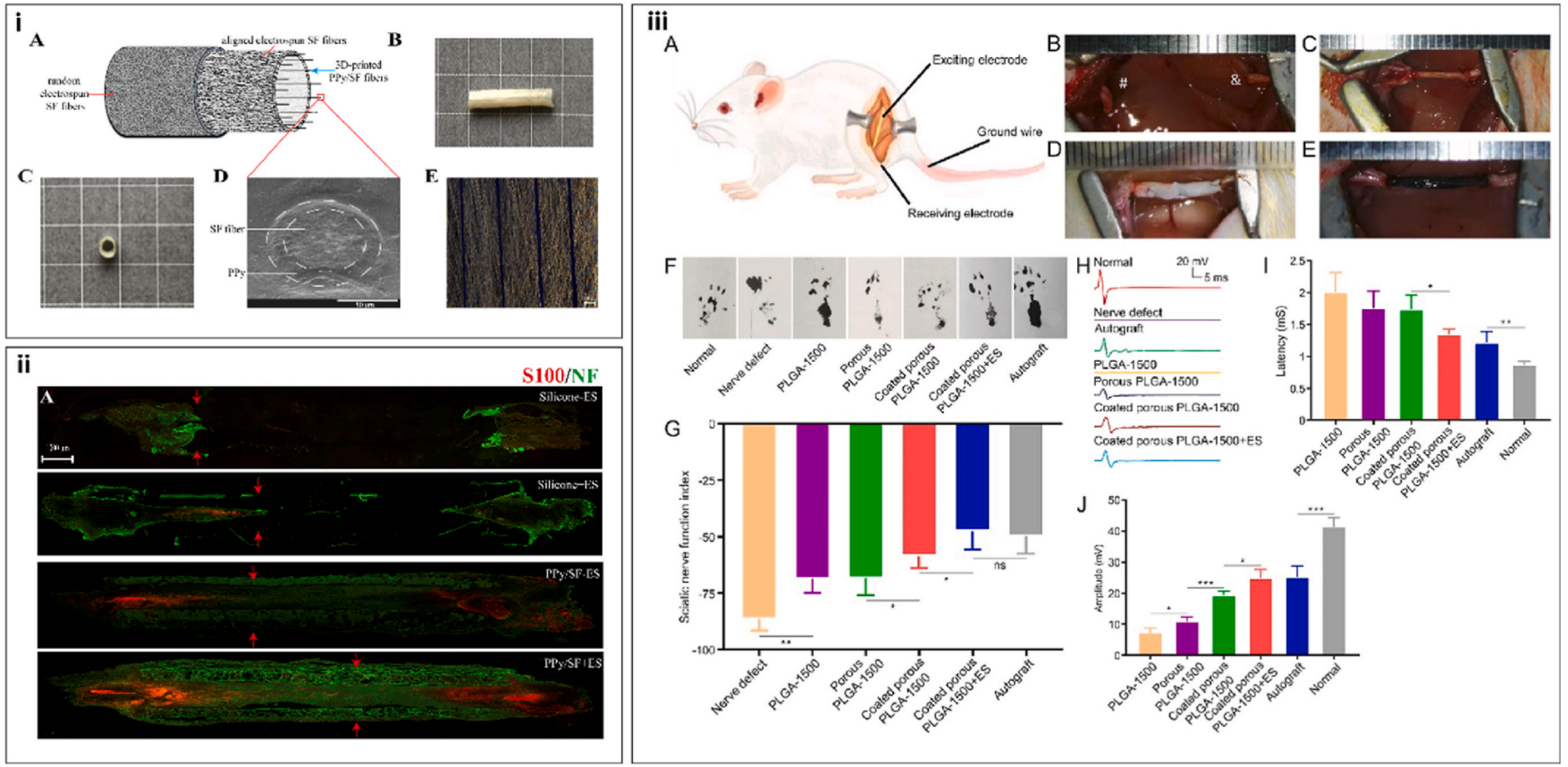

Fig. 8. (i & ii) Conductive PPy/SF NGC for electrically stimulated PNR. i. (A) Schematic diagram, (B) full view, of (C) cross-section of PPy/SF NGC; (D) SEM of PPy/SF composite film, (scale bar = 50 μm) and (E) inner micropatterning (scale bar = 100 μm). ii. PPy/SF with ES promoted neurite growth (anti-NF, green) and Schwann cell (anti-S100, red) infiltration in 10-mm rat sciatic nerve defects as compared to autograft and other groups as indicated after 14 d post-grafting. *Reprinted and adapted from Zhao* et al. *2020, Copyright Elsevier (2020) [Ref. 172]*. iii. Porous aligned PEDOT:PSS-coated PLGA electrospinning NGC for promoting nerve regeneration under ES. Animal experimental procedures and assessment of motor function and neurophysiology in rats after 3 months. (A) Schematic of ES and electrophysiology electrode positions. (B) Nerve defect model with proximal (&) and distal (#) nerve ends. (C–E) Groups: autograft, uncoated NGC, coated NGC (n = 10 per group). (F) Rat footprints in each group. (G) SFI for each group (n = 5). (H–J) Neurophysiological analysis: CMAP waveform, latency, and amplitude after 3 months (n = 4). Data shown as mean ± SD (*P < 0.05, **P < 0.01, ***P < 0.001). *Reprinted and adapted from Liu et al. 2024, Copyright Elsevier (2024) [Ref. 203]*. (For interpretation of the references to colour in this figure legend, the reader is referred to the Web version of this article.)

Table 3
PAni based neural scaffolds or NGCs assessed for electrically stimulated neural regeneration in-vitro and in-vivo, highlighting their electrical or electrochemical properties and ES paradigms (parameters and delivery method).

Materials	Electrical/Electrochemical properties	ES Parameters	In vitro/In vivo	Outcome	Key points	References
PAni/PCL/ gelatin	Maximum current response in mA range under bias voltage ±40 V	Steady potential, 1.5 V, duration of 15, 30, 60 min	Neural stem cells (NSCs)	Enhanced cell proliferation and neurite outgrowth under ES	• Electrospinning of PAni/PCL/gelatin blend. • Wired ES protocol employed in direct with the scaffold	184
PAni/PLLA	Conductivity: 3×10^{-9} S	100 mV/mm, 1 h	NSCs	ES induced increased neurite outgrowth	• Electrospinning of PAni/PLLA blend. • Wired ES protocol employed in direct with the scaffold	189
PAni/PLCL/ SF	Conductivity: 30.5 ± 3.1 mS/cm	100 mV/cm, 1 h/day	PC12 cells	ES combined with NGF release from the scaffold, promoted neurite outgrowth and neural differentiation	• Co-axial electrospinning of PAni/PLCL/SF blend with NGF. • Wired ES protocol employed in direct with the scaffold	185
PAni/ITO	Resistivity: 25.9 ± 2.5 Ω	Biphasic rectangular current, 0.8 ms, 60 Hz, 100 μA, duration of 1, 2, and 4 h	PC12 cells	ES promoted neurite outgrowth through serum protein adsorption	• Oxidative polymerization of PAni over ITO. • Wired ES protocol employed in direct with the scaffold.	190
PAni/P (VDT-VI)	Conductivity: 16.7 mS/cm	Charge balanced biphasic waveform, 200 Hz, 75 mV, 6 h/day	NSCs	ES promoted neural and glial differentiation	• PVDT and PVI were crosslinked using PEGDA4K to produce mechanically stable hydrogel followed by dip coating o of PAni	191
PAni/ Graphene	NA	±500 mV/cm, 1–3 h/day	PC12 cells	ES induced increased neurite length	• PAni/Graphene was prepared by polymerization-enhanced edge-functional ball-milling method, followed by spin coating on ITO. • Wired ES protocol employed in direct with the scaffold.	192
PAni/ Chitosan	Resistance: 10^6–10^7 Ω/cm	500 mV/cm, 2 h/day	PC12 cells	Enhanced neurite extension and neural differentiation under ES	• Oxidative polymerization of PAni nanofibers followed by blending with Chitosan. • Wired ES protocol employed in direct with the scaffold.	181
PAni/PCL	Conductivity: 0.2 S/cm	100 Hz, 1 V, 12 h	NSCs	ES showed increased neural differentiation and elevated expression of neural markers.	• Electrospinning of PAni/PCL blend. • Wired ES protocol employed in direct with the scaffold	193
HEC/SPI/ PAni	Conductivity: 1.7 S/m	3 V, 1 h	SD rat	ES through conductive conduit promoted recovery of nerve motor function and morphology.	• PAni was polymerized over the HEC/SPI conduits. • ES was delivered via wires attached to the conduit. • Tested in a 10 mm sciatic nerve injury model	194

5.3. Polythiophene (PT) and its derivatives

Polythiophene (PT) is another candidate ECP with high electrical conductivity up to 2.0 × 10^2 S/cm [195]. It is polymerized from thiophene consisting of one or more atoms other than carbon (sulfur), resulting in a polyheterocyle akin to PPy. However, due to the absence of functional groups, brittleness, and poor solubility, processing 3D scaffolds from PT is challenging. Although PT has shown effective functionality within neural electrodes when interacting with neurons [196,197], there is limited evidence supporting its use in nerve repair applications. Interestingly, several thiophene derivatives exist, such as 3, 4-ethylenedioxythiophene (EDOT), 3-hexylthiophene (3HT), and 3-methylthiophene (3 MT). These derivatives form ECPs like poly(3, 4-ethylenedioxythiophene) (PEDOT), P3HT, and P3MT, respectively, which exhibit improved physicochemical properties compared to PT [12,198]. Particularly, the bandgap in the resulting PEDOT is drastically reduced by the dioxyalkylene group that is present at positions 3 and 4, leading to its enhanced electrical conductivity (~10–10^3 S/cm) and electrochemical stability [20,199]. Besides, when doped with polystyrene sulfonate (PSS), the resulting formulation PEDOT:PSS becomes partially water soluble or stably dispersed due to the anionic tosylate ions (SO_3^-). Over the past few years, PEDOT:PSS has emerged as a highly promising ECP in the field of organic bioelectronics. It possesses a unique blend of electronic and ionic conductivity [44,45], making it an excellent candidate for seamless integration with biological tissues. While the pi electron delocalization due to the alternating single and double bonds provide the electronic conductivity, the deprotonated sulphonate group or tosylate anion (SO_3^-) contributes for ionic conductivity in a hydrated environment. The polymerization of PEDOT oligomers onto long PSS chains results in a porous structured PEDOT:PSS, which facilitates efficient ion permeability. Thus, PEDOT:PSS is highly susceptible to volumetric electrochemical doping, resulting in improved charge-transfer efficiency and charge injection capacity when interacting with biological tissues for neuronal stimulation. Therefore, PEDOT:PSS based scaffolds or NGCs have been successfully assessed for electrically stimulated axonal growth in vitro and in vivo. For instance, an aligned PLGA porous NGC coated with PEDOT:PSS was assessed in a 10 mm gap rat sciatic nerve defect under ES of 100 mV (20 Hz), which showed significantly enhanced axonal growth, remyelination, and functional recovery than the controls [200]. Histological analysis, immunofluorescence staining, and electrophysiological assessments revealed better nerve fiber alignment, thicker myelin sheaths, increased SC infiltration, and improved CMAPs in the ES-treated groups [Fig. 8 (iii)]. Table 4 further summarizes various PEDOT based neural scaffolds for neural tissue engineering applications in conjunction with ES. Another intriguing thiophene-based ECP is P3HT, which has a remarkably low band gap and excellent optical properties. Zhang et al. demonstrated that the conductivity of PLGA/P3HT membranes can be tuned by adjusting the doping duration with $FeCl_3$ [201]. Specifically, the membrane doped for 5 min achieved a conductivity of 10^{-2} S/cm, significantly higher than the 10^{-6} S/cm observed after just 6 s of doping. The 5 min doped membrane having higher conductivity exhibited enhanced neurite growth in PC12 cells. Aligned electrospun nanofibers of this P3HT/PLGA also demonstrated improved adhesion and proliferation, indicating its potential for neural applications [202]. In addition, P3HT has the advantage of being easily modified or blended with electron acceptor materials that are relevant to biological applications [23]. Therefore, P3HT is widely regarded as a highly suitable material for organic photovoltaic applications [203]. In recent years, this feature has been employed to convert light energy into electrical energy and applied for optoelectronic stimulation of neurons and peripheral nerves [204,205]. A more detailed discussion on this topic is provided in Section 9.5 of this review.

5.4. Other ECPs

Having reviewed ECPs that have been majorly exploited for nerve repair applications there exists a minority which are less reported in the literature. One such material; a PPV based derivative MEH-PPV, has investigated for electrically stimulated neuronal growth potential. Unlike other ECPs, MEH-PPV has better solubility options in common organic solvents such as chloroform, dichloromethane, tetrahydrofuran, toluene, and chlorobenzene due to its branched alkoxy chains [217]. Due to this ease of ease of processing, reproducibility, and versatility, MEH-PPV has been investigated for various applications including organic polymer photovoltaics, light-emitting diodes, and light emitting electrochemical cells, as well as in biosensor applications [155,165,218–220]. However, a just a handful of studies are reported which assess MEH-PPV for tissue engineering applications although it offers interesting properties for biological applicatiosn by readily aiding the immobilization of biomolecules via high density hole-traps. MEH-PPV is a p-type semiconducting polymer that has low conductivity due to its low hole and electron mobilities. However, it has been shown that suitable doping can enhance the electrical conductivity of MEH-PPV for a desired application. For instance, Shin Sakiyama et al. reported a significant increase in the conductivity of MEH-PPV using $FeCl_3$ (p-type dopant) and Cs_2CO_3 (n-type dopant) [221]. The cytocompatibility of MEH-PPV was first reported with L929 fibroblast cells [206]. In contrast to ECPs such as PPy, PAni and PEDOT, MEH-PPV based biomaterials for neural applications are less reported. MEH-PPV based neural scaffolds in combination with ES has been assessed with neuronal like PC12 cells [155,165,219] whereby nanofibrillar meshes of MEH-PPV were fabricated along with a biocompatible PCL in a blended and core-shell formulation using blended and co-axial electrospinning techniques. Core-sheath nanofibers with MEH-PPV as shell material, showed superior conductivity than those electrospun nanofibers fomed by blending MEH-PPV and PCL. Consequently, nanofibers with higher conductivity exhibited enhanced neurite formation and outgrowth in PC12 cells, especially under ES at 500 mV/cm. These studies also demonstrated neuronal differentiation with or without NGF in presence of ES, reestablishing the impact of ES on cellular differentiation as discussed in Section 2. In fact, a mechanistic insight on charge transport properties of theses electrospun nanofibers revealed that increased charge carrier mobility and low filed conductance enabled efficient delivery of ES to cells for membrane depolarization, leading to improved cytoskeletal remodeling and neurite elongation [165]. Other ECPs, such as polyindole, polyphenylene (PPP), polythiophene-vinylene (PTh-V), poly(3-octylthiophene-3-methylthiophene) (POTMT), Poly(3-alkylthiophene) (PAT), polyfluorene (PFO), polyfuran (PFu), poly(phenylene sulfide) (PPS), and polypyridazine (PPd), are emerging that require further exploration. Detailed studies on their synthesis and biomedical properties are needed before they can be fully utilized in tissue engineering applications, including nerve repair.

6. Engineering strategies of ECP based NGCs

6.1. Synthesis of ECPs

ECPs are synthesized from their corresponding monomers, mainly chemical polymerization and electrochemical synthesis methods [23,39]. Owing to their unique semiconducting feature along with traditional polymer like flexibility, ECPs have been extensively explored for energy, sensor, actuator, and electrochromic display applications in addition to range of biomedical applications [39,222]. Depending on the final application, a variety of synthesis parameters, such as the dopant, oxidant, solvent, relative reagent concentration, reaction duration, temperature, and so on, can be selected. Therefore, ECP synthesis strategies designed for applications other than biomedical use often involve toxic and corrosive reagents, whereas biologically compatible dopants, oxidants, and solvents are preferred for ECPs intended for biomaterial fabrication. In chemical polymerization, carbon-carbon (C-C) bonds are formed by combining simple monomers under various physico-chemical

Table 4
PT derivatives (PEDOT & P3HT) based neural scaffolds or NGCs assessed for electrically stimulated neural regeneration in-vitro and in-vivo, highlighting their electrical or electrochemical properties and ES paradigms (parameters and delivery method).

Materials	Electrical/Electrochemical properties	ES Parameters	In-vitro/ In-vivo	Outcome	Key points	References
PEDOT:PSS	Conductivity: 5.8 S/m	1 V/cm, 100 Hz, 24 h (4 days) & 12 h (8 days)	Human NSCs	ES showed increased neural differentiation and neurite outgrowth; Enhanced protein synthesis and adsorption under ES	• PEDOT:PSS film was fabricated using GOPS as cross-linker • Wired ES protocol was employed	206
PEDOT/rGO	Conductivity: 1.68–2.41 S/cm	3000 pulses/day from TENG (Output: 300 V, 30 μA)	MSCs	ES generated by TENG promoted neural differentiation	• PEDOT/rGO microfibers were fabricated by modified capillary hydrothermal method • ES was delivered using TENG through wires attached to the microfibrous scaffold	207
PEDOT	Good charge storage and charge injection capacity	Biphasic waveform, 100 μs, 250 Hz, ±0.25 mA/cm^2	PC12 cells	Increased neural differentiation, neurite length and branching	• PEDOT film was synthesized electrochemically • Wired ES protocol was employed	208
PEG/PEDOT:PSS	Higher charge storage capacity	Steady state DC, 1000 mV	ADMSCs	ES induced improved neurogenic differentiation	• PEG/PEDOT:PSS hydrogel was casted over a micropatterned PDMS mod followed by photo-crosslinking • Electrodes were placed in culture media without direct contact with sample for ES	209
PEO/PEDOT:PSS	High charge injection capacity	Biphasic square waveform, 100 mV/cm, 100 ms, 1 h/day	PC12 cells	ES on aligned nanofibers showed increased neurite extension and elevated expression of neural genes	• Electrospinning of PEO/PEDOT:PSS blend • Wired ES protocol was used	210
PEGDA/ PEDOT:PSS	Resistance: ~660–1000 Ω	Steady-state DC electric field, 1000 mV, 2 days	DRG neurons	Conductive hydrogel combined with ES showed elevated expression of neural markers.	• Stereolithography 3D printing of PEGDA/PEDOT:PSS blend followed by photo crosslinking • Electrodes were placed in culture media without direct contact with sample for ES	211
PEDOT:PSS/ Chitosan	Conductivity:0.1945 S/cm Impedance: 15 kΩ CSC: 5.704 × 10^{-6} C	0.1 Hz, 400 mV/cm, frequency: 0.1 Hz, duration of1, 2, and 3 h	BNCs	ES resulted higher density of axons	• PEDOT:PSS was spin coated over electrospun chitosan nanofibers • Wired ES protocol was used	212
PVA/PEDOT:PSS	Conductivity: 2 × 10^{-3} S/m	100 mV/m, 2h each day from day 10–13.	Rat MSCs	ES showed elevated expression of neural specific markers	• Electrospinning of PVA/PEDOT:PSS blend • Electrodes were placed in culture media without direct contact with sample for ES	213
PEDOT:PSS/ SF	Conductivity: 1.003 S/cm Resistance: 3.833 × 10^3 Ω	50 mV/day, 5 h/day	PC12 cells	Enhanced neural differentiation with significant axonal growth after ES	• PEDOT:PSS was dip coated over SF film • Wired ES protocol was used	214
PEDOT:PSS/ PLGA	Conductivity: 0.07 ± 0.01 S/cm	20 Hz, 50 % duty cycle, 100 mV, 2 h	SD rats	ES through the conductive NGC enhanced functional recovery of injured nerve; ES along with conductive coating and porous morphology of NGC promoted M2 polarization in vivo	• Electrospun aligned PLGA nanofibers were coated with PEDOT:PSS • Tested in a 10 mm sciatic nerve injury model • Wired ES protocol was employed	200
GelMA/ Chitosan/ PEDOT	Conductivity: 0.18 S/m	Electrical field of 2, 10, 50 & 100 mV/mm, Duration of 0.5, 1 and 2 h/day	SD rats	ES through the conductive hydrogel NGC showed enhanced functional nerve repair and muscle reinnervation	• Digital light processing (DLP) printing of GelMA/Chitosan hydrogel followed by freeze drying; PEDOT was polymerized over the freeze dried hydrogel tubes • Tested in a 10 mm sciatic nerve injury model • Wired ES protocol was used	215
EC/P3HT	NA	Steady state potential of 5 V, 300 min/day	PC12 cells	ES showed increased cell behaviour	• P3HT was polymerized over EC electrospun mats • Wired ES protocol was used	216

conditions such as temperature, pressure, and a catalyst. The chemical synthesis process involves the oxidation or reduction of monomers in presence of dopant and oxidant, followed by polymerization of succeeding monomers. Chemical synthesis of ECPs is simple, affordable and efficient in terms of large-scale production. Electrochemical synthesis of ECPs involve oxidation of the monomer in electrochemical cell consisting of three electrodes (working, counter and reference). Electrochemical polymerization can be carried out utilizing potentiodynamic processes with either continuous current or voltage. This polymerization procedure is normally carried out in highly acidic conditions to obtain ECP with longer polymer backbone. In addition, there are other methods like as vapor phase synthesis, self-assembly, photo-chemical approach, and plasma-assisted polymerization that are used to synthesize various ECPs [39].

6.2. Design considerations for ECP based NGCs

As already mentioned; artificial NGCs have emerged as promising alternative for bridging damaged nerve ends addressing the shortcomings of autologous nerve grafts and allografts. Various designs of NGCs with adequate physical, topographical, chemical, and biological cues have been documented thus far, and this also applies to ECP-based NGCs [4,16,223]. While linking the injured nerve ends, NGCs provide structural and trophic support and protection to both, allowing for the invasion of surrounding tissues and axon regrowth along the conduit. An ideal NGC should be biocompatible and biodegradable, with a physical design that closely resembles the nerve anatomy to facilitate axonal regeneration in the longitudinal direction, as well as appropriate porosity to provide nutritional support. Furthermore, it should be electrically conductive, allowing for signal transmission between the wounded ends, as well as mechanically durable and flexible. ECP based NGCs designed for wired ES, in particular, must be mechanically sturdy enough to survive electrode placement or wiring. To replicate nerve architecture, NGCs are crafted into various configurations, including grooved aligned structures, intraluminal channels, fillers with intraluminal fibers, and multilayered conduits [Fig. 9]. Additionally, biochemical cues, such as nerve growth-promoting factors (e.g., NGF, BDNF), can be integrated during the fabrication of ECP-based NGCs [224]. Tissue-engineered conductive NGCs have also been developed by growing neural supporting cells on them before implantation in nerve injury models [168]. For further insights into essential NGC features and their alignment with the biological processes of nerve regeneration, readers are encouraged to consult recent reviews by Zhou et al. [14], Rahman et al. [223], Zarrintaj et al. [225], and Marques-Almeida et al. [50] The various design considerations for a suitable ECP based NGC are outlined in Fig. 9.

6.3. Fabrication methods of ECP based NGCs

Due to poor solubility, fashioning NGCs into grooved multilayer configurations using ECPs alone is challenging. To meet the growing demand for creating an electroconductive microenvironment in NGCs, various ECPs have been incorporated into NGC configurations by blending them with other natural or synthetic materials/polymers or employing various deposition and coating techniques [15,23,223]. ECP based NGCs in single tube format or with 3D neural anatomical architectures (e.g., porous, grooved, hollow, intraluminal channels or fibers) have been fabricated using a variety of conventional techniques such as freeze-drying [226,227], dip coating [200], solvent casting [228], salt leaching [229], and electrospinning [155,165,219], as well as through various additive manufacturing methods like melt electrowriting [230], 3D printing [231,232] and bioprinting [233] [Fig. 9].However, studies

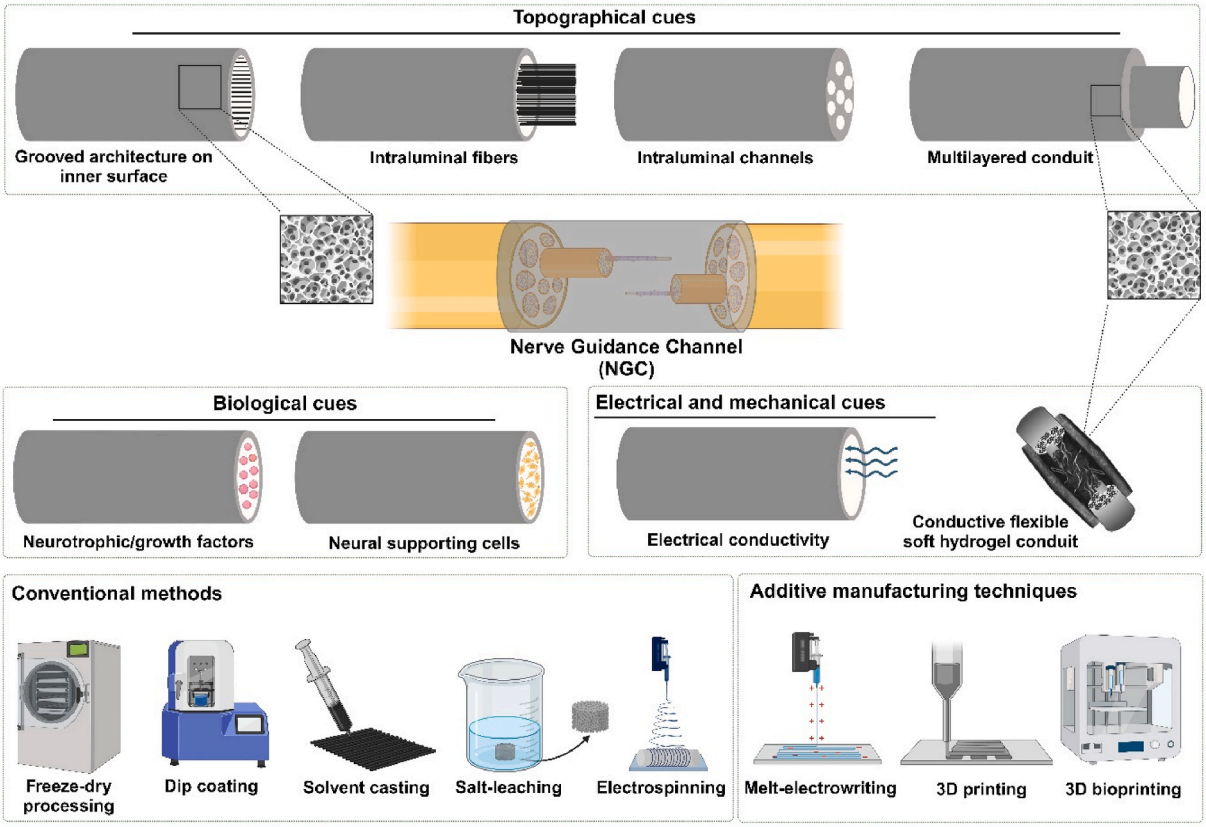

Fig. 9. Different designs of NGCs with various topographical, electrical, mechanical, and biological cues being explored for PNR applications. (Lower panel) Schematic depiction of various conventional and additive manufacturing techniques employed for fabrication of NGCs into different architectures as shown in the upper panel.

utilizing ECPs for NGCs remain limited due to their inherently poor solubility, which hinders their ability to replicate the complex microstructural anatomy of nerves. In contrast, widely used non-conductive synthetic polymers such as PCL and PLGA offer better processability and can be easily fabricated into multilumen or multichannel structures using advanced additive manufacturing techniques like 3D printing and electro-writing [234–236]. A common approach to create conductive ECP-based NGCs is by coating the outer layer of an already fabricated NGC made from non-conductive synthetic or naturally derived polymers or their composites. This outer coating can be applied through techniques such as dip coating [200] or in-situ chemical polymerization of ECPs [237]. Alternatively, ECPs can be incorporated as conductive fillers in a blend with non-conductive polymers. This requires the homogeneous distribution of ECPs within the blend to achieve the percolation threshold and ensure optimal electrical conductivity for effective ES [32]. Previously, a PPy/PLGA-based NGC was fabricated with parallel-aligned conductive fibers encased within a conductive tubular structure, designed to facilitate axonal growth and create a biomimetic environment for nerve regeneration [237]. The parallel-aligned PLGA fibres were created via electrospinning, which were subsequently coated with PPy through in-situ polymerization, following integration into a conductive tubular structure fabricated by dip-coating a PPy/PLGA emulsion onto a cylindrical mandrel. Similarly in a separate study, aligned electrospun PLGA fibers were coated with PEDOT:PSS, while the porosity of the resultant NGC was optimized through phase separation by varying solvent ratios during electrospinning [200]. Another study has reported fabrication of a hollow tubular conductive NGCs using a composite of sodium alginate, PAni, and graphene through a solution extrusion technique [238].

7. ES paradigm using ECP based biomaterial scaffold for PNR

7.1. ES delivery methods

ES can be applied via three common methods that rely on the coupling mechanism between the externally applied electrical signal and the cells or tissues; and can be categorized as direct coupling, capacitive coupling, and inductive coupling [20,76,239]. Direct coupling is the most common and straightforward method for delivering ES, involving the placement of two conductive electrodes in a cell culture medium or at the injury site in vivo. For electroconductive scaffolds, such as ECP based biomaterials or NGCs, one electrode is directly attached to the scaffold, while the other is positioned around the cell-seeded scaffold in the culture medium [155,219] or surrounding soft tissue in vivo [168]. Although this is a well-established and widely used method, careful attention is needed during the development of ECP based scaffolds/NGCs to prevent unwanted electrochemical degradation reactions, which could result in the production of toxic byproducts, sudden temperature increases, and pH changes. In capacitive coupling, two electrodes are positioned at opposite ends of the culture medium or target tissue without direct contact, with the electric field driving the ES. This non-invasive approach allows electrodes to be placed outside the stimulation site in vivo [240]. However, the delivered ES may not be localized, potentially affecting surrounding tissues undesirably. Moreover, the applied electric field may not be uniform across the cell system or injury site, resulting in inefficient stimulation. Inductive coupling for ES is also non-invasive, using a conductive coil placed around the cell culture system or target tissue to generate an electromagnetic field for stimulation. However, this approach requires a magnetic material and is rarely employed with ECP based scaffolds.

7.2. ES regime for PNR

An ES regime involves various parameters, including the type of waveform, frequency, amplitude, pulse width, and duration of the signal. These parameters must be carefully optimized based on the conductivity and electrochemical properties of the ECP based scaffold, as well as the target cell or tissue type. Such optimisation is crucial to effectively trigger the desired biological response, such as an action potential for nerve repair. Careful calibration enhances the safety and efficacy of therapeutic interventions, ensuring effective treatment while minimizing potential adverse effects.

Waveforms that have been investigated for ES of neuronal tissue include cathodic monophasic, charge balanced and imbalanced biphasic and charge balanced with interphase delay [20]. Although effective, a monophasic waveform involves unidirectional current flow, which can lead to irreversible faradaic reactions and potentially cause tissue damage [Table 5] [20,148,242]. A charge balanced waveform has been widely used for neural applications [148,241,243]. While irreversible faradaic reactions can still occur during both the cathodic and anodic phases with metal or carbon nanomaterial-based electrodes, they are less likely with ECP based electrodes or scaffolds due to their unique reversible doping/de-doping (oxidation/reduction) behaviour. A charge-imbalanced biphasic waveform or the inclusion of an interphase delay further reduces the likelihood of faradaic reactions, thereby minimizing the risk of tissue damage. Additionally, charge-balanced symmetric biphasic waveforms, asymmetric biphasic waveforms, and monophasic capacitor-coupled waveforms have also been used for neuronal stimulation [20,148].

As discussed in Section 3, the aim of ES should be to evoke a functional response in nerve cells during stimulation. In other words, ES should drive the resting potential of a typical nerve cell from −70 mV to +30 mV for membrane depolarization and trigger an action potential. Motor neurons can produce action potentials at frequencies ranging from 5 to 100 Hz, depending on their state-whether at rest, active, or undergoing maximal or continuous contraction [244]. Previous research has shown nerve regeneration occurring in rat models when utilizing various ES settings (without using any biomaterials), which includes frequencies ranging from 1 to 20 Hz, amplitudes between 50 mV and 3 V, and pulse widths of 0.1–1 ms for 1 h durations [83,245–248]. In these studies, ES was applied in voltage mode, which involves applying a constant potential across the electrodes, causing current flow (charge transport). In voltage mode, the current flow or charge transfer process is heavily influenced by the impedance of the biological tissue and the electroconductive scaffold (if any). Alternatively, ES can be used in current mode, which involves setting a certain current across the

Table 5
Overview of various waveform types, their descriptions, and their effects in specific applications [20,241–243].

Waveform Type	Description	Effects
Cathodic Monophasic	Unidirectional current flow	Highly effective in stimulation but can cause irreversible faradaic reactions and tissue damage
Charge-Balanced Biphasic	Alternates current flow between cathodic and anodic phases, maintaining net charge balance	Reduces faradaic reactions compared to monophasic waveforms; safer for tissue
Charge-Imbalanced Biphasic	Slight imbalance in charge between cathodic and anodic phases	Further minimizes faradaic reactions; lowers risk of tissue damage
Biphasic with Interphase Delay	Includes a delay between cathodic and anodic phases	Reduces overlap of reactions, minimizing faradaic reactions and enhancing safety
Charge-Balanced Symmetric Biphasic	Equal amplitude and duration for cathodic and anodic phases	Effective for stimulation with minimal tissue damage
Charge-Balanced Asymmetric Biphasic	Unequal amplitude or duration for cathodic and anodic phases	Customizable for specific nerve responses; reduces adverse reactions
Monophasic Capacitor-Coupled	Includes a capacitor to limit current flow	Prevents direct current buildup, reducing faradaic reactions

electrodes and automatically adjusting the voltage across the biological tissue or scaffold to match the specified current. Tang et al., for example, used ES at 2 Hz for 20 min with a current of less than 6 mA to repair a damaged ulnar nerve using acupuncture needles [249]. Typically, ES in voltage mode is considered safer (than the current mode) since it allows for the selection of a potential below the water electrolysis window, reducing the likelihood of harmful electrochemical reactions in the target tissue or conductive scaffold. The ES regime for PNR becomes more complex when administered via electroconductive biomaterials, such as ECP based scaffolds as intrinsic conductivity and electrochemical properties, such as redox potentials, charge carrier concentration and mobility, charge injection capacity, and electrochemical charge-transfer resistance, have a significant impact on stimulation efficiency [20,32,165]. As a result, ES parameters used with different ECP based scaffolds can vary greatly, both in vitro and in vivo. Tables 2–4 give a summary of these parameters across several in vitro studies and studies in nerve injury models. However, irrespective of the variation of the ES parameters across studies, most ECP-based NGCs demonstrate good conductivity in the range of 5–17 S/cm [Tables 2–4], which is well above the conductivity of peripheral nerve tissue (0.003–0.026 S/cm) [12,250] which drives an enhanced nerve regeneration under ES. In addition, Hsiao et al. showed NIR driven electric field generation in P3HT based scaffold in the range of 220–980 mV for electrically stimulated axonal growth [Table 7] [251]. All these clearly indicate the ability of the ECP based neural scaffold to mimic or support the endogenous electric field following an injury or to drive neuron cell resting potential for membrane depolarization.

Table 6
Quantitative and qualitative comparison of functional recovery using ECP-based NGC with exogenous ES in a small animal nerve injury model following PNI.

ECP based NGC	Study details	Sciatic Function Index (SFI)	Electrophysiological Measurements		Histological & Immunofluorescence Outcomes
			Nerve Conduction Velocity (NCV) (m/s)	Peak Amplitude (PA) (mV)	
PPy/Chitosan [171]	Injury model: Rat Nerve gap: 15 mm Study duration: 12 weeks ES parameter: 3 V, 20 Hz, 1 h every 2 days for 8 sessions post-surgery	PPy/Chitosan + ES: 60.3 ±3.25 PPy/Chitosan-ES: 72.5±5.66 Chitosan + ES: 71.5±3.62 Chitosan -ES: 72.5±5.66	PPy/Chitosan + ES: 23.6±0.71 PPy/Chitosan-ES: 21.5 ± 0.82 Chitosan + ES: 20.9 ± 0.73	PPy/Chitosan + ES: 18.9 ± 0.93 PPy/Chitosan-ES: 17.9 ± 0.93 Chitosan + ES: 17.1 ± 0.85	Regenerated axonal area, myelinated axonal density and diameter are higher on PPy/Chitosan + ES
PPy/PLCL [172]	Injury model: Rat Nerve gap: 15 mm Study duration: 8 weeks ES parameter: 100 mV/cm, 20 Hz, 1 h per day on days 1, 3, 5, and 7 post-implantation	PPy/PLCL + ES: 23.5 ± 1.2 PPy/PLCL-ES: 34.1 ± 2.1 Autograft: 21.4 ± 1.1	PPy/PLCL + ES: 61.34 ± 4.21 PPy/PLCL-ES: 41.23 ± 1.54 Autograft: 63.32 ± 2.54	PPy/PLCL + ES: 8.07 ± 0.24 PPy/PLCL-ES: 6.27 ± 0.14 Autograft: 9.34 ± 0.12	Total myelinated fiber counts, the myelinated fiber diameter, the average axon diameter, and myelin sheath thickness are higher on PPy/PLCL + ES than the unstimulated group
PPy/SF [169]	Injury model: Rat Nerve gap: 10 mm Study duration: 24 weeks ES parameter: 3 V, 20 Hz, 1 h per day on every 2 days for 7 sessions	PPy/SF + ES: 48.2 ± 5.1 PPy/SF-ES: 56.8 ± 6.2 Autograft: 30.5 ± 4.0	–	–	PPy/SF + ES group showed enhanced myelin sheath thickness, axon diameter, and number of myelin lamellae, outperforming the non-stimulated (PPy/SF - ES)
PPy [168]	Injury model: Rat Nerve gap: 10 mm Study duration: 12 weeks ES parameter: 40 V/m, 100 Hz, 1 h per session, applied on days 1, 3, and 5 post-implantation	–	PPy + hNPC + ES: 60 ≥ NCV≥80 PPy + hNPC-ES: 40 ≥ NCV≥60 PPy + ES: PPy-ES: Autograft: 80 ≥ NCV≥100	PPy + hNPC + ES: 0.7 ≥ NCV≥0.9 PPy + hNPC-ES: 0.2 ≥ PA≥0.7 PPy + ES: PPy-ES: Autograft: 2.1 ≥ NCV≥2.3	PPy + ES group showed a greater number of myelinated nerve fibers, increased myelin thickness, and better-organized axonal structures compared to unstimulated controls
C-GO/PPy/PLLA [178]	Injury model: Rat Nerve gap: 10 mm Study duration: 12 weeks ES parameter: 1 V, 20 Hz, 0.1 ms, 1 h per day for 7 days	–	C-GO/PPy/PLLA + ES: ~34.59 C-GO/PPy/PLLA-ES: ~28.06 Autograft: ~36.87	C-GO/PPy/PLLA + ES: ~2.96 C-GO/PPy/PLLA-ES: ~2.51 Autograft: ~3.12	C-GO/PPy/PLLA + ES showed significant improvement in axon diameter (~3.4 μm) and myelin thickness (~0.43 μm) compared to the non-ES group (axon diameter: 2.6 μm; myelin thickness: 0.38 μm)
HEC/SPI/PAni [194]	Injury model: Rat Nerve gap: 10 mm Study duration: 12 weeks ES parameter: 3 V, 20 Hz, 1 h every 2 days for 7 days	HEC/SPI/PAni + ES: 55.9 HEC/SPI/PAni-ES: 61.5 HEC/SPI/PAni + BDNF: 55.9 Autograft: 53.5	NA	HEC/SPI/PAni + ES: 15.6 HEC/SPI/PAni-ES: 10.5 HEC/SPI/PAni + BDNF: 9.6 Autograft: 18.5	Enhanced myelinated fiber density, axon diameter, and myelin thickness were observed on HEC/SPI/PAni + ES as compared to the non-ES groups
PEDOT:PSS/PLGA [200]	Injury model: Rat Nerve gap: 10 mm Study duration: 12 weeks ES parameter: 100 mV, 20 Hz, 2 h every other day for 5 sessions post-surgery	PEDOT:PSS/PLGA + ES: −55 ≤ SFI ≤ −45 PEDOT:PSS/PLGA-ES: −70 ≤ SFI ≤ −50 PLGA: −75 ≤ SFI ≤ −55 Autograft: −55 ≤ SFI ≤ −45	PEDOT:PSS/PLGA + ES: 1 ≥ NCV ≥1.5 PEDOT:PSS/PLGA-ES: 1.5 ≥ NCV ≥2 PLGA: 1.5 ≥ NCV ≥2 Autograft: 0.5 ≥ NCV ≥1	PEDOT:PSS/PLGA + ES: 20 ≥ PA ≥ 30 PEDOT:PSS/PLGA-ES: 15 ≥ PA ≥ 25 PLGA: 10 ≥ PA ≥ 15 Autograft: 20 ≥ PA ≥ 30	PEDOT:PSS/PLGA + ES group showed enhanced axon diameter, myelin thickness, and functional recovery compared to non-stimulated conduits and control groups.

Table 7
P3HT based conductive photovoltaic biomaterials assessed for optoelectronic neuronal stimulation, highlighting their optoelectronic properties (photoelectrical conversion) and light stimulation parameters.

Materials	Optoelectronic/other relevant properties	Light Stimulation Parameters	In-vitro/In-vivo	Outcome	Key points	References
P3HT:PCBM	Photocurrent: ~2 nA	10 mW/mm^2, 50 ms, 532 nm	Hippocampal neurons	OptoES showed membrane potential modulation in neurons	• P3HT and PCBM mixer was spin coated over a ITO glass substrate • First demonstration of OptoES modulation of neurons via photovoltaic (capacitive) mechanism	291
P3HT/ Graphene	Surface potential: 1–2 mV at 1 mW/mm^2	1–15 mW/mm^2, 50–500 ms, 550 nm	Hippocampal neurons, Retinal explants	OptoES induced current injection mediated voltage modulation in hippocampal neurons and promoted light-sensitivity recovery in blind retina explants	• Graphene was chemical vapor deposited on PET substrate, followed by P3HT spin-coating	204
ZnO/PbS/ P3HT/ITO: RuO_2/ITO	Photocurrent & photovoltage density: ~500 μA/cm^2 and ~180 mV at 10 ms pulse, 1 mW/mm^2, 1 Hz	7 mW/mm^2, 20 ms, 780 nm	Hippocampal neurons	Incorporation P3HT led to higher photocurrent response; OptoES induced photovoltaic capacitive ionic current resulting modulation of neuronal action potentials	• ZnO, PbS, and P3HT were spin coated over ITO/PET substrate • NIR (780 nm) was used for photostimulation (Possibility of photochemical effect was mitigated)	297
P3HT	Photocurrent density & photovoltage: ~ −36 mA/cm^2 and ~0.45 V at 10 ms pulse, 1 mW/mm^2, 1 Hz	1 s, 1 Hz, 30 min, 7 mW/cm^2, 539 nm	Human NSCs	OptoES showed increased neuronal differentiation and maturation	• Nanofibrils of P3HT was spin coated over a glass slide to form a nanoweb substrate	288
β-carotene/ PTCDI-C8/ PEDOT: P3HT/ PCBM/ PEDOT	Photocurrent density & photovoltage: ~0.17 mA/cm and ~0.42 V at 100 mW/cm^2	780 nm NIR light driven generated electric fields in the range of 255–1260 mV/cm, were used for neuronal stimulation	PC12 cells	NIR based OptoES generated electric field in the range of 220–980 mV/m, resulting in enhanced neurite outgrowth	• β-carotene & PTCDI-C8 were deposited over PEDOT:PSS layer on ITO; Similarly, P3HT & PCBM were also deposited over PEDOT: PSS in a separate configuration. Photovoltaic device was developed by integrating both of these configurations	251
PCL/P3HT/ Collagen	Photocurrent: 20–80 pA at 3–10 mW/cm^2 and 530 nm	500 ms, 1 Hz, 6 mW/ cm^2, 30 min, 530 nm	PC12 cells	OptoES promoted neurit outgrowth through L-type voltage-gated calcium channel activation	• P3HT NPs were synthesized by microemulsion technique, followed by electrospinning of PCL/P3HT blend • Collagen was coated over PCL/ P3HT electrospun fibers by electrospraying	295
ZnO/P3HT/ PCBM/ PEDOT:PSS	Photocurrent density & photovoltage: 3.1 mA/ cm^2 and 470 mV, at 50 ms, 2 Hz, 100 mW/cm^2 at 445, 530 & 630 nm	10 ms, 100 mW/cm^2 at 445, 530 and 630 nm	SH-SY5Y cells	OptoES promoted effective modulation of membrane potential in neuronal cells	• Photovoltaic device was device was fabricated by successive deposition of ZnO, P3HT/PCBM and PEDOT:PSS over ITO glass	298
P3HT/ Collagen/ MAH	Photocurrent: ~60 pA at 500 ms, 1 Hz, 2–10 mW/ cm^2, 530 nm	500 ms, 1 Hz, 6 mW/ cm^2, 30 min, 530 nm	Cortical neurons, BMSCs	OptoES promoted growth of cortical neurons in the photoactive conductive hydrogel as well as neural differentiation of BMSCs	• P3HT NPs synthesis by miniemulsion method • Self-assembled P3HT/Collagen hydrogel was modified by MAH	296
PCL-P3HT/PPy	NA	40 mW/cm^2, 532 nm, 1 h/day	PC12 cells	The fabricated system had low impedance, showed free radical scavenging; Improved neurogenesis under OptoES	• Electrospinning of PCL/P3HT blend followed by in situ polymerization of PPy	287
Patterned P3HT film & P3HT/PCL	NA	28.8 W/m, 623 nm, 30 min	PC12 cells	Enhanced neurite outgrowth under OptoES	• Patterned P3HT film was fabricated by photolithography • Electrospinning of P3HT/PCL blend	299
P3HT/PCBM/ ITO	Photocurrent: ~142 pA at 20 ms, 15 mW/mm^2, 532 nm	Hippocampal neurons: 20 ms, 15 mW/mm^2, 532 nm; Retinal explant: 10 ms, 4 mW/ mm^2, 532 nm	Hippocampal neurons, Retinal explant	High light responsivity at lower threshold of 0.3 μW/ mm; OptoES promoted neuronal activity in neurons and restored light sensitivity in the retinal explant	• P3HT/PCBM blend was spin coated over ITO glass substrate • Photoactivity of P3HT as a single component was tested	286
P3HT/PEDOT: PSS/SF	NA	Visual cortical responses were recorded at flash stimuli of 20 cd/m^2, 100 ms, 0.5 Hz at 30 and 180 DPI	RCS rats	Conductive photovoltaic formulations retained photoactivity after 10 month of implantation; Visual restoration achieved by OptoES in RCS rats	• PEDOT:PSS and P3HT were sequentially spin-coated on silk substrate • Demonstrated vision restoration using photovoltaic OptoES in-vivo	205

8. ECP based NGCs toward clinical translation and challenges

The pathophysiology following PNI is highly complex, which is why only a few FDA-approved NGCs exist. These NGCs are based on selective ECM proteins or synthetic biodegradable/bioresorbable polymers, including collagen (e.g., NeuroMatrix, NeuroMend, NeuroFlex, NeuraGen, NeuraWrap, COVA ORTHO NERVE, NervAlign), chitosan (e.g., NeuroShield, ProVeil), calcium alginate and glycosaminoglycan (VersaWrap), PLCL (e.g., Neurolac, NEUROCAP, Vivosorb), poly(glycolic acid) (PGA) (Neurotube), PGA/collagen (Nerbridge), and porcine ECM (e.g., AxoGuard, Nerve Tape) [252]. Interestingly, there are currently only a few ongoing clinical trials focused on PNR, involving the use of processed human nerve grafts (Avance), PCL/PLLA (Polynerve), and decellularized, allogeneic grafts of arteries or veins (NerVFIX) [Source: https://clinicaltrials.gov/]. Obtaining FDA approval for commercialization is a lengthy and complex process, as reflected in the limited number of clinical trials for PNR. This process requires the safety and efficacy of the intended medical device or implant to be thoroughly validated from the preclinical stages. In this regard, various ECP based NGCs have been mostly validated in small animal models [100,169,253]. Despite this, preclinical studies have shown promising results using ECP-based bioelectronics and NGCs for neural recording and nerve repair, suggesting their potential for clinical translation. PEDOT, PPy, and more recently, P3HT have been leading contenders in this category. Notably, a PEDOT:PSS electrocorticogram electrode has already been tested in 30 human subjects [254]. However, a significant challenge in the clinical translation of ECP based NGCs is their poor biodegradability and bioresorbability. Additionally, delamination from the bulk scaffold in aqueous environments poses a concern for long-term stability, which is crucial for effective nerve repair. The integration of an ES module with an ECP-based NGC offers significant advantages over its non-ES counterpart and can potentially yield outcomes that are comparable to or superior to the autograft group in terms of functional recovery following PNI in small animal models [Table 6]. In addition, the absence of an effective non-invasive ES protocol, along with the practical limitations of traditional wired ES systems, remains a major constraint in preclinical studies involving ECP based NGCs in conjunction with ES. While performing ES through conductive NGCs in a sciatic nerve injury models, practical issues are often encountered such as exposed wired electrodes causing itching in the animals and health deterioration from repeated anaesthesia during ES sessions. These challenges introduce variability, complicating accurate comparisons with control groups. Most existing studies have used conventional wired ES approaches with transcutaneous electrode placement, which is intrusive and unsuited for delicate tissues such as nerve. Additionally, secondary surgeries to remove electrode wires may impede nerve regeneration further.

9. Emerging strategies for ECP based biomaterials in ES mediated PNR

9.1. Improving electrochemical performance

When implanted, neural scaffolds come into direct contact with ion-rich biological tissues and fluids. As a result, ECP based electroconductive NGCs will experience electrochemical reactions during ES in the presence of such biological fluids. The well-established reversible redox activity of ECPs causes the polymer chains to undergo continuous cycles of oxidation and reduction, interacting with ions in biological fluid. Typically, the ECP chains or networks swell during reduction and shrink during oxidation due to the influx and efflux of ions from the biological fluid. This continuous volume change induces significant structural alterations, mechanical stress, and disruption of the π-conjugation. In light of this, ECP based materials can store a large amount of charge through volumetric faradaic processes, but can suffer from poor cyclic stability [146,147]. Hence, it is always desirable to maintain a stable conductive network for efficient charge transport during ES in a hydrated environment. Besides, the volumetric change during reversible redox activity also leads to reduced bulk electrical conductivity in the polymer. As discussed in Section 4, ECP can inject charges into biological tissues and vice versa via volumetric electrochemical doping mechanism, which is favorable for an ideal bioelectronic interface. An ideal bioelectronic interface in the form of a conductive NGC for neuronal stimulation should also offer efficient charge-transfer reactions so that electron flow in the bulk of the polymer induce ion flow in the biological tissue. During the optimisation of NGCs to mimic the neural anatomy, the bulk conductivity and charge mobility of the ECP network are often compromised. Therefore, in order to develop a highly efficient bioelectronic interface for NGC with high electrical conductivity, charge density, and low electrochemical impedance, that can trigger an action potential for membrane depolarization at low stimulation potentials for neural applications, ECPs can be blended with other conductive materials including carbon based nanomaterials [207,255] and metal nanoparticles [256,257] [Fig. 10(a)]. There are reports of highly conductive CNTs blended with PEDOT yielded a three fold higher charge injection capacity (CIC) of 10.9 ± 1.9 mC cm^{-2} than a conventional TiN electrode [258]. Subsequently, this CNT/PEDOT electrode stimulated retinal ganglion neurons at a lower voltage threshold with less energy consumption, safe for biological tissues. This study combined the complementary properties of PEDOT and CNT to enhance performance: PEDOT's ability to facilitate charge transfer through valence changes in its polymer chain improves CIC, while CNT contributes high electrical conductivity, rapid charge mobility, and an increased surface area for greater electrochemical interaction and charge storage density. Xiao et al. similarly reported nitrogen doped graphene blended with PEDOT to generate an enhanced electrochemical performance with low charge transfer resistance, higher charge density and long-term stability for robust neurite outgrowth [259]. PPy was also coated over the electrospun PLA/rGO nanofibers through oxidative polymerization resulting in their increased conductivity, which showed accelerated neurite outgrowth of PC12 cells under ES [260]. Furthermore, the electroactivity of a PPy-based aligned NGC has been enhanced by incorporating fMWCNTs, which resulted in improved SC proliferation and migration, as well as promoted neural differentiation of PC12 cells [27]. The importance of low power stimulation is recognised in terms of therapeutic feasibility, and hence, there is still opportunity for further improvement in creating highly electroactive NGC. MXenes, a unique class of two-dimensional nanomaterials of transition metal carbides, nitrides, or carbonitrides, with high surface area, excellent conductivity and electrochemical properties, superior electrochemical stability, and unique surface chemistry (e.g., hydrophilicity), are expected to be one of the key players with ECP based highly electroactive bioelectronic interface for NGC development. For instance, a PLA based nerve conduit coated with PPy and titanium carbide ($Ti_3C_2T_x$) showed effective neurite growth and macrophage polarization under ES [261]. PEDOT:PSS film when incorporated with Ti_3C_2 MXene showed exceptionally high volumetric capacitance (607.0 ± 85.3 F cm^{-3}) and electrochemically stability [262], which further validates this perspective.

9.2. Integration with self-powered stimulation module

The majority of reports in clinical or laboratory settings use standard electrical stimulators to administer ES to cells or tissues via NGCs. In most situations, conventional electrical stimulators rely on external AC or DC power supplies, which are costly, bulky and non-portable. Furthermore, an electrical stimulator connected to a 220 V power source attached to a patient's body may be painful, unpleasant, and risky. Battery-based power sources like Li-ion batteries, have also limitations in terms of their functionality, their rigid structure, conformity, potential toxicity and limited lifetime. An additional concern that is the removal of the battery after the desired function through a secondary surgery, which is again a costly and risky process for a patient with nerve injury. Consequently, numerous studies have underscored the necessity

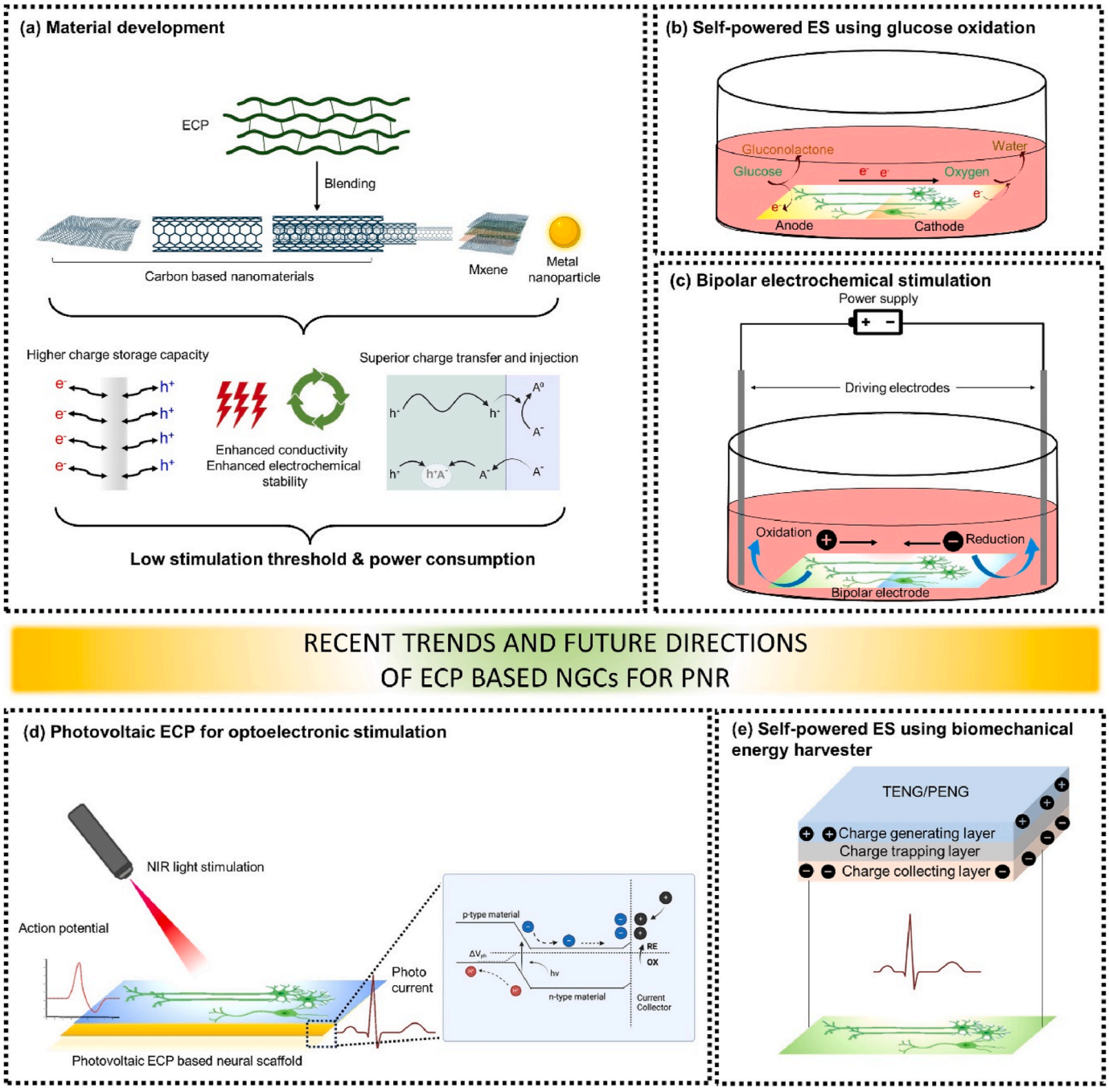

Fig. 10. Schematic illustration showing recent strategies employed for development for ECP based NGCs combined with ES delivery methods for PNR focussing on (a) Material development, (b) Self-powered ES using glucose oxidation, (c) Bipolar electrochemical stimulation, (d) Photovoltaic ECP for optoelectronic stimulation, and (e) Self-powered ES using biomechanical energy harvester.

of creating a self-powered ES system that is both portable and durable, with a compact size and minimal weight, and that can be integrated with an NGC based on ECP for neuronal stimulation.

Implantable piezoelectric nanogenerators (PENGs) or triboelectric nanogenerators (TENGs), can harvest irregular biomechanical human energy and convert it into useable electrical energy, [136,263]. The development of both PENG and TENG technologies has been pioneered by Z. L. Wang's research group at the Georgia Institute of Technology, USA. Their work has demonstrated the effective use of these technologies to harness bodily movements, such as muscle contractions, walking, or heartbeat, to produce functional electrical outputs [264–266]. Although such electrical output depends on the material's durability and the source frequency, it can align with the endogenous electric field observed during nerve injury. These outputs (PENGs: 40 mV-30 V, 36–80 μA; TENGs: 50 mV-47 V, 0.6–30 μA), harvested from ambient irregular biomechanical energy, are sufficient to enable therapeutic ES for nerve repair [76,263,267–274].

PENGs utilize the electric charges generated during mechanical stress through the piezoelectric effect [269–271]. The implementation of PENG or self-powered piezoelectrical systems in PNR has recently commenced [269–274]. These studies have successfully demonstrated the fabrication of implantable PENGs or self-powered piezoelectrical systems using biocompatible synthetic polymers, such as polyvinylidene fluoride (PVDF), poly-ε-caprolactone (PCL), poly(L-lactic acid) (PLLA),

and poly(3-hydroxybutyrateco-3-hydroxyvalerate) (PHBV) [269–271]. The electricity generated was then utilized for electrically stimulated nerve regeneration [Fig. 10(e)]. Most of these or self-powered piezoelectrical devices were mainly focussed on delivering the ES (not localized and controlled) with or without having any scaffolding role in PNR, with ultrasound or body movement as the source for mechanical stimulation of the material. It is to be noted that efficient energy harvesting depends on the choice of piezoelectric materials (i.e., dielectric constant) and design configuration of the piezoelectrical device. Hence, it is very challenging to achieve energy harvesting with an ideal piezoelectric NGC design architecture. A notable advancement in this area involved the integration of a piezoelectric device, composed of potassium sodium niobate nanowires, PLLA, and PHBV encapsulated with PCL or PLA, with a NGC made of hydroxyethyl cellulose (HEC), soy protein isolate (SPI), and conductive black phosphorus (BP) nanosheets [271]. This system demonstrates an ultrasound-driven (100 kHz) piezoelectric effect for delivering ES (12 V, 36 μA) in a rat sciatic nerve injury model. Another strategically designed piezoelectric scaffold (not in ideal NGC architecture) composed of silk fibroin (SF), PVDF-HFP, and Ti_3C_2Tx MXene was used to generate electrical output of ~100 mV and body movement was utilized as mechanical energy source for ES to promote nerve repair in vivo [272]. Studies in this direction have just recently emerged and only very recently, a PVDF/PLCL piezoelectrical device was integrated successfully with an ECP based PEDOT/SF cryogel scaffold [273]. The system used mechanical deformation from body movement and surrounding tissue forces to generate piezoelectric stimulation (~500 mV) in a rat sciatic nerve injury model. Hence, integration of ECP based NGCs with PENGs can be viable option for self-powered ES in PNR. The viability of this approach is also inspired by effective integration of TENGs with ECP based neural scaffolds for self-powered electrically stimulated nerve repair [Fig. 7(e)] [207]. TENGs can convert biomechanical energy into electricity with the coupling of triboelectric effects and electrostatic induction [263]. In both PENGs and TENGs, a highly conductive current collector is essential to collect the electric charges, generated during the piezoelectric process and triboelectrification. ECPs or a hybrid blend of ECPs with carbon based nanomaterials can effectively play this role and can ensure efficient utilisation of harvested electricity for ES. Guo et al. fabricated a highly conductive rGO/PEDOT microfibrous neural scaffold (up to 2.41 S/cm) [207]. This conductive microfibrous scaffold was integrated with a TENG with current output 30 μA for delivering ES to promote the neural differentiation of mesenchymal stem cells (MSCs). However, the current output obtained from PENGs/piezoelectrical systems or TENGs are generally very low, ranging from several pA to few μA [47,136,263,269–271]. Therefore, while integration of such sustainable power sources with conductive NGCs is fascinating, one need to mindful to enhance the electroactivity of the NGC sufficiently so that they can effectively utilize low current output for ES purpose. For this, strategies discussed in the preceding section can be adopted.

9.3. Bipolar ECP based scaffolds for wireless ES

The majority of ES studies which employs ECP or other conducting materials have used standard wired ES modules for nerve repair with a very high efficiency [32,155,168,219,275]. Nevertheless, difficulties that arise from using wired electrodes on a target site have not been adequately addressed. The highly invasive wiring that connects the power supply to the tissue or conductive scaffold at the stimulation site, raises concerns regarding infection, bleeding, loosening, secondary nerve injury, and anaesthetic complications [276]. The hardwired power supply can also limit patient movement during ES in clinical settings, thereby decreasing stimulation efficacy. Device failure owing to persistent fatigue on wires, patient discomfort, and post-surgical pain are all additional risks related with the wired ES approach. In the last decade, non-invasive wireless stimulation techniques have evolved as an alternative to traditional wired ES methods, effectively overcoming the constraints noted above. In tandem, ECP based scaffolds have been investigated in connection with one of the new wireless stimulation techniques, which works on the principle of bipolar electrochemistry for neural applications [276–280].

A pioneering work Rajnicek et al. showed that dipole polarization can be induced in conducting substrates, preferably one with mixed ionic-electronic features or species of different redox behaviours, under the influence of an externally applied electric field [Fig. 10(c)] [277]. The electric field was generated in the culture medium by two driving electrodes connected to a power supply (not connected to the conducted substrate). The generated electric field induces electrochemical interactions/changes in the conducting substrate including charge transfer with the cell culture medium and the neuronal cells seeded on them. Therefore, the conducting scaffold needs to possess sufficient bipolar characteristics potentially at the two extremities for oxidation and reduction reactions, which can induce charge carrier movement in the bulk of the polymer. The first bipolar electroactivity in an ECP was reported by Ishiguro et al., in a polythiophene based derivative, poly (3-methylthiophene) (P3MT) [281]. Since then, various ECPs, such as PEDOT, PAni and PPy, have been shown to exhibit bipolar electroactivity [280], which can be further enhanced by incorporating different dopants or blending with suitable redox-active species. This is attributed to their ease of processing, versatility, and high redox activity. However, the development of ECP-based bipolar neural scaffolds for bipolar electrochemical stimulation is still in its early stages, with only limited evidence available. In a significant development in this direction, Qin et al. of the Intelligent Polymer Research Group at University of Wollongong demonstrated reversible and recoverable bipolar electrochemical activity of PPy based films using biologically relevant dopants dextran sulfate (DS) and collagen [276]. The resultant PPy film was capable to direct neurite outgrowth in PC12 cells under bipolar electrochemical stimulation, which was achieved at a much lower driving voltage ($\leq$1 V/cm) compared to metallic bipolar electrodes. Recently, the same research group developed a tissue compatible soft, and flexible ECP based bipolar scaffold, with superior bipolar electrochemical properties, using PPy co-doped with redox active poly (2-methoxyaniline-5-sulfonic acid) (PMAS) and collagen, which was further blended with PEDOT:PSS [280]. Wireless bipolar electrochemical stimulation was successfully administrated to PC12 and SH-SY5Y cells for enhanced neural differentiation using the same scaffold. Research in this area is still emerging, and considerable effort is required to develop ECP-based bipolar scaffolds that mimic neural anatomy, to effectively apply this wireless, non-invasive ES for PNR.

9.4. Glucose oxidation for self-powered wireless ES

In one interesting approaches of wireless self-powered energy generation, endogenous glucose in bodily fluid can be oxidized to generate electrical energy, which can be used to power implantable medical devices [282]. This technique was utilized to develop both implantable and external glucose biofuel cells to energy generation [283]. Typically, in a glucose biofuel cell, glucose is oxidized at an anode and oxygen is reduced to water at the cathode [Fig. 10(b)]. The anode and cathode are often divided into distinct chambers by an ion-selective membrane, which allows protons produced by oxidation at the anode to travel unidirectionally to the cathode. Charge neutrality in the whole cell is restored via a redox process involving the protons that arrive at the cathode through the solution, the electrons that arrive at the cathode through the external circuit, and the oxidant at the cathode. A suitable bioelectronic interface with a distinct anodic and cathodic region can carefully be designed, by incorporating an oxidizing agent at the anode for glucose oxidation. For instance, Rapoport et al. devised a bioelectronic substrate for glucose fuel cells based on nanostructured Pt and single-walled carbon nanotubes that can provide up to 180 mW cm^{-2} of peak power and 3.4 mW cm^{-2} of steady-state power as brain-machine interface [284]. Inspired by this, a PPy/bacterial cellulose based

nanofibrous scaffold was designed using Pt deposition at one side (anode), while depositing nitrogen doped CNTs (cathode) for glucose oxidation [285]. The study demonstrated an electric potential generation up to 300 mV in PBS with glucose concentration of 5×10^{-3} M. This self-powered ES system in presence of glucose showed longer neurite outgrowth in DRGs than that without glucose oxidation. Additional research is required to thoroughly investigate the potential of physiologic glucose oxidation-based self-powered ES technology when combined with ECP-based neural scaffolds for PNR.

9.5. Photovoltaic ECP based scaffolds for optoelectronic stimulation (OptoES)

One other wireless ES approach involves utilisation of optoelectronic or photovoltaic materials, which can convert light energy into photocurrent through an internal conversion mechanism [286–290]. This optoelectronic wireless stimulation offers several advantages, including deep cell and tissue penetration (e.g., with NIR light), improved spatial localization and resolution, and no harmful effects on biological tissue [204,286,291]. Light sources in the red to near-infrared range have been shown to successfully achieve optoelectronic stimulation for nerve regeneration in vivo. Optoelectronic stimulation using white, and red to NIR laser were successfully demonstrated for restoration of vision in blind rats P3HT based retinal implants [205,286,292]. Recently, Sun et al. developed an optoelectronic device using a thin-film silicon diode interfaced with molybdenum (Mo), which enabled highly efficient charge injection and ES for the functional recovery of injured facial nerves, as well as sciatic nerve stimulation in SD rats using a 635 nm laser [290]. Photovoltaic materials, like inorganic silicon based optoelectronics have been demonstrated to convert light inputs into electric signals to stimulate neurons and peripheral nerve [289,290,293]. However, most of these devices have been optimized for dry environments, and their rigidity and susceptibility to corrosion under physiological conditions make them less suitable for interfacing with biological tissues [204]. In this context, organic photovoltaic materials, such as ECP based optoelectronics, are better suited for biological tissues due to their soft, flexible nature and mixed ionic-electronic transport behaviour. However, not all ECPs exhibit photovoltaic properties, with only a few polythiophene-based derivatives, such as P3HT and P3MT, demonstrating such capabilities. In addition to being electrically conductive, a photovoltaic material must also be capable of absorbing light and converting it into electricity. Organic semiconductors can induce neuromodulation through photovoltaic conversion, or/and photothermal conversion or/and photocatalytic reactions [294]. In ECP based photovoltaics, all three processes co-exist depending upon light illumination parameters (wavelength, duration, power, intensity) as well as on the material or device properties. Organic photovoltaics stimulate neural activity via capacitive coupling or reversible Faradaic processes at the material's surface or within its bulk. When light is absorbed, charges either accumulate at the surface, affecting the surface-electrolyte double layer, or are transferred into the solution via Faradaic reactions [Fig. 10(d)]. Effective stimulation is based on energetic asymmetry in the semiconductor, which facilitates charge transfer at the electrolyte interface. Spatial asymmetry, which is commonly achieved using heterojunctions, increases carrier generation and potential difference in the surrounding electrolyte. When a semiconductor is combined with conductors as anode and/or cathode, efficiency increases. The specific stimulation mechanism is determined by the interfaced materials, favouring capacitive coupling or Faradaic processes. Organic semiconductors allow for photovoltaic neurostimulation with pulse durations ranging from a few to several tens of milliseconds and intensity levels below 1 mW/mm^2, falling within the conventional neurostimulation range. A pioneering work showing optoelectronic stimulation of hippocampal neurons via photovoltaic (capacitive) mechanism using P3HT based bulk heterojunction blended with [6, 6]-Phenyl C61-butyric acid methyl ester (PC60BM) and ITO, was reported by Ghezzi et al. [291] whereby a laser pulse of 532 nm at 10 mW/mm^2 was used for photostimulation, which yielded a photocurrent in pA range. To optimize energy conversion based on the solar cell principle, the bulk heterojunction architecture should be designed to expand the interface between the donor (p-type) and acceptor (n-type) materials. Additionally, a highly conductive layer is integrated with the heterojunction to enhance the likelihood of charge pair separation under stimulation and subsequent charge collection. For example, a P3HT-based implant with a standard solar cell configuration was shown to induce photostimulation of retinal neurons through a photovoltaic mechanism and successfully demonstrated visual restoration in a Royal College of Surgeons (RCS) rat model of retinal dystrophy [205]. The implant was constructed in a multilayered configuration, featuring a semiconducting P3HT layer attached to a highly conductive PEDOT:PSS layer on a biocompatible and flexible silk fibroin substrate. The conductive PEDOT:PSS layer serves to collect the holes generated during light stimulation through capacitive charging and accumulates negative charges at the polymer/biological fluid interface. In an effort to further improve the photoconversion efficiency, PEDOT:PSS layer was substituted with a more conductive graphene layer for effective charge extraction from photovoltaic P3HT layer [204]. The implant was shown to modulate action potentials in primary hippocampal neurons and restore light sensitivity in blind retinal explants. This emerging field of using organic photovoltaic materials for neuronal stimulation holds significant promise for wireless ES in nerve repair. Recently, there has been a notable increase in research utilizing P3HT-based photovoltaic interfaces for neuronal stimulation [287,295,296]. However, the efficiency, particularly in terms of generated photocurrent, remains low (in the pA range) and needs to be improved. Additionally, the application of ECP based photovoltaic materials in the design and fabrication of NGCs is still in its early stages, and it is crucial to maintain the essential heterojunction architecture for effective electron-hole generation under light illumination. Table 7 summarizes the studies on P3HT based conductive photovoltaic biomaterials involving optoelectronic neuronal stimulation.

10. Future perspectives and conclusions

While numerous in vitro studies have explored the fundamental principles of using ECP based bioactive scaffolds to deliver ES to neural cells, resulting in enhanced neurite outgrowth, neural differentiation, and proliferation; there is not enough of pre-clinical or in vivo studies investigating the use of ES with ECP-based NGCs, a short-coming that limits clinical translation of ECP based biomaterials. Although several studies have demonstrated that PPy and PEDOT based NGCs support functional recovery in sciatic nerve injury models after long-term implantation with little to no immune response; safety and efficacy still remain significant limitations for ECP based NGCs. When blended with non-conductive materials prior to 3D scaffold fabrication techniques (e.g., electrospinning, 3D printing, freeze-drying, etc.), it is essential to ensure that the ECP fillers are evenly distributed within the blend or dispersion to achieve the percolation threshold, thereby forming a well-connected conductive network. Such reduction in electroactivity necessitates higher ES parameters, such as increased electric field or current, to facilitate charge transfer at the scaffold-tissue interface, but use of high stimulation parameters also raises the risk of electrochemical degradation and tissue damage.

An additional challenge is administering ES to nerve injury site in a living body. Clinically, ES is typically applied externally via adhesive electrodes or through invasive microelectrode implantation for conditions like Parkinson's disease or neurotrophic pain. However, no standardized protocol exists for ES delivery in PNR using ECP based NGCs We have summarized various non-invasive ES modules currently being evaluated with ECP based scaffolds, including self-powered approaches using implantable TENG/PENG devices or glucose oxidation, bipolar electrochemical stimulation, and opto-electronic photovoltaic

stimulation.

The synthesis and fabrication procedures have a considerable impact on the characteristics and performance of ECP based NGCs, as is commonly acknowledged. These procedures entail selecting various processing components, such as appropriate reagents (such as dopants and oxidants), to produce specified material properties. These qualities include conductivity, mechanical properties, biocompatibility, biodegradability, target tissue architecture, component spatial distribution, and anisotropic properties. While there are significant efforts are currently being devoted, it is equally important to address their biodegradability and bioresorbability to align with the bioactive properties of existing commercial NGCs (e.g., NeuraGen, Neurolac, etc.). One potential approach is to leverage the flexible chemical synthesis process of ECPs or their unique doping-dedoping characteristics. Since ECPs are susceptible to anionic dopants, various negatively charged biomolecules can be incorporated into their structure. Indeed, anionic biomolecules such as hyaluronic acid (HA), chondroitin sulfate (CS), amino acids like lysine and glutamate, and even the RGD peptide, have been used as primary or secondary dopants for various ECPs, demonstrating enhanced conductive properties [300–304]. ECPs synthesized or modified through this bioactive doping approach can also be blended with other electrochemically stable conductive materials (e.g., carbon based nanomaterials) to create biohybrid electroactive biomaterials with improved biodegradability and bioresorbability.

Similarly, the recently demonstrated non-invasive bipolar electrochemical stimulation has only been tested in vitro. It is still unclear how 'the driving electrodes' can be positioned non-invasively for in vivo ES. One potential solution is to replace these electrodes with TENG/PENG systems, which could generate an electric field at the injury site and induce redox reactions on the ECP based bipolar NGC, enabling non-invasive ES. Another area that has received limited attention is the study of immunoregulation mechanisms under ES during PNI, which remain poorly understood. Gaining a clearer understanding of these mechanisms could pave the way for more effective therapeutic interventions in PNR. Stem cell therapy combined with ECP-based ES has shown potential for promoting functional nerve regeneration, as demonstrated by Song et al. [168], and this approach should be further explored using recent innovative wireless ES strategies.

Future research efforts also need to consider and embrace artificial intelligence (AI) and machine learning (ML) approaches, which can offer innovative and advanced solutions for NGC design, optimisation of ES protocols and their integration. AI has rapidly evolved due to advancements in computer hardware and deep learning technologies, particularly in healthcare applications, which has been acknowledged by FDA as well as 26 AI based healthcare solutions which were approved by 2019. Stewart et al. highlighted how AI can enable the creation of personalized NGCs by analysing patient-specific anatomical data, such as nerve dimensions and injury characteristics, to tailor conduit designs for optimal outcomes [305]. Deep learning models could potentially optimize scaffold architectures, biomaterial properties (e.g., conductivity, biodegradability), and electrical parameters to ensure effective axonal growth and functional nerve regeneration. Furthermore, AI enhances 3D bioprinting processes by reducing variability and enhancing precision and scalability. Iterative enhancements and the reduction of experimental time can be facilitated by such predictive algorithms, which can evaluate the performance of NGC under various conditions. ML models can be used to effectively optimize the ES protocols (e.g. amplitude, frequency, pulse width, duration) based on the real time feedback from the neural environment with the help of electroneurograms or other sensors [306–308]. Advanced techniques like convolutional neural networks and genetic algorithms can further be employed to fine tune these protocols for precise and selective neural activation depending on treatment requirement. This domain, which is highly interdisciplinary, has only recently emerged and has the potential to significantly improve the machine-assisted production and design of NGC by incorporating data from advanced imaging and computational modelling.

In addition to the technological advancements, the development of appropriate ethical and regulatory frameworks is essential as ES technology becomes more prevalent in clinical settings, particularly for treating neurological disorders. Since ES can alter neurological functions and other biological processes, ethical considerations such as consent, privacy, and the risk of misuse of information, must be carefully addressed. Regulatory bodies will need to establish stringent standards for future ES devices and therapies to strike a balance between innovation and patient safety.

A deeper understanding of the complex interactions between ECP based biomaterials, electrical signals, nerve tissue, and surrounding tissues could pave the way for more efficient, personalized, and integrated therapeutic strategies for functional nerve regeneration. This knowledge could also be applied to the repair of other electrically excitable tissues, making the combined use of ES and ECP based biomaterials a promising approach to address some of the most pressing medical challenges and ultimately improve patient quality of life.

Any data reported in this review will be available upon reasonable request.

CRediT authorship contribution statement

Rajiv Borah: Writing – review & editing, Writing – original draft, Validation, Methodology, Investigation, Formal analysis, Data curation, Conceptualization. **Daniel Diez Clarke:** Writing – review & editing, Writing – original draft, Formal analysis. **Jnanendra Upadhyay:** Writing – review & editing, Writing – original draft. **Michael G. Monaghan:** Writing – review & editing, Writing – original draft, Validation, Supervision, Project administration, Methodology, Funding acquisition, Data curation, Conceptualization.

Declaration of competing interest

The authors declare that they have no known competing financial interests or personal relationships that could have appeared to influence the work reported in this paper.

Acknowledgements

This project has received funding from the European Union's Horizon 2020 research and innovation programme under the Marie Skłodowska-Curie grant agreement No 101067283, and from the European Research Council (ERC) under the European Union's Horizon 2020 research and innovation programme (Grant agreement No. 101125153. MM and DDC acknowledge CRY Ireland for Michael Greene Cardiac Risk in the Young (CRY) summer scholarship (CRYUG/2023/001).

Data availability

Data will be made available on request.

References

[1] Y. Huang, Y. Li, H. Pan, L. Han, Global, regional, and national burden of neurological disorders in 204 countries and territories worldwide, Journal of global health 13 (2023).
[2] K. Houschyar, A. Momeni, M. Pyles, J. Cha, Z. Maan, D. Duscher, O. Jew, F. Siemers, J.v. Schoonhoven, The role of current techniques and concepts in peripheral nerve repair, Plastic surgery international 2016 (1) (2016) 4175293.
[3] K.S. Katiyar, S. Das, J.C. Burrell, D.K. Cullen, Scaffolds for bridging sciatic nerve gaps, in: Handbook of Tissue Engineering Scaffolds: Volume Two, Elsevier, 2019, pp. 67–93.
[4] S. Vijayavenkataraman, Nerve guide conduits for peripheral nerve injury repair: a review on design, materials and fabrication methods, Acta Biomater. 106 (2020) 54–69.
[5] M. Anderson, N.B. Shelke, O.S. Manoukian, X. Yu, L.D. McCullough, S.G. Kumbar, Peripheral nerve regeneration strategies: electrically stimulating polymer based

nerve growth conduits, Critical Reviews™ in Biomedical Engineering 43 (2–3) (2015).
[6] E.W. Wang, J. Zhang, J.H. Huang, Repairing peripheral nerve injury using tissue engineering techniques, Neural regeneration research 10 (9) (2015) 1393–1394.
[7] D. Cinteza, I. Persinaru, B.M.M. Zarnescu, D. Ionescu, I. Lascar, Peripheral nerve regeneration–an appraisal of the current treatment options, Maedica 10 (1) (2015) 65.
[8] R.N. Murphy, C. de Schoulepnikoff, J.H. Chen, M.O. Columb, J. Bedford, J. K. Wong, A.J. Reid, The incidence and management of peripheral nerve injury in England (2005–2020), J. Plast. Reconstr. Aesthetic Surg. 80 (2023) 75–85.
[9] A.C. Ruijs, J.-B. Jaquet, S. Kalmijn, H. Giele, S.E. Hovius, Median and ulnar nerve injuries: a meta-analysis of predictors of motor and sensory recovery after modern microsurgical nerve repair, Plast. Reconstr. Surg. 116 (2) (2005) 484–494.
[10] X. Jia, M.I. Romero-Ortega, Y.D. Teng, Peripheral nerve regeneration: mechanism, cell biology, and therapies, BioMed Res. Int. 2014 (2014).
[11] A.K. Singh, Peripheral nerve injuries–A call for better evaluation and preventive measures, Neurol. India 65 (3) (2017) 556–557.
[12] E. Manousiouthakis, J. Park, J.G. Hardy, J.Y. Lee, C.E. Schmidt, Towards the translation of electroconductive organic materials for regeneration of neural tissues, Acta Biomater. 139 (2022) 22–42.
[13] C.E. Schmidt, J.B. Leach, Neural tissue engineering: strategies for repair and regeneration, Annu. Rev. Biomed. Eng. 5 (1) (2003) 293–347.
[14] W. Zhou, M.S.U. Rahman, C. Sun, S. Li, N. Zhang, H. Chen, C.C. Han, S. Xu, Y. Liu, Perspectives on the novel multifunctional nerve guidance conduits: from specific regenerative procedures to motor function rebuilding, Adv Mater 36 (14) (2024) 2307805.
[15] C. Zhang, J. Gong, J. Zhang, Z. Zhu, Y. Qian, K. Lu, S. Zhou, T. Gu, H. Wang, Y. He, Three potential elements of developing nerve guidance conduit for peripheral nerve regeneration, Adv. Funct. Mater. 33 (40) (2023) 2302251.
[16] M. Sarker, S. Naghieh, A.D. McInnes, D.J. Schreyer, X. Chen, Strategic design and fabrication of nerve guidance conduits for peripheral nerve regeneration, Biotechnol. J. 13 (7) (2018) 1700635.
[17] B. Song, M. Zhao, J. Forrester, C. McCaig, Nerve regeneration and wound healing are stimulated and directed by an endogenous electrical field in vivo, J. Cell Sci. 117 (20) (2004) 4681–4690.
[18] C. McCaig, A. Rajnicek, Electrical fields, nerve growth and nerve regeneration, Exp. Physiol.: Translation and Integration 76 (4) (1991) 473–494.
[19] N. Haan, B. Song, Therapeutic application of electric fields in the injured nervous system, Adv. Wound Care 3 (2) (2014) 156–165.
[20] Y. Huang, K. Yao, Q. Zhang, X. Huang, Z. Chen, Y. Zhou, X. Yu, Bioelectronics for electrical stimulation: materials, devices and biomedical applications, Chem. Soc. Rev. 53 (2024) 8632–8712.
[21] F. Jin, T. Li, T. Yuan, L. Du, C. Lai, Q. Wu, Y. Zhao, F. Sun, L. Gu, T. Wang, Physiologically self-regulated, fully implantable, battery-free system for peripheral nerve restoration, Adv Mater 33 (48) (2021) 2104175.
[22] Z. Wei, F. Jin, T. Li, L. Qian, W. Zheng, T. Wang, Z.Q. Feng, Physical cue-based strategies on peripheral nerve regeneration, Adv. Funct. Mater. 33 (3) (2023) 2209658.
[23] H. Yi, R. Patel, K.D. Patel, L.-S. Bouchard, A. Jha, A.W. Perriman, M. Patel, Conducting polymer-based scaffolds for neuronal tissue engineering, J. Mater. Chem. B 11 (46) (2023) 11006–11023.
[24] M.R. Abidian, E.D. Daneshvar, B.M. Egeland, D.R. Kipke, P.S. Cederna, M. G. Urbanchek, Hybrid Conducting Polymer–Hydrogel Conduits for Axonal Growth and Neural Tissue Engineering, 2012.
[25] R.A. Nasser, S.S. Arya, K.H. Alshehhi, J.C. Teo, C. Pitsalidis, Conducting polymer scaffolds: a new frontier in bioelectronics and bioengineering, Trends Biotechnol. 42 (6) (2024) 760–779.
[26] C.E. Schmidt, V.R. Shastri, J.P. Vacanti, R. Langer, Stimulation of neurite outgrowth using an electrically conducting polymer, Proc. Natl. Acad. Sci. USA 94 (17) (1997) 8948–8953.
[27] S. Shrestha, B.K. Shrestha, J.I. Kim, S. Won Ko, C.H. Park, C.S. Kim, Electrodeless coating polypyrrole on chitosan grafted polyurethane with functionalized multiwall carbon nanotubes electrospun scaffold for nerve tissue engineering, Carbon 136 (2018) 430–443, https://doi.org/10.1016/j.carbon.2018.04.064.
[28] H.-S. Ahn, J.-Y. Hwang, M.S. Kim, J.-Y. Lee, J.-W. Kim, H.-S. Kim, U.S. Shin, J. C. Knowles, H.-W. Kim, J.K. Hyun, Carbon-nanotube-interfaced glass fiber scaffold for regeneration of transected sciatic nerve, Acta Biomater. 13 (2015) 324–334.
[29] C. Dong, F. Qiao, W. Hou, L. Yang, Y. Lv, Graphene-based conductive fibrous scaffold boosts sciatic nerve regeneration and functional recovery upon electrical stimulation, Appl. Mater. Today 21 (2020) 100870.
[30] P.C. Sherrell, B.C. Thompson, J.K. Wassei, A.A. Gelmi, M.J. Higgins, R.B. Kaner, G.G. Wallace, Maintaining cytocompatibility of biopolymers through a graphene layer for electrical stimulation of nerve cells, Adv. Funct. Mater. 24 (6) (2014) 769–776.
[31] J. Wang, Y. Cheng, L. Chen, T. Zhu, K. Ye, C. Jia, H. Wang, M. Zhu, C. Fan, X. Mo, In vitro and in vivo studies of electroactive reduced graphene oxide-modified nanofiber scaffolds for peripheral nerve regeneration, Acta Biomater. 84 (2019) 98–113.
[32] J.M. Das, J. Upadhyay, M.G. Monaghan, R. Borah, Impact of the reduction time-dependent electrical conductivity of graphene nanoplatelet-coated aligned Bombyx mori silk scaffolds on electrically stimulated axonal growth, ACS Appl. Bio Mater. 7 (4) (2024) 2389–2401.
[33] M. Liao, Y. Hu, Y. Zhang, K. Wang, Q. Fang, Y. Qi, Y. Shen, H. Cheng, X. Fu, M. Tang, 3D Ti3C2T x MXene–matrigel with electroacoustic stimulation to promote the growth of spiral ganglion neurons, ACS Nano 16 (10) (2022) 16744–16756.
[34] R. Guo, M. Xiao, W. Zhao, S. Zhou, Y. Hu, M. Liao, S. Wang, X. Yang, R. Chai, M. Tang, 2D Ti3C2TxMXene couples electrical stimulation to promote proliferation and neural differentiation of neural stem cells, Acta Biomater. 139 (2022) 105–117.
[35] F. Qi, R. Liao, L. Yang, M. Yang, H. Li, G. Chen, S. Peng, S. Yang, C. Shuai, Photoexcited wireless electrical stimulation elevates nerve cell growth, Colloids Surf. B Biointerfaces 220 (2022) 112890.
[36] J.S. Park, K. Park, H.T. Moon, D.G. Woo, H.N. Yang, K.-H. Park, Electrical pulsed stimulation of surfaces homogeneously coated with gold nanoparticles to induce neurite outgrowth of PC12 cells, Langmuir 25 (1) (2009) 451–457.
[37] G. Zhao, H. Zhou, G. Jin, B. Jin, S. Geng, Z. Luo, Z. Ge, F. Xu, Rational design of electrically conductive biomaterials toward excitable tissues regeneration, Prog. Polym. Sci. 131 (2022) 101573.
[38] C.J. Bettinger, J.P. Bruggeman, A. Misra, J.T. Borenstein, R. Langer, Biocompatibility of biodegradable semiconducting melanin films for nerve tissue engineering, Biomaterials 30 (17) (2009) 3050–3057.
[39] K. Namsheer, C.S. Rout, Conducting polymers: a comprehensive review on recent advances in synthesis, properties and applications, Rsc Adv 11 (10) (2021) 5659–5697.
[40] J. Upadhyay, T.M. Das, R. Borah, K. Paul, K. Acharjya, Ternary nanocomposites of rGO: RuO2: pani based flexible electrode for supercapacitor applications, Solid State Commun. 334 (2021) 114382.
[41] J. Upadhyay, T.M. Das, R. Borah, K. Acharjya, Electrochemical performance evaluation of polyaniline nanofibers and polypyrrole nanotubes, Mater. Today: Proc. 32 (2020) 274–279.
[42] J. Jang, Conducting polymer nanomaterials and their applications, Emissive materials nanomaterials (2006) 189–260.
[43] A.B. Kaiser, V. Skákalová, Electronic conduction in polymers, carbon nanotubes and graphene, Chem. Soc. Rev. 40 (7) (2011) 3786–3801.
[44] J. Rivnay, S. Inal, A. Salleo, R.M. Owens, M. Berggren, G.G. Malliaras, Organic electrochemical transistors, Nat. Rev. Mater. 3 (2) (2018) 1–14.
[45] J. Rivnay, S. Inal, B.A. Collins, M. Sessolo, E. Stavrinidou, X. Strakosas, C. Tassone, D.M. Delongchamp, G.G. Malliaras, Structural control of mixed ionic and electronic transport in conducting polymers, Nat. Commun. 7 (1) (2016) 11287.
[46] Y. Liu, X. Zhang, C. Xiao, B. Liu, Engineered hydrogels for peripheral nerve repair, Materials Today Bio 20 (2023) 100668.
[47] L.E. Shlapakova, M.A. Surmeneva, A.L. Kholkin, R.A. Surmenev, Revealing an important role of piezoelectric polymers in nervous-tissue regeneration: a review, Materials Today Bio (2024) 100950.
[48] Y. Xu, X. Liu, M.A. Ahmad, Q. Ao, Y. Yu, D. Shao, T. Yu, Engineering cell-derived extracellular matrix for peripheral nerve regeneration, Materials Today Bio 27 (2024) 101125.
[49] Y. Zhang, S. Chen, Z. Xiao, X. Liu, C. Wu, K. Wu, A. Liu, D. Wei, J. Sun, L. Zhou, Magnetoelectric nanoparticles incorporated biomimetic matrix for wireless electrical stimulation and nerve regeneration, Adv. Healthcare Mater. 10 (16) (2021) 2100695.
[50] T. Marques-Almeida, S. Lanceros-Mendez, C. Ribeiro, State of the Art and Current challenges on Electroactive Biomaterials and strategies for neural tissue regeneration, Adv. Healthcare Mater. 13 (1) (2024) 2301494.
[51] Y. Zhao, Y. Liu, S. Kang, D. Sun, Y. Liu, X. Wang, L. Lu, Peripheral nerve injury repair by electrical stimulation combined with graphene-based scaffolds, Front. Bioeng. Biotechnol. 12 (2024) 1345163.
[52] S. Sunderland, A classification of peripheral nerve injuries producing loss of function, Brain 74 (4) (1951) 491–516.
[53] S.S. Sunderland, The anatomy and physiology of nerve injury, Muscle Nerve: Official Journal of the American Association of Electrodiagnostic Medicine 13 (9) (1990) 771–784.
[54] T. Matsuyama, M. Mackay, R. Midha, Peripheral nerve repair and grafting techniques: a review, Neurol. Med.-Chir. 40 (4) (2000) 187–199.
[55] M. Sarker, S. Naghieh, A.D. McInnes, D.J. Schreyer, X. Chen, Regeneration of peripheral nerves by nerve guidance conduits: influence of design, biopolymers, cells, growth factors, and physical stimuli, Progress in neurobiology 171 (2018) 125–150.
[56] D. Arslantunali, T. Dursun, D. Yucel, N. Hasirci, V. Hasirci, Peripheral nerve conduits: technology update, Med. Dev. Evid. Res. (2014) 405–424.
[57] A. Faroni, S.A. Mobasseri, P.J. Kingham, A.J. Reid, Peripheral nerve regeneration: experimental strategies and future perspectives, Adv. Drug Deliv. Rev. 82 (2015) 160–167.
[58] A.H. Koeppen, Wallerian degeneration: history and clinical significance, Journal of the neurological sciences 220 (1) (2004) 115–117.
[59] R. López-Cebral, J. Silva-Correia, R. Reis, T. Silva, J. Oliveira, Peripheral nerve injury: current challenges, conventional treatment approaches, and new trends in biomaterials-based regenerative strategies, Acs Biomater Sci Eng 3 (12) (2017) 3098–3122.
[60] L. Kong, X. Gao, Y. Qian, W. Sun, Z. You, C. Fan, Biomechanical microenvironment in peripheral nerve regeneration: from pathophysiological understanding to tissue engineering development, Theranostics 12 (11) (2022) 4993.
[61] G. Wu, X. Wen, R. Kuang, K.W. Lui, B. He, G. Li, Z. Zhu, Roles of macrophages and their interactions with schwann cells after peripheral nerve injury, Cell. Mol. Neurobiol. 44 (1) (2024) 11.
[62] X. Dong, P. Wu, L. Yan, K. Liu, W. Wei, Q. Cheng, X. Liang, Y. Chen, H. Dai, Oriented nanofibrous P (MMD-co-LA)/Deferoxamine nerve scaffold facilitates

peripheral nerve regeneration by regulating macrophage phenotype and revascularization, Biomaterials 280 (2022) 121288.
[63] L. Ghasemi-Mobarakeh, M.P. Prabhakaran, M. Morshed, M.H. Nasr-Esfahani, H. Baharvand, S. Kiani, S.S. Al-Deyab, S. Ramakrishna, Application of conductive polymers, scaffolds and electrical stimulation for nerve tissue engineering, Journal of tissue engineering and regenerative medicine 5 (4) (2011) e17–e35.
[64] S. Meng, M. Rouabhia, Z. Zhang, D. De, F. De, U. Laval, Electrical stimulation in tissue regeneration, Applied biomedical engineering (2011) 37–62.
[65] M. Mattioli-Belmonte, G. Giavaresi, G. Biagini, L. Virgili, M. Giacomini, M. Fini, F. Giantomassi, D. Natali, P. Torricelli, R. Giardino, Tailoring biomaterial compatibility: in vivo tissue response versus in vitro cell behavior, Int. J. Artif. Organs 26 (12) (2003) 1077–1085.
[66] J. Tang, F. Yuan, X. Shen, Z. Wang, M. Rao, Y. He, Y. Sun, X. Li, W. Zhang, Y. Li, Bridging biological and artificial neural networks with emerging neuromorphic devices: fundamentals, progress, and challenges, Adv Mater 31 (49) (2019) 1902761.
[67] L. Abdul Kadir, M. Stacey, R. Barrett-Jolley, Emerging roles of the membrane potential: action beyond the action potential, Front. Physiol. 9 (2018) 1661.
[68] G. Marsh, H. Beams, In vitro control of growing check nerve fibers by applied electric currents, J. Cell. Comp. Physiol. 27 (3) (1946) 139–157.
[69] S. Ingvar, Reaction of cells to the galvanic current in tissue cultures, PSEBM (Proc. Soc. Exp. Biol. Med.) 17 (8) (1920) 198–199.
[70] L.F. Jaffe, M.M. Poo, Neurites grow faster towards the cathode than the anode in a steady field, J. Exp. Zool. 209 (1) (1979) 115–127.
[71] B.F. Sisken, S.D. Smith, The effects of minute direct electrical currents on cultured chick embryo trigeminal ganglia, Development 33 (1) (1975) 29–41.
[72] E.M. Steel, H.G. Sundararaghavan, Electrically conductive materials for nerve regeneration. Neural Engineering: from Advanced Biomaterials to 3D Fabrication Techniques, 2016, pp. 145–179.
[73] Q. Liu, B. Song, Electric field regulated signaling pathways, Int. J. Biochem. Cell Biol. 55 (2014) 264–268, https://doi.org/10.1016/j.biocel.2014.09.014.
[74] L. Leppik, K.M.C. Oliveira, M.B. Bhavsar, J.H. Barker, Electrical stimulation in bone tissue engineering treatments, Eur. J. Trauma Emerg. Surg. 46 (2) (2020) 231–244, https://doi.org/10.1007/s00068-020-01324-1.
[75] S. Zhao, A.S. Mehta, M. Zhao, Biomedical applications of electrical stimulation, Cell. Mol. Life Sci. 77 (14) (2020) 2681–2699, https://doi.org/10.1007/s00018-019-03446-1.
[76] S. Luo, C. Zhang, W. Xiong, Y. Song, Q. Wang, H. Zhang, S. Guo, S. Yang, H. Liu, Advances in electroactive biomaterials: through the lens of electrical stimulation promoting bone regeneration strategy, Journal of Orthopaedic Translation 47 (2024) 191–206.
[77] N. Patel, M.-M. Poo, Orientation of neurite growth by extracellular electric fields, J. Neurosci. 2 (4) (1982) 483–496.
[78] C.D. Rae, V.H.-C. Lee, R.J. Ordidge, A. Alonzo, C. Loo, Anodal transcranial direct current stimulation increases brain intracellular pH and modulates bioenergetics, Int. J. Neuropsychopharmacol. 16 (8) (2013) 1695–1706.
[79] J.R. Jacobson, S.M. Dudek, P.A. Singleton, I.A. Kolosova, A.D. Verin, J.G. Garcia, Endothelial cell barrier enhancement by ATP is mediated by the small GTPase Rac and cortactin, Am. J. Physiol. Lung Cell Mol. Physiol. 291 (2) (2006) L289–L295.
[80] G. Thrivikraman, S.K. Boda, B. Basu, Unraveling the mechanistic effects of electric field stimulation towards directing stem cell fate and function: a tissue engineering perspective, Biomaterials 150 (2018) 60–86.
[81] H.S. Venkatesh, W. Morishita, A.C. Geraghty, D. Silverbush, S.M. Gillespie, M. Arzt, L.T. Tam, C. Espenel, A. Ponnuswami, L. Ni, Electrical and synaptic integration of glioma into neural circuits, Nature 573 (7775) (2019) 539–545.
[82] J. Freeman, P. Manis, G. Snipes, B. Mayes, P. Samson, J. Wikswo Jr, D. Freeman, Steady growth cone currents revealed by a novel circularly vibrating probe: a possible mechanism underlying neurite growth, J. Neurosci. Res. 13 (1-2) (1985) 257–283.
[83] A.N. Koppes, A.L. Nordberg, G.M. Paolillo, N.M. Goodsell, H.A. Darwish, L. Zhang, D.M. Thompson, Electrical stimulation of schwann cells promotes sustained increases in neurite outgrowth, Tissue Eng Pt A 20 (3–4) (2014) 494–506.
[84] J. Huang, Z. Ye, X. Hu, L. Lu, Z. Luo, Electrical stimulation induces calcium-dependent release of NGF from cultured Schwann cells, Glia 58 (5) (2010) 622–631.
[85] D. Kamber, H. Erez, M.E. Spira, Local calcium-dependent mechanisms determine whether a cut axonal end assembles a retarded endbulb or competent growth cone, Exp. Neurol. 219 (1) (2009) 112–125.
[86] M. Guillot-Ferriols, S. Lanceros-Méndez, J.G. Ribelles, G.G. Ferrer, Electrical stimulation: effective cue to direct osteogenic differentiation of mesenchymal stem cells? Biomater. Adv. 138 (2022) 212918.
[87] J.N. Wong, J.L. Olson, M.J. Morhart, K.M. Chan, Electrical stimulation enhances sensory recovery: a randomized controlled trial, Ann. Neurol. 77 (6) (2015) 996–1006, https://doi.org/10.1002/ana.24397.
[88] A.A. Al-Majed, S.L. Tam, T. Gordon, Electrical stimulation accelerates and enhances expression of regeneration-associated genes in regenerating rat femoral motoneurons, Cell. Mol. Neurobiol. 24 (2004) 379–402.
[89] A.A. Al-Majed, T.M. Brushart, T. Gordon, Electrical stimulation accelerates and increases expression of BDNF and trkB mRNA in regenerating rat femoral motoneurons, Eur. J. Neurosci. 12 (12) (2000) 4381–4390.
[90] M. Hronik-Tupaj, W.K. Raja, M. Tang-Schomer, F.G. Omenetto, D.L. Kaplan, Neural responses to electrical stimulation on patterned silk films, J. Biomed. Mater. Res. 101 (9) (2013) 2559–2572.
[91] T. Gordon, Electrical stimulation to enhance axon regeneration after peripheral nerve injuries in animal models and humans, Neurotherapeutics 13 (2) (2016) 295–310, https://doi.org/10.1007/s13311-015-0415-1.
[92] A. Soltani Khaboushan, A. Azimzadeh, S. Behboodi Tanourlouee, M. Mamdoohi, A.-M. Kajbafzadeh, K.V. Slavin, V. Rahimi-Movaghar, Z. Hassannejad, Electrical stimulation enhances sciatic nerve regeneration using a silk-based conductive scaffold beyond traditional nerve guide conduits, Sci Rep-Uk 14 (1) (2024) 15196.
[93] X.-L. Chu, X.-Z. Song, Q. Li, Y.-R. Li, F. He, X.-S. Gu, D. Ming, Basic mechanisms of peripheral nerve injury and treatment via electrical stimulation, Neural regeneration research 17 (10) (2022) 2185–2193.
[94] C. Henríquez-Olguín, F. Altamirano, D. Valladares, J.R. López, P.D. Allen, E. Jaimovich, Altered ROS production, NF-κB activation and interleukin-6 gene expression induced by electrical stimulation in dystrophic mdx skeletal muscle cells, Biochimica et Biophysica Acta (BBA)-Molecular Basis of Disease 1852 (7) (2015) 1410–1419.
[95] R.E. Zigmond, Cytokines that promote nerve regeneration, Exp. Neurol. 238 (2) (2012) 101.
[96] H. Bai, J.V. Forrester, M. Zhao, DC electric stimulation upregulates angiogenic factors in endothelial cells through activation of VEGF receptors, Cytokine 55 (1) (2011) 110–115.
[97] M. Schmelter, B. Ateghang, S. Helmig, M. Wartenberg, H. Sauer, Embryonic stem cells utilize reactive oxygen species as transducers of mechanical strain-induced cardiovascular differentiation, Faseb. J. 20 (8) (2006).
[98] A. Görlach, K. Bertram, S. Hudecova, O. Krizanova, Calcium and ROS: a mutual interplay, Redox Biol. 6 (2015) 260–271.
[99] K. Ohl, K. Tenbrock, Reactive oxygen species as regulators of MDSC-mediated immune suppression, Front. Immunol. 9 (2018) 2499.
[100] Q. Wang, Y. Wei, X. Yin, G. Zhan, X. Cao, H. Gao, Engineered PVDF/PLCL/PEDOT dual electroactive nerve conduit to mediate peripheral nerve regeneration by modulating the immune microenvironment, Adv. Funct. Mater. (2024) 2400217.
[101] S.A. O'Rourke, A. Dunne, M.G. Monaghan, The role of macrophages in the infarcted myocardium: orchestrators of ECM remodeling, Frontiers in cardiovascular medicine 6 (2019) 101.
[102] S. Zhong, C. Lu, H.-Y. Liu, J. Zhang, J. Wang, Y. Liu, Y. Chen, X. Zhang, Electrical and immune stimulation-based hydrogels synergistically realize scarless wound healing via amplifying endogenous electrophysiological function and promoting Macrophage Phenotype-Switching, Chem. Eng. J. 491 (2024) 152048.
[103] C.D. McCaig, A.M. Rajnicek, B. Song, M. Zhao, Controlling cell behavior electrically: current views and future potential, Physiol. Rev. 85 (3) (2005) 943–978.
[104] S. O'Rourke, Engineering Innate Immunology in Cardiovascular Disease Models and Regenerative Medicine, University of Dublin, 2023.
[105] S. Roy Barman, S. Jhunjhunwala, Electrical stimulation for immunomodulation, ACS Omega 9 (1) (2023) 52–66.
[106] J. Gu, C. Wu, X. He, X. Chen, L. Dong, W. Weng, K. Cheng, D. Wang, Z. Chen, Enhanced M2 polarization of oriented macrophages on the P (Vdf-Trfe) film by coupling with electrical stimulation, Acs Biomater Sci Eng 9 (5) (2023) 2615–2624.
[107] K. Srirussamee, S. Mobini, N.J. Cassidy, S.H. Cartmell, Direct electrical stimulation enhances osteogenesis by inducing Bmp2 and Spp1 expressions from macrophages and preosteoblasts, Biotechnol. Bioeng. 116 (12) (2019) 3421–3432.
[108] J. Xu, Y. Jia, W. Huang, Q. Shi, X. Sun, L. Zheng, M. Wang, P. Li, Y. Fan, Non-contact electrical stimulation as an effective means to promote wound healing, Bioelectrochemistry 146 (2022) 108108.
[109] Y. Jia, J. Xu, Q. Shi, L. Zheng, M. Liu, M. Wang, P. Li, Y. Fan, Study on the effects of alternating capacitive electric fields with different frequencies on promoting wound healing, Medicine in Novel Technology and Devices 16 (2022) 100142.
[110] H. Wu, H. Dong, Z. Tang, Y. Chen, Y. Liu, M. Wang, X. Wei, N. Wang, S. Bao, D. Yu, Electrical stimulation of piezoelectric BaTiO3 coated Ti6Al4V scaffolds promotes anti-inflammatory polarization of macrophages and bone repair via MAPK/JNK inhibition and OXPHOS activation, Biomaterials 293 (2023) 121990.
[111] Z.-C. Hu, J.-Q. Lu, T.-W. Zhang, H.-F. Liang, H. Yuan, D.-H. Su, W. Ding, R.-X. Lian, Y.-X. Ge, B. Liang, Piezoresistive MXene/Silk fibroin nanocomposite hydrogel for accelerating bone regeneration by Re-establishing electrical microenvironment, Bioact. Mater. 22 (2023) 1–17.
[112] Y. Li, L. Yang, Y. Hou, Z. Zhang, M. Chen, M. Wang, J. Liu, J. Wang, Z. Zhao, C. Xie, Polydopamine-mediated graphene oxide and nanohydroxyapatite-incorporated conductive scaffold with an immunomodulatory ability accelerates periodontal bone regeneration in diabetes, Bioact. Mater. 18 (2022) 213–227.
[113] H. Wu, H. Dong, Z. Tang, Y. Chen, Y. Liu, M. Wang, X. Wei, N. Wang, S. Bao, D. Yu, et al., Electrical stimulation of piezoelectric BaTiO3 coated Ti6Al4V scaffolds promotes anti-inflammatory polarization of macrophages and bone repair via MAPK/JNK inhibition and OXPHOS activation, Biomaterials 293 (2023) 121990, https://doi.org/10.1016/j.biomaterials.2022.121990.
[114] Y. Kong, F. Liu, B. Ma, J. Duan, W. Yuan, Y. Sang, L. Han, S. Wang, H. Liu, Wireless localized electrical stimulation generated by an ultrasound-driven piezoelectric discharge regulates proinflammatory macrophage polarization, Adv. Sci. 8 (13) (2021) 2100962.
[115] Y. Yan, Y. Zhang, K. Li, Y. Li, W. Qian, W. Zhang, Y. Wang, W. Ma, L. Li, Synergistic effects of graphene microgrooves and electrical stimulation on M2 macrophage polarization, Biochem. Biophys. Res. Commun. 711 (2024) 149911.
[116] X. Dai, B.C. Heng, Y. Bai, F. You, X. Sun, Y. Li, Z. Tang, M. Xu, X. Zhang, X. Deng, Restoration of electrical microenvironment enhances bone regeneration under

diabetic conditions by modulating macrophage polarization, Bioact. Mater. 6 (7) (2021) 2029–2038.
[117] T. Jiang, F. Yu, Y. Zhou, R. Li, M. Zheng, Y. Jiang, Z. Li, J. Pan, N. Ouyang, Synergistic effect of ultrasound and reinforced electrical environment by bioinspired periosteum for enhanced osteogenesis via immunomodulation of macrophage polarization through Piezo1, Materials Today Bio 27 (2024) 101147.
[118] C. Li, M. Levin, D.L. Kaplan, Bioelectric modulation of macrophage polarization, Sci Rep-Uk 6 (1) (2016) 21044.
[119] H. Shirakawa, E.J. Louis, A.G. MacDiarmid, C.K. Chiang, A.J. Heeger, Synthesis of electrically conducting organic polymers: halogen derivatives of polyacetylene, (CH) x, J. Chem. Soc., Chem. Commun. (16) (1977) 578–580.
[120] T.-H. Le, Y. Kim, H. Yoon, Electrical and electrochemical properties of conducting polymers, Polymers-Basel 9 (4) (2017) 150.
[121] D.M. Mohilner, R.N. Adams, W.J. Argersinger, Investigation of the kinetics and mechanism of the anodic oxidation of aniline in aqueous sulfuric acid solution at a platinum electrode, J. Am. Chem. Soc. 84 (19) (1962) 3618–3622.
[122] H. Letheby, On the physiological properties of nitro-benzole and aniline, Boston Med. Surg. J. 69 (16) (1863) 313–320.
[123] B. Anft, Friedlieb Ferdinand Runge: a forgotten chemist of the nineteenth century, J. Chem. Educ. 32 (11) (1955) 566.
[124] H. Shirakawa, Y.-X. Zhang, K. Akagi, Synthesis of highly conducting polyacetylene thin films, Prog. Theor. Phys. Suppl. 113 (1993) 107–113.
[125] C.K. Chiang, C. Fincher Jr, Y.W. Park, A.J. Heeger, H. Shirakawa, E.J. Louis, S. C. Gau, A.G. MacDiarmid, Electrical conductivity in doped polyacetylene, Phys. Rev. Lett. 39 (17) (1977) 1098.
[126] A. Diaz, Electrochemical preparation and characterization of conducting polymers, Chem. Scripta 17 (1–5) (1981) 145–148.
[127] A.J. Heeger, Nobel Lecture: semiconducting and metallic polymers: the fourth generation of polymeric materials, Rev. Mod. Phys. 73 (3) (2001) 681.
[128] E. Stelmach, E. Jaworska, V.D. Bhatt, M. Becherer, P. Lugli, A. Michalska, K. Maksymiuk, Electrolyte gated transistors modified by polypyrrole nanoparticles, Electrochim. Acta 309 (2019) 65–73.
[129] Q. Zhang, M. Kaisti, A. Prabhu, Y. Yu, Y.-A. Song, M.H. Rafailovich, A. Rahman, K. Levon, Polyaniline-functionalized ion-sensitive floating-gate FETs for the on-chip monitoring of peroxidase-catalyzed redox reactions, Electrochim. Acta 261 (2018) 256–264.
[130] Y. Huang, H. Li, Z. Wang, M. Zhu, Z. Pei, Q. Xue, , C. Zhi, Nanostructured polypyrrole as a flexible electrode material of supercapacitor, Nano Energy 22 (2016) 422–438.
[131] D. Zhao, Q. Zhang, W. Chen, X. Yi, S. Liu, Q. Wang, Y. Liu, J. Li, X. Li, H. Yu, Highly flexible and conductive cellulose-mediated PEDOT: PSS/MWCNT composite films for supercapacitor electrodes, Acs Appl Mater Inter 9 (15) (2017) 13213–13222.
[132] J.C. Yu, J.A. Hong, E.D. Jung, D.B. Kim, S.-M. Baek, S. Lee, S. Cho, S.S. Park, K. J. Choi, M.H. Song, Highly efficient and stable inverted perovskite solar cell employing PEDOT: GO composite layer as a hole transport layer, Sci Rep-Uk 8 (1) (2018) 1070.
[133] W. Hou, Y. Xiao, G. Han, D. Fu, R. Wu, Serrated, flexible and ultrathin polyaniline nanoribbons: an efficient counter electrode for the dye-sensitized solar cell, J. Power Sources 322 (2016) 155–162.
[134] J.D. Larson, C.V. Fengel, N.P. Bradshaw, I.S. Romero, J.M. Leger, A.R. Murphy, Enhanced actuation performance of silk-polypyrrole composites, Mater. Chem. Phys. 186 (2017) 67–74.
[135] Y.Y. Zhang, G.L. Wang, J. Zhang, K.H. Ding, Z.F. Wang, M. Zhang, Preparation and properties of core-shell structured calcium copper titanate@ polyaniline/ silicone dielectric elastomer actuators, Polym. Compos. 40 (S1) (2019) E62–E68.
[136] B. Dudem, A.R. Mule, H.R. Patnam, J.S. Yu, Wearable and durable triboelectric nanogenerators via polyaniline coated cotton textiles as a movement sensor and self-powered system, Nano Energy 55 (2019) 305–315.
[137] R.M. Lima, J.J. Alcaraz-Espinoza, F.A. da Silva Jr, H.P. de Oliveira, Multifunctional wearable electronic textiles using cotton fibers with polypyrrole and carbon nanotubes, Acs Appl Mater Inter 10 (16) (2018) 13783–13795.
[138] A.M. Kumar, A.Y. Adesina, M. Hussein, S. Ramakrishna, N. Al-Aqeeli, S. Akhtar, S. Saravanan, PEDOT/FHA nanocomposite coatings on newly developed Ti-Nb-Zr implants: biocompatibility and surface protection against corrosion and bacterial infections, Mater. Sci. Eng. C 98 (2019) 482–495.
[139] K. Cai, S. Zuo, S. Luo, C. Yao, W. Liu, J. Ma, H. Mao, Z. Li, Preparation of polyaniline/graphene composites with excellent anti-corrosion properties and their application in waterborne polyurethane anticorrosive coatings, Rsc Adv 6 (98) (2016) 95965–95972.
[140] A.J. Heeger, Semiconducting and Metallic Polymers: the Fourth Generation of Polymeric Materials, vol. 105, ACS Publications, 2001, pp. 8475–8491.
[141] T.A. Skotheim, Handbook of Conducting Polymers, CRC Press, 1997.
[142] A.G. MacDiarmid, R. Mammone, R. Kaner, L. Porter, The concept of 'doping'of conducting polymers: the role of reduction potentials, Phil. Trans. Roy. Soc. Lond. Math. Phys. Sci. 314 (1528) (1985) 3–15.
[143] M. Kertesz, C.H. Choi, S. Yang, Conjugated polymers and aromaticity, Chemical reviews 105 (10) (2005) 3448–3481.
[144] A. Burnstine-Townley, Y. Eshel, N. Amdursky, Conductive scaffolds for cardiac and neuronal tissue engineering: governing factors and mechanisms, Adv. Funct. Mater. 30 (18) (2020) 1901369.
[145] G.G. Wallace, P.R. Teasdale, G.M. Spinks, L.A. Kane-Maguire, Conductive Electroactive Polymers: Intelligent Polymer Systems, CRC Press, 2008.
[146] J. Upadhyay, R. Borah, T.M. Das, J.M. Das, Fabrication of flexible supercapacitor of Polypyrrole nanotubes embedded with Ruthenium oxide nanoparticles for enhanced electrochemical performance, Electrochim. Acta (2024) 144858.
[147] J. Upadhyay, R. Borah, T.M. Das, J.M. Das, Flexible solid-state supercapacitor based on ternary nanocomposites of reduced graphene oxide and ruthenium oxide nanoparticles bridged by polyaniline nanofibers, J. Energy Storage 72 (2023) 108600.
[148] S.F. Cogan, Neural stimulation and recording electrodes, Annu. Rev. Biomed. Eng. 10 (1) (2008) 275–309.
[149] B. Lu, H. Yuk, S. Lin, N. Jian, K. Qu, J. Xu, X. Zhao, Pure pedot: pss hydrogels, Nat. Commun. 10 (1) (2019) 1043.
[150] G. Shi, M. Rouabhia, Z. Wang, L.H. Dao, Z. Zhang, A novel electrically conductive and biodegradable composite made of polypyrrole nanoparticles and polylactide, Biomaterials 25 (13) (2004) 2477–2488.
[151] C. Dusemund, G. Schwitzgebel, Ion-exchange properties of conducting polypyrrole films, Synth. Met. 55 (2–3) (1993) 1396–1401.
[152] W.W. Focke, G.E. Wnek, Y. Wei, Influence of oxidation state, pH, and counterion on the conductivity of polyaniline, J. Phys. Chem. 91 (22) (1987) 5813–5818.
[153] R. Balint, N.J. Cassidy, S.H. Cartmell, Conductive polymers: towards a smart biomaterial for tissue engineering, Acta Biomater. 10 (6) (2014) 2341–2353.
[154] N.K. Guimard, N. Gomez, C.E. Schmidt, Conducting polymers in biomedical engineering, Prog. Polym. Sci. 32 (8–9) (2007) 876–921.
[155] R. Borah, G.C. Ingavle, S.R. Sandeman, A. Kumar, S.V. Mikhalovsky, Amine-functionalized electrically conductive core–sheath MEH-PPV: PCL electrospun nanofibers for enhanced cell–biomaterial interactions, Acs Biomater Sci Eng 4 (9) (2018) 3327–3346.
[156] J.Y. Lee, C.A. Bashur, A.S. Goldstein, C.E. Schmidt, Polypyrrole-coated electrospun PLGA nanofibers for neural tissue applications, Biomaterials 30 (26) (2009) 4325–4335.
[157] I. Rajzer, M. Rom, E. Menaszek, P. Pasierb, Conductive PANI patterns on electrospun PCL/gelatin scaffolds modified with bioactive particles for bone tissue engineering, Mater. Lett. 138 (2015) 60–63.
[158] K. Sajesh, R. Jayakumar, S.V. Nair, K. Chennazhi, Biocompatible conducting chitosan/polypyrrole–alginate composite scaffold for bone tissue engineering, Int. J. Biol. Macromol. 62 (2013) 465–471.
[159] A.G. Guex, J.L. Puetzer, A. Armgarth, E. Littmann, E. Stavrinidou, E.P. Giannelis, G.G. Malliaras, M.M. Stevens, Highly porous scaffolds of PEDOT: PSS for bone tissue engineering, Acta Biomater. 62 (2017) 91–101.
[160] T.H. Qazi, R. Rai, D. Dippold, J.E. Roether, D.W. Schubert, E. Rosellini, N. Barbani, A.R. Boccaccini, Development and characterization of novel electrically conductive PANI–PGS composites for cardiac tissue engineering applications, Acta Biomater. 10 (6) (2014) 2434–2445.
[161] M. Björninen, K. Gilmore, J. Pelto, R. Seppänen-Kaijansinkko, M. Kellomäki, S. Miettinen, G. Wallace, D. Grijpma, S. Haimi, Electrically stimulated adipose stem cells on polypyrrole-coated scaffolds for smooth muscle tissue engineering, Ann. Biomed. Eng. 45 (2017) 1015–1026.
[162] N.A. Chowdhury, A.M. Al-Jumaily, Regenerated cellulose/polypyrrole/silver nanoparticles/ionic liquid composite films for potential wound healing applications, Wound Medicine 14 (2016) 16–18.
[163] Y. Wang, M. Rouabhia, Z. Zhang, PPy-coated PET fabrics and electric pulse-stimulated fibroblasts, J. Mater. Chem. B 1 (31) (2013) 3789–3796.
[164] A. Kotwal, C.E. Schmidt, Electrical stimulation alters protein adsorption and nerve cell interactions with electrically conducting biomaterials, Biomaterials 22 (10) (2001) 1055–1064.
[165] R. Borah, G.C. Ingavle, A. Kumar, S.R. Sandeman, S.V. Mikhalovsky, Surface-functionalized conducting nanofibers for electrically stimulated neural cell function, Biomacromolecules 22 (2) (2021) 594–611.
[166] D. Ateh, H. Navsaria, P. Vadgama, Polypyrrole-based conducting polymers and interactions with biological tissues, Journal of the royal society interface 3 (11) (2006) 741–752.
[167] L. Forciniti, J. Ybarra III, M.H. Zaman, C.E. Schmidt, Schwann cell response on polypyrrole substrates upon electrical stimulation, Acta Biomater. 10 (6) (2014) 2423–2433.
[168] S. Song, K.W. McConnell, D. Amores, A. Levinson, H. Vogel, M. Quarta, T. A. Rando, P.M. George, Electrical stimulation of human neural stem cells via conductive polymer nerve guides enhances peripheral nerve recovery, Biomaterials 275 (2021) 120982.
[169] Y. Zhao, Y. Liang, S. Ding, K. Zhang, H.-q. Mao, Y. Yang, Application of conductive PPy/SF composite scaffold and electrical stimulation for neural tissue engineering, Biomaterials 255 (2020) 120164.
[170] Z.-F. Zhou, F. Zhang, J.-G. Wang, Q.-C. Chen, W.-Z. Yang, N. He, Y.-Y. Jiang, F. Chen, J.-J. Liu, Electrospinning of PELA/PPY fibrous conduits: promoting peripheral nerve regeneration in rats by self-originated electrical stimulation, Acs Biomater Sci Eng 2 (9) (2016) 1572–1581.
[171] J. Huang, L. Lu, J. Zhang, X. Hu, Y. Zhang, W. Liang, S. Wu, Z. Luo, Electrical stimulation to conductive scaffold promotes axonal regeneration and remyelination in a rat model of large nerve defect, PLoS One 7 (6) (2012) e39526.
[172] J. Song, B. Sun, S. Liu, W. Chen, Y. Zhang, C. Wang, X. Mo, J. Che, Y. Ouyang, W. Yuan, Polymerizing pyrrole coated poly (l-lactic acid-co-ε-caprolactone) (PLCL) conductive nanofibrous conduit combined with electric stimulation for long-range peripheral nerve regeneration, Front. Mol. Neurosci. 9 (2016) 117.
[173] S.M. Broas, I.A. Banerjee, Design of peptide-PEG-Thiazole bound polypyrrole supramolecular assemblies for enhanced neuronal cell interactions, Soft Mater. 19 (4) (2021) 428–443.
[174] Y. Li, Z. Huang, X. Pu, X. Chen, G. Yin, Y. Wang, D. Miao, J. Fan, J. Mu, Polydopamine/carboxylic graphene oxide-composited polypyrrole films for promoting adhesion and alignment of Schwann cells, Colloids Surf. B Biointerfaces 191 (2020) 110972.

[175] M. Patel, J.H. Min, M.-H. Hong, H.-J. Lee, S. Kang, S. Yi, W.-G. Koh, Culture of neural stem cells on conductive and microgrooved polymeric scaffolds fabricated via electrospun fiber-template lithography, Biomedical Materials 15 (4) (2020) 045007.
[176] R.P. Trueman, O. Guillemot-Legris, H.T. Lancashire, A.S. Mehta, J. Tropp, R. E. Daso, J. Rivnay, A.B. Tabor, J.B. Phillips, B.C. Schroeder, Aligned bioelectronic polypyrrole/collagen constructs for peripheral nerve interfacing, Adv. Eng. Mater. 26 (6) (2024) 2301488.
[177] P. Moroder, M.B. Runge, H. Wang, T. Ruesink, L. Lu, R.J. Spinner, A. J. Windebank, M.J. Yaszemski, Material properties and electrical stimulation regimens of polycaprolactone fumarate–polypyrrole scaffolds as potential conductive nerve conduits, Acta Biomater. 7 (3) (2011) 944–953.
[178] X. Chen, C. Liu, Z. Huang, X. Pu, L. Shang, G. Yin, C. Xue, Preparation of carboxylic graphene oxide-composited polypyrrole conduits and their effect on sciatic nerve repair under electrical stimulation, J. Biomed. Mater. Res. 107 (12) (2019) 2784–2795, https://doi.org/10.1002/jbm.a.36781.
[179] R. Karimi-Soflou, I. Shabani, A. Karkhaneh, Enhanced neural differentiation by applying electrical stimulation utilizing conductive and antioxidant alginate-polypyrrole/poly-l-lysine hydrogels, Int. J. Biol. Macromol. 237 (2023) 124063.
[180] P. Zarrintaj, M.K. Yazdi, H. Vahabi, P.N. Moghadam, M.R. Saeb, Towards advanced flame retardant organic coatings: expecting a new function from polyaniline, Prog. Org. Coating 130 (2019) 144–148.
[181] R. Borah, A. Kumar, Enhanced cellular activity on conducting polymer: chitosan nanocomposite scaffolds for tissue engineering application. In *polymer Nanocomposites for advanced Engineering and military applications*, IGI Global (2019) 150–189.
[182] P. Humpolicek, V. Kasparkova, P. Saha, J. Stejskal, Biocompatibility of polyaniline, Synth. Met. 162 (7–8) (2012) 722–727.
[183] Y. Guo, M. Li, A. Mylonakis, J. Han, A.G. MacDiarmid, X. Chen, P.I. Lelkes, Y. Wei, Electroactive oligoaniline-containing self-assembled monolayers for tissue engineering applications, Biomacromolecules 8 (10) (2007) 3025–3034.
[184] L. Ghasemi-Mobarakeh, M.P. Prabhakaran, M. Morshed, M.H. Nasr-Esfahani, S. Ramakrishna, Electrical stimulation of nerve cells using conductive nanofibrous scaffolds for nerve tissue engineering, Tissue Eng Pt A 15 (11) (2009) 3605–3619.
[185] J. Zhang, K. Qiu, B. Sun, J. Fang, K. Zhang, E.-H. Hany, S.S. Al-Deyab, X. Mo, The aligned core–sheath nanofibers with electrical conductivity for neural tissue engineering, J. Mater. Chem. B 2 (45) (2014) 7945–7954.
[186] G. Wang, W. Wu, H. Yang, P. Zhang, J.Y. Wang, Intact polyaniline coating as a conductive guidance is beneficial to repairing sciatic nerve injury, J. Biomed. Mater. Res. B Appl. Biomater. 108 (1) (2020) 128–142.
[187] S. Das, M. Sharma, D. Saharia, K.K. Sarma, E.M. Muir, U. Bora, Electrospun silk-polyaniline conduits for functional nerve regeneration in rat sciatic nerve injury model, Biomedical Materials 12 (4) (2017) 045025.
[188] M.S. Zaman, Z.F. Khosravieh, M. Ahssan, M. Salehiamin, S. Ghoraishizadeh, F. Darvishnia, E. Rahmani, J. Esmaeili, Fabrication of a conduit for future peripheral nerve regeneration using decellularized plant tissue modified with polyaniline/graphene oxide nanosheet, Mater. Today Commun. 39 (2024) 109204.
[189] M.P. Prabhakaran, L. Ghasemi-Mobarakeh, G. Jin, S. Ramakrishna, Electrospun conducting polymer nanofibers and electrical stimulation of nerve stem cells, J. Biosci. Bioeng. 112 (5) (2011) 501–507.
[190] L. Wang, Q. Huang, J.-Y. Wang, Nanostructured polyaniline coating on ITO glass promotes the neurite outgrowth of PC 12 cells by electrical stimulation, Langmuir 31 (44) (2015) 12315–12322.
[191] B. Xu, T. Bai, A. Sinclair, W. Wang, Q. Wu, F. Gao, H. Jia, S. Jiang, W. Liu, Directed neural stem cell differentiation on polyaniline-coated high strength hydrogels, Mater. Today Chem. 1 (2016) 15–22.
[192] Z. Zheng, L. Huang, L. Yan, F. Yuan, L. Wang, K. Wang, T. Lawson, M. Lin, Y. Liu, Polyaniline functionalized graphene nanoelectrodes for the regeneration of PC12 cells via electrical stimulation, Int. J. Mol. Sci. 20 (8) (2019) 2013.
[193] F.F. Garrudo, P.E. Mikael, C.A. Rodrigues, R.W. Udangawa, P. Paradiso, C. A. Chapman, P. Hoffman, R. Colaço, J.M. Cabral, J. Morgado, Polyaniline-polycaprolactone fibers for neural applications: electroconductivity enhanced by pseudo-doping, Mater. Sci. Eng. C 120 (2021) 111680.
[194] P. Wu, Y. Zhao, F. Chen, A. Xiao, Q. Du, Q. Dong, M. Ke, X. Liang, Q. Zhou, Y. Chen, Conductive hydroxyethyl cellulose/soy protein isolate/polyaniline conduits for enhancing peripheral nerve regeneration via electrical stimulation, Front. Bioeng. Biotechnol. 8 (2020) 709.
[195] Y. Furukawa, M. Akimoto, I. Harada, Vibrational key bands and electrical conductivity of polythiophene, Synth. Met. 18 (1–3) (1987) 151–156.
[196] S. Ostrovsky, S. Hahnewald, R. Kiran, P. Mistrik, R. Hessler, A. Tscherter, P. Senn, J. Kang, J. Kim, M. Roccio, Conductive hybrid carbon nanotube (CNT)–polythiophene coatings for innovative auditory neuron-multi-electrode array interfacing, Rsc Adv 6 (48) (2016) 41714–41723.
[197] A.S. Widge, M. Jeffries-El, X. Cui, C.F. Lagenaur, Y. Matsuoka, Self-assembled monolayers of polythiophene conductive polymers improve biocompatibility and electrical impedance of neural electrodes, Biosens. Bioelectron. 22 (8) (2007) 1723–1732.
[198] L. Yang, S.K. Sontag, T.W. LaJoie, W. Li, N.E. Huddleston, J. Locklin, W. You, Surface-initiated poly (3-methylthiophene) as a hole-transport layer for polymer solar cells with high performance, Acs Appl Mater Inter 4 (10) (2012) 5069–5073.
[199] A.K. Panda, B. Basu, Biomaterials-based bioengineering strategies for bioelectronic medicine, Mater. Sci. Eng. R Rep. 146 (2021) 100630.
[200] K. Liu, S. Yan, Y. Liu, J. Liu, R. Li, L. Zhao, B. Liu, Conductive and alignment-optimized porous fiber conduits with electrical stimulation for peripheral nerve regeneration, Materials Today Bio 26 (2024) 101064.
[201] S. Zhang, H. Yan, J.M. Yeh, X. Shi, P. Zhang, Electroactive composite of FeCl3-doped P3HT/PLGA with adjustable electrical conductivity for potential application in neural tissue engineering, Macromol. Biosci. 19 (10) (2019) 1900147.
[202] A. Subramanian, U.M. Krishnan, S. Sethuraman, Axially aligned electrically conducting biodegradable nanofibers for neural regeneration, J. Mater. Sci. Mater. Med. 23 (2012) 1797–1809.
[203] P. Berger, M. Kim, Polymer solar cells: P3HT: PCBM and beyond, J. Renew. Sustain. Energy 10 (1) (2018).
[204] M.L. DiFrancesco, E. Colombo, E.D. Papaleo, J.F. Maya-Vetencourt, G. Manfredi, G. Lanzani, F. Benfenati, A hybrid P3HT-Graphene interface for efficient photostimulation of neurons, Carbon 162 (2020) 308–317.
[205] J.F. Maya-Vetencourt, D. Ghezzi, M.R. Antognazza, E. Colombo, M. Mete, P. Feyen, A. Desii, A. Buschiazzo, M. Di Paolo, S. Di Marco, A fully organic retinal prosthesis restores vision in a rat model of degenerative blindness, Nat. Mater. 16 (6) (2017) 681–689.
[206] F. Pires, Q. Ferreira, C.A. Rodrigues, J. Morgado, F.C. Ferreira, Neural stem cell differentiation by electrical stimulation using a cross-linked PEDOT substrate: expanding the use of biocompatible conjugated conductive polymers for neural tissue engineering, Biochimica et Biophysica Acta (BBA)-General Subjects 1850 (6) (2015) 1158–1168.
[207] W. Guo, X. Zhang, X. Yu, S. Wang, J. Qiu, W. Tang, L. Li, H. Liu, Z.L. Wang, Self-powered electrical stimulation for enhancing neural differentiation of mesenchymal stem cells on graphene–poly (3, 4-ethylenedioxythiophene) hybrid microfibers, ACS Nano 10 (5) (2016) 5086–5095.
[208] P.J. Molino, L. Garcia, E.M. Stewart, M. Lamaze, B. Zhang, A.R. Harris, P. Winberg, G.G. Wallace, PEDOT doped with algal, mammalian and synthetic dopants: polymer properties, protein and cell interactions, and influence of electrical stimulation on neuronal cell differentiation, Biomater Sci-Uk 6 (5) (2018) 1250–1261.
[209] D.N. Heo, N. Acquah, J. Kim, S.-J. Lee, N.J. Castro, L.G. Zhang, Directly induced neural differentiation of human adipose-derived stem cells using three-dimensional culture system of conductive microwell with electrical stimulation, Tissue Eng Pt A 24 (7–8) (2018) 537–545.
[210] N.C. Tsai, J.W. She, J.G. Wu, P. Chen, Y.S. Hsiao, J. Yu, Poly (3, 4-ethylenedioxythiophene) polymer composite bioelectrodes with designed chemical and topographical cues to manipulate the behavior of pc12 neuronal cells, Adv. Mater. Interfac. 6 (5) (2019) 1801576.
[211] D.N. Heo, S.-J. Lee, R. Timsina, X. Qiu, N.J. Castro, L.G. Zhang, Development of 3D printable conductive hydrogel with crystallized PEDOT: PSS for neural tissue engineering, Mater. Sci. Eng. C 99 (2019) 582–590.
[212] L. Du, T. Li, F. Jin, Y. Wang, R. Li, J. Zheng, T. Wang, Z.-Q. Feng, Design of high conductive and piezoelectric poly (3, 4-ethylenedioxythiophene)/chitosan nanofibers for enhancing cellular electrical stimulation, J. Colloid Interface Sci. 559 (2020) 65–75.
[213] A. Babaie, B. Bakhshandeh, A. Abedi, J. Mohammadnejad, I. Shabani, A. Ardeshirylajimi, S.R. Moosavi, J. Amini, L. Tayebi, Synergistic effects of conductive PVA/PEDOT electrospun scaffolds and electrical stimulation for more effective neural tissue engineering, Eur. Polym. J. 140 (2020) 110051.
[214] A. Zhuang, X. Huang, S. Fan, X. Yao, B. Zhu, Y. Zhang, One-step approach to prepare transparent conductive regenerated silk fibroin/PEDOT: PSS films for electroactive cell culture, Acs Appl Mater Inter 14 (1) (2021) 123–137.
[215] Y. Han, M. Sun, X. Lu, K. Xu, M. Yu, H. Yang, J. Yin, A 3D printable gelatin methacryloyl/chitosan hydrogel assembled with conductive PEDOT for neural tissue engineering, Compos. B Eng. 273 (2024) 111241, https://doi.org/10.1016/j.compositesb.2024.111241.
[216] F. Zha, W. Chen, L. Hao, C. Wu, M. Lu, L. Zhang, D. Yu, Electrospun cellulose-based conductive polymer nanofibrous mats: composite scaffolds and their influence on cell behavior with electrical stimulation for nerve tissue engineering, Soft Matter 16 (28) (2020) 6591–6598.
[217] B.R. Hsieh, Y. Yu, A.C. VanLaeken, H. Lee, General methodology toward soluble poly (p-phenylenevinylene) derivatives, Macromolecules 30 (25) (1997) 8094–8095.
[218] A. Reshak, M. Shahimin, N. Juhari, S. Suppiah, Electrical behaviour of MEH-PPV based diode and transistor, Prog. Biophys. Mol. Biol. 113 (2) (2013) 289–294.
[219] R. Borah, G.C. Ingavle, S.R. Sandeman, A. Kumar, S. Mikhalovsky, Electrically conductive MEH-PPV: PCL electrospun nanofibres for electrical stimulation of rat PC12 pheochromocytoma cells, Biomater Sci-Uk 6 (9) (2018) 2342–2359.
[220] Z. Matharu, S.K. Arya, S. Singh, V. Gupta, B. Malhotra, Langmuir–Blodgett film based on MEH-PPV for cholesterol biosensor, Anal. Chim. Acta 634 (2) (2009) 243–249.
[221] S. Sakiyama, N. Mizutani, K. Fujita, Controllable p-and n-type doping of poly [2-methoxy-5-(2′-methyl-hexyloxy)-p-phenylenevinylene] films prepared by evaporative spray deposition using ultradilute solution, Jpn. J. Appl. Phys. 55 (4S) (2016) 04EL03.
[222] R. Borah, S. Banerjee, A. Kumar, Surface functionalization effects on structural, conformational, and optical properties of polyaniline nanofibers, Synth. Met. 197 (2014) 225–232.
[223] M. Rahman, T. Mahady Dip, R. Padhye, S. Houshyar, Review on electrically conductive smart nerve guide conduit for peripheral nerve regeneration, J. Biomed. Mater. Res. 111 (12) (2023) 1916–1950.
[224] J. Zeng, Z. Huang, G. Yin, J. Qin, X. Chen, J. Gu, Fabrication of conductive NGF-conjugated polypyrrole–poly (l-lactic acid) fibers and their effect on neurite outgrowth, Colloids Surf. B Biointerfaces 110 (2013) 450–457.
[225] P. Zarrintaj, E. Zangene, S. Manouchehri, L.M. Amirabad, N. Baheiraei, M. R. Hadjighasem, M. Farokhi, M.R. Ganjali, B.W. Walker, M.R. Saeb, Conductive

biomaterials as nerve conduits: recent advances and future challenges, Appl. Mater. Today 20 (2020) 100784.
[226] A. Manzari-Tavakoli, R. Tarasi, R. Sedghi, A. Moghimi, H. Niknejad, Fabrication of nanochitosan incorporated polypyrrole/alginate conducting scaffold for neural tissue engineering, Sci Rep-Uk 10 (1) (2020) 22012.
[227] Y. Bu, H.-X. Xu, X. Li, W.-J. Xu, Y.-x. Yin, H.-l. Dai, X.-b. Wang, Z.-J. Huang, P.-H. Xu, A conductive sodium alginate and carboxymethyl chitosan hydrogel doped with polypyrrole for peripheral nerve regeneration, Rsc Adv 8 (20) (2018) 10806–10817.
[228] Y. Wang, H. Yu, H. Liu, Y. Fan, Double coating of graphene oxide–polypyrrole on silk fibroin scaffolds for neural tissue engineering, J. Bioact. Compat Polym. 35 (3) (2020) 216–227.
[229] I.S. Romero, M.L. Schurr, J.V. Lally, M.Z. Kotlik, A.R. Murphy, Enhancing the interface in silk–polypyrrole composites through chemical modification of silk fibroin, Acs Appl Mater Inter 5 (3) (2013) 553–564.
[230] D. Olvera, M. Sohrabi Molina, G. Hendy, M.G. Monaghan, Electroconductive melt electrowritten patches matching the mechanical anisotropy of human myocardium, Adv. Funct. Mater. 30 (44) (2020) 1909880.
[231] M. Namhongsa, D. Daranarong, M. Sriyai, R. Molloy, S. Ross, G.M. Ross, A. Tuantranont, J. Tocharus, S. Sivasinprasasn, P.D. Topham, Surface-modified polypyrrole-coated PLCL and PLGA nerve guide conduits fabricated by 3D printing and electrospinning, Biomacromolecules 23 (11) (2022) 4532–4546.
[232] L.M. Leahy, I. Woods, J. Gutierrez-Gonzalez, J. Maughan, C. O'Connor, M. Stasiewicz, K. Kaur, M.G. Monaghan, A. Dervan, F.J. O'Brien, Electrostimulation via a 3D-printed, biomimetic, neurotrophic, electroconductive scaffold for the promotion of axonal regrowth after spinal cord injury, Mater. Today 79 (2024) 60–72.
[233] S. Vijayavenkataraman, N. Vialli, J.Y. Fuh, W.F. Lu, Conductive collagen/polypyrrole-b-polycaprolactone hydrogel for bioprinting of neural tissue constructs, International Journal of Bioprinting 5 (2.1) (2019).
[234] S.-J. Lee, M. Nowicki, B. Harris, L.G. Zhang, Fabrication of a highly aligned neural scaffold via a table top stereolithography 3D printing and electrospinning, Tissue Eng Pt A 23 (11–12) (2017) 491–502.
[235] C. Darroch, G.A. Asaro, C. Gréant, M. Suku, N. Pien, S. Van Vlierberghe, M. G. Monaghan, Melt electrowriting of a biocompatible photo-crosslinkable poly (D, L-lactic acid)/poly (ε-caprolactone)-based material with tunable mechanical and functionalization properties, J. Biomed. Mater. Res. 111 (6) (2023) 851–862.
[236] J.C. Kade, P.D. Dalton, Polymers for melt electrowriting, Adv. Healthcare Mater. 10 (1) (2021) 2001232.
[237] W. Jing, Q. Ao, L. Wang, Z. Huang, Q. Cai, G. Chen, X. Yang, W. Zhong, Constructing conductive conduit with conductive fibrous infilling for peripheral nerve regeneration, Chem. Eng. J. 345 (2018) 566–577.
[238] A. Bayat, A. Ramazani Sa, Biocompatible conductive alginate/polyaniline-graphene neural conduits fabricated using a facile solution extrusion technique, International Journal of Polymeric Materials and Polymeric Biomaterials 70 (7) (2021) 486–495.
[239] B. Ferrigno, R. Bordett, N. Duraisamy, J. Moskow, M.R. Arul, S. Rudraiah, S. P. Nukavarapu, A.T. Vella, S.G. Kumbar, Bioactive polymeric materials and electrical stimulation strategies for musculoskeletal tissue repair and regeneration, Bioact. Mater. 5 (3) (2020) 468–485.
[240] A. Gangrade, B. Gawali, P.K. Jadi, V.G. Naidu, B.B. Mandal, Photo-electro active nanocomposite silk hydrogel for spatiotemporal controlled release of chemotherapeutics: an in vivo approach toward suppressing solid tumor growth, Acs Appl Mater Inter 12 (25) (2020) 27905–27916.
[241] S.J. Wilks, S.M. Richardson-Burn, J.L. Hendricks, D. Martin, K.J. Otto, Poly (3, 4-ethylene dioxythiophene)(PEDOT) as a micro-neural interface material for electrostimulation, Front. Neuroeng. 2 (2009) 591.
[242] D.R. Merrill, M. Bikson, J.G. Jefferys, Electrical stimulation of excitable tissue: design of efficacious and safe protocols, J. Neurosci. Methods 141 (2) (2005) 171–198.
[243] Y.J. Lee, H.-J. Kim, S.H. Do, J.Y. Kang, S.H. Lee, Characterization of nerve-cuff electrode interface for biocompatible and chronic stimulating application, Sensor. Actuator. B Chem. 237 (2016) 924–934.
[244] R.M. Brownstone, Beginning at the end: repetitive firing properties in the final common pathway, Progress in neurobiology 78 (3–5) (2006) 156–172.
[245] B. Singh, Q.-g. Xu, C.K. Franz, R. Zhang, C. Dalton, T. Gordon, V.M. Verge, R. Midha, D.W. Zochodne, Accelerated axon outgrowth, guidance, and target reinnervation across nerve transection gaps following a brief electrical stimulation paradigm, J. Neurosurg. 116 (3) (2012) 498–512.
[246] K. Elzinga, N. Tyreman, A. Ladak, B. Savaryn, J. Olson, T. Gordon, Brief electrical stimulation improves nerve regeneration after delayed repair in Sprague Dawley rats, Exp. Neurol. 269 (2015) 142–153.
[247] M. Vivó, A. Puigdemasa, L. Casals, E. Asensio, E. Udina, X. Navarro, Immediate electrical stimulation enhances regeneration and reinnervation and modulates spinal plastic changes after sciatic nerve injury and repair, Exp. Neurol. 211 (1) (2008) 180–193.
[248] X. Zhang, N. Xin, L. Tong, X.-J. Tong, Electrical stimulation enhances peripheral nerve regeneration after crush injury in rats, Mol. Med. Rep. 7 (5) (2013) 1523–1527.
[249] Y.-J. Tang, M.H. Wu, C.-J. Tai, Direct electrical stimulation on the injured ulnar nerve using acupuncture needles combined with rehabilitation accelerates nerve regeneration and functional recovery—a case report, Compl. Ther. Med. 24 (2016) 103–107.
[250] J.H. Lee, Y.C. Yoon, H.S. Kim, J. Lee, E. Kim, C. Findeklee, U. Katscher, In vivo electrical conductivity measurement of muscle, cartilage, and peripheral nerve around knee joint using MR-electrical properties tomography, Sci Rep-Uk 12 (1) (2022) 73.
[251] Y.-S. Hsiao, Y.-H. Liao, H.-L. Chen, P. Chen, F.-C. Chen, Organic photovoltaics and bioelectrodes providing electrical stimulation for PC12 cell differentiation and neurite outgrowth, Acs Appl Mater Inter 8 (14) (2016) 9275–9284.
[252] Global unique device identification database (GUDID) created by national library of medicine (NLM), in collaboration with the FDA. https://accessgudid.nlm.nih.gov/devices/search?page=1&page_size=50&query=JXI. (Accessed 11 September 2024).
[253] T. Vishnoi, A. Singh, A.K. Teotia, A. Kumar, Chitosan-gelatin-polypyrrole cryogel matrix for stem cell differentiation into neural lineage and sciatic nerve regeneration in peripheral nerve injury model, Acs Biomater Sci Eng 5 (6) (2019) 3007–3021, https://doi.org/10.1021/acsbiomaterials.9b00242.
[254] A.C. Paulk, J.C. Yang, D.R. Cleary, D.J. Soper, M. Halgren, A.R. O'Donnell, S. H. Lee, M. Ganji, Y.G. Ro, H. Oh, Microscale physiological events on the human cortical surface, Cerebr. Cortex 31 (8) (2021) 3678–3700.
[255] C.L. Weaver, X.T. Cui, Directed neural stem cell differentiation with a functionalized graphene oxide nanocomposite, Adv. Healthcare Mater. 4 (9) (2015) 1408–1416.
[256] A.S. Pranti, A. Schander, A. Bödecker, W. Lang, PEDOT: PSS coating on gold microelectrodes with excellent stability and high charge injection capacity for chronic neural interfaces, Sensor. Actuator. B Chem. 275 (2018) 382–393.
[257] Z.D. Kojabad, S.A. Shojaosadati, S.M. Firoozabadi, S. Hamedi, Polypyrrole nanotube modified by gold nanoparticles for improving the neural microelectrodes, J. Solid State Electrochem. 23 (2019) 1533–1539.
[258] R. Samba, T. Herrmann, G. Zeck, PEDOT–CNT coated electrodes stimulate retinal neurons at low voltage amplitudes and low charge densities, J. Neural. Eng. 12 (1) (2015) 016014.
[259] Y. Xiao, X. Chen, T. Wang, X. Yang, J. Mitchell, Nitrogen-doped graphene combined with bioactive conducting polymer: an ideal platform for neural interface, Polym. Eng. Sci. 58 (9) (2018) 1548–1554.
[260] R. Liu, X. Huang, X. Wang, X. Peng, S. Zhang, Y. Liu, D. Yang, Y. Min, Electrical stimulation mediated the neurite outgrowth of PC-12 cells on the conductive polylactic acid/reduced graphene oxide/polypyrrole composite nanofibers, Appl. Surf. Sci. 560 (2021) 149965.
[261] Liu, J.; He, H.; Zhu, H.; Li, H.; Xiang, R.; Dang, J.; Ran, Z.; Zhou, Y.; Dong, Y.; Yang, Y. Ti3c2tx/Ppy Coated Pla/Oleanic Acid Multi-Layered Nerve Conduit Promotes Peripheral Nerve Regeneration through Anti-inflammatory Effects and Electrical Stimulation.
[262] S. Wustoni, A. Saleh, J.K. El-Demellawi, A. Koklu, A. Hama, V. Druet, N. Wehbe, Y. Zhang, S. Inal, MXene improves the stability and electrochemical performance of electropolymerized PEDOT films, Apl. Mater. 8 (12) (2020), https://doi.org/10.1063/5.0023187. (Accessed 9 February 2024).
[263] X. Chen, X. Xie, Y. Liu, C. Zhao, M. Wen, Z. Wen, Advances in healthcare electronics enabled by triboelectric nanogenerators, Adv. Funct. Mater. 30 (43) (2020) 2004673.
[264] F.R. Fan, W. Tang, Z.L. Wang, Flexible nanogenerators for energy harvesting and self-powered electronics, Adv Mater 28 (22) (2016) 4283–4305.
[265] Y. Yang, H. Zhang, Z.-H. Lin, Y.S. Zhou, Q. Jing, Y. Su, J. Yang, J. Chen, C. Hu, Z. L. Wang, Human skin based triboelectric nanogenerators for harvesting biomechanical energy and as self-powered active tactile sensor system, ACS Nano 7 (10) (2013) 9213–9222.
[266] B.J. Hansen, Y. Liu, R. Yang, Z.L. Wang, Hybrid nanogenerator for concurrently harvesting biomechanical and biochemical energy, ACS Nano 4 (7) (2010) 3647–3652.
[267] S. Parandeh, N. Etemadi, M. Kharaziha, G. Chen, A. Nashalian, X. Xiao, J. Chen, Advances in triboelectric nanogenerators for self-powered regenerative medicine, Adv. Funct. Mater. 31 (47) (2021) 2105169.
[268] E. Elsanadidy, I.M. Mosa, D. Luo, X. Xiao, J. Chen, Z.L. Wang, J.F. Rusling, Advances in triboelectric nanogenerators for self-powered neuromodulation, Adv. Funct. Mater. 33 (8) (2023) 2211177.
[269] R. Mao, B. Yu, J. Cui, Z. Wang, X. Huang, H. Yu, K. Lin, S.G. Shen, Piezoelectric stimulation from electrospun composite nanofibers for rapid peripheral nerve regeneration, Nano Energy 98 (2022) 107322.
[270] P. Chen, P. Wu, X. Wan, Q. Wang, C. Xu, M. Yang, J. Feng, B. Hu, Z. Luo, Ultrasound-driven electrical stimulation of peripheral nerves based on implantable piezoelectric thin film nanogenerators, Nano Energy 86 (2021) 106123.
[271] P. Wu, P. Chen, C. Xu, Q. Wang, F. Zhang, K. Yang, W. Jiang, J. Feng, Z. Luo, Ultrasound-driven in vivo electrical stimulation based on biodegradable piezoelectric nanogenerators for enhancing and monitoring the nerve tissue repair, Nano Energy 102 (2022) 107707.
[272] H. Zhang, D. Lan, B. Wu, X. Chen, X. Li, Z. Li, F. Dai, Electrospun piezoelectric scaffold with external mechanical stimulation for promoting regeneration of peripheral nerve injury, Biomacromolecules 24 (7) (2023) 3268–3282.
[273] Y. Ma, H. Wang, Q. Wang, X. Cao, H. Gao, Piezoelectric conduit combined with multi-channel conductive scaffold for peripheral nerve regeneration, Chem. Eng. J. 452 (2023) 139424.
[274] W. Pi, F. Rao, J. Cao, M. Zhang, T. Chang, Y. Han, Y. Zheng, S. Liu, Q. Li, X. Sun, Sono-electro-mechanical therapy for peripheral nerve regeneration through piezoelectric nanotracts, Nano Today 50 (2023) 101860.
[275] R. Borah, A. Kumar, Enhanced cellular activity on conducting polymer: chitosan nanocomposite scaffolds for tissue engineering application, in: Research Anthology on Emerging Technologies and Ethical Implications in Human Enhancement, IGI Global, 2021, pp. 734–773.

[276] C. Qin, Z. Yue, G.G. Wallace, J. Chen, Bipolar electrochemical stimulation using conducting polymers for wireless electroceuticals and future directions, ACS Appl. Bio Mater. 5 (11) (2022) 5041–5056.
[277] A.M. Rajnicek, Z. Zhao, J. Moral-Vico, A.M. Cruz, C.D. McCaig, N. Casañ-Pastor, Controlling nerve growth with an electric field induced indirectly in transparent conductive substrate materials, Adv. Healthcare Mater. 7 (17) (2018) 1800473.
[278] A.M. Rajnicek, N. Casañ-Pastor, Wireless control of nerve growth using bipolar electrodes: a new paradigm in electrostimulation, Biomater Sci-Uk 12 (9) (2024) 2180–2202.
[279] C. Qin, Z. Yue, Y. Chao, R.J. Forster, F.Ó. Maolmhuaidh, X.-F. Huang, S. Beirne, G. G. Wallace, J. Chen, Bipolar electroactive conducting polymers for wireless cell stimulation, Appl. Mater. Today 21 (2020) 100804.
[280] C. Qin, Z. Yue, X.-F. Huang, R.J. Forster, G.G. Wallace, J. Chen, Enhanced wireless cell stimulation using soft and improved bipolar electroactive conducting polymer templates, Appl. Mater. Today 27 (2022) 101481.
[281] Y. Ishiguro, S. Inagi, T. Fuchigami, Gradient doping of conducting polymer films by means of bipolar electrochemistry, Langmuir 27 (11) (2011) 7158–7162.
[282] V. Nishaa, B. Spoorthi, B. Soumya, U.S. Meda, V.S. Desai, Powering implantable medical devices with biological fuel cells, ECS Trans. 107 (1) (2022) 19197.
[283] Ó. Santiago, E. Navarro, M.A. Raso, T.J. Leo, Review of implantable and external abiotically catalysed glucose fuel cells and the differences between their membranes and catalysts, Applied energy 179 (2016) 497–522.
[284] B.I. Rapoport, J.T. Kedzierski, R. Sarpeshkar, A glucose fuel cell for implantable brain–machine interfaces, PLoS One 7 (6) (2012) e38436.
[285] Y. Sun, Q. Quan, H. Meng, Y. Zheng, J. Peng, Y. Hu, Z. Feng, X. Sang, K. Qiao, W. He, Enhanced neurite outgrowth on a multiblock conductive nerve scaffold with self-powered electrical stimulation, Adv. Healthcare Mater. 8 (10) (2019) 1900127.
[286] D. Ghezzi, M.R. Antognazza, R. Maccarone, S. Bellani, E. Lanzarini, N. Martino, M. Mete, G. Pertile, S. Bisti, G. Lanzani, A polymer optoelectronic interface restores light sensitivity in blind rat retinas, Nat. Photonics 7 (5) (2013) 400–406.
[287] B. Yuan, M.R.F. Aziz, S. Li, J. Wu, D. Li, R.-K. Li, An electro-spun tri-component polymer biomaterial with optoelectronic properties for neuronal differentiation, Acta Biomater. 139 (2022) 82–90.
[288] K. Yang, J.Y. Oh, J.S. Lee, Y. Jin, G.-E. Chang, S.S. Chae, E. Cheong, H.K. Baik, S.-W. Cho, Photoactive poly (3-hexylthiophene) nanoweb for optoelectrical stimulation to enhance neurogenesis of human stem cells, Theranostics 7 (18) (2017) 4591.
[289] A. Prominski, J. Shi, P. Li, J. Yue, Y. Lin, J. Park, B. Tian, M.Y. Rotenberg, Porosity-based heterojunctions enable leadless optoelectronic modulation of tissues, Nat. Mater. 21 (6) (2022) 647–655.
[290] P. Sun, C. Li, C. Yang, M. Sun, H. Hou, Y. Guan, J. Chen, S. Liu, K. Chen, Y. Ma, A biodegradable and flexible neural interface for transdermal optoelectronic modulation and regeneration of peripheral nerves, Nat. Commun. 15 (1) (2024) 4721.
[291] D. Ghezzi, M.R. Antognazza, M. Dal Maschio, E. Lanzarini, F. Benfenati, G. Lanzani, A hybrid bioorganic interface for neuronal photoactivation, Nat. Commun. 2 (1) (2011) 166.
[292] J.F. Maya-Vetencourt, G. Manfredi, M. Mete, E. Colombo, M. Bramini, S. Di Marco, D. Shmal, G. Mantero, M. Dipalo, A. Rocchi, Subretinally injected semiconducting polymer nanoparticles rescue vision in a rat model of retinal dystrophy, Nat. Nanotechnol. 15 (8) (2020) 698–708.
[293] R. Parameswaran, J.L. Carvalho-de-Souza, Y. Jiang, M.J. Burke, J.F. Zimmerman, K. Koehler, A.W. Philips, J. Yi, E. Adams, F. Bezanilla, Photoelectrochemical modulation of neuronal activity with free-standing coaxial silicon nanowires, Biophys. J. 114 (3) (2018) 393a.
[294] D.I. Medagoda, D. Ghezzi, Organic semiconductors for light-mediated neuromodulation, Communications Materials 2 (1) (2021) 111.
[295] J. Tang, C. Wu, Z. Qiao, J. Pi, Y. Zhang, F. Luo, J. Sun, D. Wei, H. Fan, A photoelectric effect integrated scaffold for the wireless regulation of nerve cellular behavior, J. Mater. Chem. B 10 (10) (2022) 1601–1611.
[296] C. Wu, Y. Pu, Y. Zhang, X. Liu, Z. Qiao, N. Xin, T. Zhou, S. Chen, M. Zeng, J. Tang, A bioactive and photoresponsive platform for wireless electrical stimulation to promote neurogenesis, Adv. Healthcare Mater. 11 (20) (2022) 2201255.
[297] O. Karatum, H.N. Kaleli, G.O. Eren, A. Sahin, S. Nizamoglu, Electrical stimulation of neurons with quantum dots via near-infrared light, ACS Nano 16 (5) (2022) 8233–8243.
[298] M. Han, S.B. Srivastava, E. Yildiz, R. Melikov, S. Surme, I.B. Dogru-Yuksel, I. H. Kavakli, A. Sahin, S. Nizamoglu, Organic photovoltaic pseudocapacitors for neurostimulation, Acs Appl Mater Inter 12 (38) (2020) 42997–43008.
[299] Y. Wu, Y. Peng, H. Bohra, J. Zou, V.D. Ranjan, Y. Zhang, Q. Zhang, M. Wang, Photoconductive micro/nanoscale interfaces of a semiconducting polymer for wireless stimulation of neuron-like cells, Acs Appl Mater Inter 11 (5) (2019) 4833–4841.
[300] Y. Yuan, S. Adeloju, G. Wallace, In-situ electrochemical studies on the redox properties of polypyrrole in aqueous solutions, Eur. Polym. J. 35 (10) (1999) 1761–1772.
[301] Y. Li, C. Yu, RGD peptide doped polypyrrole film as a biomimetic electrode coating for impedimetric sensing of cell proliferation and cytotoxicity, J. Appl. Biomed. 15 (4) (2017) 256–264.
[302] J. Jin, Z. Huang, G. Yin, A. Yang, S. Tang, Fabrication of polypyrrole/proteins composite film and their electro-controlled release for axons outgrowth, Electrochim. Acta 185 (2015) 172–177.
[303] H. Zhang, K. Wang, Y. Xing, Q. Yu, Lysine-doped polypyrrole/spider silk protein/poly (l-lactic) acid containing nerve growth factor composite fibers for neural application, Mater. Sci. Eng. C 56 (2015) 564–573.
[304] K.J. Gilmore, M. Kita, Y. Han, A. Gelmi, M.J. Higgins, S.E. Moulton, G.M. Clark, R. Kapsa, G.G. Wallace, Skeletal muscle cell proliferation and differentiation on polypyrrole substrates doped with extracellular matrix components, Biomaterials 30 (29) (2009) 5292–5304.
[305] C.E. Stewart, C.F.K. Kan, B.R. Stewart, H.W. Sanicola, J.P. Jung, O.A.R. Sulaiman, D. Wang, Machine intelligence for nerve conduit design and production, J. Biol. Eng. 14 (1) (2020) 25, https://doi.org/10.1186/s13036-020-00245-2.
[306] S. Zhang, Y. Qin, J. Wang, Y. Yu, L. Wu, T. Zhang, Noninvasive electrical stimulation neuromodulation and digital brain technology: a review, Biomedicines 11 (2023).
[307] S. Romeni, D. Zoccolan, S. Micera, A machine learning framework to optimize optic nerve electrical stimulation for vision restoration, Patterns 2 (7) (2021), https://doi.org/10.1016/j.patter.2021.100286, 2024/11/28.
[308] S. Eickhoff, A. Garcia-Agundez, D. Haidar, B. Zaidat, M. Adjei-Mosi, P. Li, C. Eickhoff, A feasibility study on AI-controlled closed-loop electrical stimulation implants, Sci Rep-Uk 13 (1) (2023) 10163, https://doi.org/10.1038/s41598-023-36384-x.